



**Università  
degli Studi  
di Palermo**

**AREA QUALITÀ, PROGRAMMAZIONE E SUPPORTO STRATEGICO  
SETTORE STRATEGIA PER LA RICERCA  
U. O. DOTTORATI**

Dottorato di Ricerca in Scienze della Terra e del Mare  
Dipartimento di Scienze della Terra e del Mare  
Settore Scientifico Disciplinare BIO/07

# **The role of seagrass meadows as Blue Carbon ecosystems and nutrient and pollutant traps: supporting factors and threats**

LA DOTTORESSA  
**Laura Caviglia**

IL COORDINATORE  
**Prof. Alessandro Aiuppa**

IL TUTOR  
**Prof.ssa Salvatrice Vizzini**

CICLO XXXVI  
ANNO CONSEGUIMENTO TITOLO 2024

# Table of Contents

<b>Introduction.....</b>	<b>4</b>
<b>Chapter 1 - Factors determining the variability in carbon and nitrogen stocks in seagrass sediments along a hydrodynamic gradient in a coastal marine ecosystem.....</b>	<b>8</b>
Introduction .....	10
Materials and Methods .....	12
Results .....	17
Discussion.....	27
Conclusion .....	31
<b>Chapter 2 - Microplastic pollution in seagrass ecosystems from a coastal marine area in the western Mediterranean Sea.....</b>	<b>32</b>
Introduction .....	33
Materials and Methods .....	35
Results .....	41
Discussion.....	65
Conclusion .....	69
<b>Chapter 3 - Analysis of carbon and nitrogen stocks, stable isotopes and trace metals from different <i>P. oceanica</i> habitats (natural meadow, reforestation, dead matte) from an anthropized coastal area.....</b>	<b>70</b>
Introduction .....	72
Materials and Methods .....	74
Results .....	82
Discussion.....	98
Conclusion .....	101
<b>General conclusion .....</b>	<b>102</b>

**References.....105**

**Acknowledgements.....127**

## Introduction

For centuries, human society has grown in coastal areas, benefiting from the ecosystem goods and services that coastal habitats provide. Although coastal areas occupy only about 4% of the total land area and 11% of the oceans (Millennium Ecosystem Assessment, 2005), they are among the most productive ecosystems on the planet and provide cumulative and unique benefits because they are located at the interface between land and watersheds and are usually inhabited by aquatic vegetation (Barbier et al., 2011). Seagrasses, salt marshes and mangroves characterize the coastal environments and are referred to as Blue Carbon ecosystems, as they act as carbon sinks, capturing and sequestering carbon from the atmosphere, providing an important role in climate change mitigation (Macreadie et al., 2014). Other services include the provision of nursery habitats and the maintenance of fisheries, coastal protection and erosion control, the improvement of water quality through filtration and detoxification processes, tourism, recreation, education and research (Himes-Cornell et al., 2018). However, due to increasing anthropogenic pressure in coastal zones and the growing demand for coastal resources, coastal ecosystems are among the most threatened natural systems worldwide. About half of all salt marshes worldwide and a third of mangroves, coral reefs and seagrass beds have already been lost or degraded (Barbieri et al., 2017), leading to a consecutive loss of their important services. This concern is particularly pronounced in densely populated areas such as the Mediterranean basin, where Blue Carbon ecosystems are represented by saltmarshes and seagrass meadows. The most important seagrass species, the endemic *Posidonia oceanica* (L.) Delile and the pioneer *Cymodocea nodosa* (Ucria) Ascherson, have been predicted to lose 75% and 45% of suitable habitat by 2050, respectively (Chefaoui et al., 2018). Among the threats that affect seagrass ecosystem health and functionality the most relevant include direct mechanical damages (anchoring, trawling, dredging), invasive species, climate change, nutrient enrichment, pollution, and contamination (Orth et al., 2006; Lewis and Devereus, 2009).

Seagrasses are aquatic angiosperms widely distributed in estuarine and coastal waters, able to sequester large amount of organic carbon in their underlying sediments, due to their high primary productivity and their physical properties that reduce the water flow, increasing sedimentation and aiding particle trapping (Fourqurean et al., 2012). Carbon sequestered in seagrass sediments derives from senescent above- and below-ground biomass and allochthonous organic matter (Mazarrasa et al., 2021). It can remain trapped for centuries to millennia (Duarte et al., 2005), due to the anaerobic state of seagrass sediments, saturated of water, that slowdown the decomposition rates, leading to continuous build-up of stocks over time (Duarte et al., 2013).

Seagrass meadows are also known as filtering habitat for incoming nutrients, especially nitrogen, and act as contaminant buffers between the continental and marine systems, playing a central role in the mitigation of water eutrophication (Aoki et al., 2020). Seagrasses improve water quality enhancing nitrogen removal from the water column through its burial in the sediment and coupled nitrification-denitrification processes that lead to the microbial transformation of biologically available nitrates into inert dinitrogen gas (Aoki and McGlathery, 2018).

Seagrasses can also absorb trace metals from seawater and sediments, exhibiting high tolerance to metal stress (Y. Li et al., 2023), and have been recognized as natural metal pollution biomonitors (Govers et al., 2014). Recent studies speculated on the phytoremediation capacity of seagrasses and seagrass recolonization and transplantation processes have been indicated as a viable tool to rehabilitate contaminated ecosystems (Oliveira et al., 2023; Lee et al., 2019). Furthermore, seagrass sediment cores have been used as natural archives, representing a useful tool to reconstruct centennial-scale fluxes and trends of chemical contamination at local, regional and global scales (Serrano et al., 2016).

Recently, as seagrass meadows favour the deposition of suspended particles through their canopy, it has been speculated that they also act as a filter for microplastics, representing a hotspot for microplastics (Sanchez-Vidal et al., 2021). Seagrass beds inhabit shallow coastal waters that have been found to be heavily contaminated with microplastics due to dense populations and inadequate waste disposal (Kaardorp et al. 2020). However, some authors have found an enrichment factor of 2.9 in seagrass sediments, compared to bare sediments (Huang et al., 2020), while some others have found no difference in microplastic concentration between seagrass and unvegetated sediments, suggesting a general build-up of microplastics in the wider environment driven by other factors such as hydrodynamics and plastic sources (Unsworth et al., 2021). Microplastics are among the emerging problems in the field of marine pollution and have recently caused great concern in the international community (Li et al., 2023). Microplastics are small (<5 mm) plastic fragments, fibres, granules, foams, pellets, which are directly produced for cosmetic and personal care industry (primary microplastics) or derived from the physical, chemical or biological degradation of macroplastics (secondary microplastics), that are ubiquitous in the marine environment and due to their small size are considered bioavailable to organisms throughout the food-web (Cole et al., 2011). Several studies have taken into account the toxicological effects of microplastics on the marine biota, which consist in physical injuries such as intestinal perforation, blockage of the digestive tract, choking (Ahrendt et al., 2020; Kim et al., 2022) or in the alteration of immunological parameters, oxidative stress, neurotoxicity, genotoxicity (Guzzetti et al., 2018). As seagrass beds support a great biodiversity but can also be characterized by high concentrations of microplastics, these ecosystems must be given

priority when assessing the impact of microplastics on marine life.

Unfortunately, direct or indirect human disturbance leading to the loss of seagrass can result in the exposure of buried organic carbon, total nitrogen and pollutants to hydrodynamic forces, erosion processes and aerobic conditions, favouring the remineralization of organic matter, the resuspension of nutrients and any potential contaminants trapped within (e.g., trace metals or microplastics), turning seagrass ecosystems from carbon, nutrients and pollutants sinks to sources (Macreadie et al, 2015; Moksnes et al, 2021; Unsworth et al., 2022).

Furthermore, carbon and nitrogen storage in seagrass sediments proved to be very heterogeneous, even within the same species (Lavery et al., 2013; Ricart et al., 2020; Kindeberg et al., 2018). This underlines the importance of also considering environmental conditions when assessing the storage of elements in seagrass sediments to improve the accuracy of seagrass ecosystem services assessments and management. Recently, several studies have focused on the seagrass traits and the environmental factors that influence seagrass sediment stocks (Rohr et al., 2016; Dahl et al., 2020; Mazarrasa et al., 2021; Kennedy et al., 2022). Different environmental parameters determine the distribution, growth and functionality of seagrass meadows, such as temperature, salinity, depth, substrate type, nutrients availability and water currents (Unsworth et al., 2014). Indeed, a correct management of these coastal vegetated ecosystems require a good understanding of the habitat characteristics that drive seagrass stocks and filtering capacities (Mazarrasa et al., 2018), and further site-specific research is needed in order to overcoming this challenge (Novak et al., 2020).

Given the ongoing risks that seagrass ecosystems are facing at a global scale and in the Mediterranean Sea, conservation and restoration strategies are among the most important challenges for marine science and coastal management (Ruiz et al., 2009). A better understanding of seagrass ecology and functionality, of the major threats affecting them and of the strategies that could be used to reverse the downward trend is needed (Unsworth et al., 2019). Nowadays, efforts to prevent seagrass regression have focused in reducing physical stressors and general human pressures, promoting conservation of existing meadows and carrying on transplantation activities to sustain the resilience of endangered species (Calvo et al., 2021). There is a growing number of seagrass restoration successes globally (Tan et al., 2020), but deep knowledge of the general state of the transplanting site and long-term monitoring programs are needed to understand the real success of the restoration projects.

This work aims to expand our knowledge of the ability of seagrass ecosystems to act as Blue Carbon systems and as filters for nutrients and pollutants, considering their interaction with the environmental factors that characterize the coastal environment. This work also aims to contribute to the science of seagrass restoration, as there is an urgent need to find solutions to the overall decline of these important ecosystems. The topics developed in this introduction will be discussed in three chapters:

- Chapter 1 deals with the interaction between seagrass traits and environmental factors affecting the carbon and nitrogen storage capacity of seagrass meadows, considering the main species of the Mediterranean Sea: *P. oceanica* and *C. nodosa*.
- Chapter 2 focuses on microplastic pollution of seagrass ecosystems in a coastal basin, with the aim of drawing conclusions on how environmental factors influence the abundance and distribution of these pollutants in seagrass sediment, water and biota and how the trophic ecology of the fish species that characterize the seagrass fauna influences the probability of ingestion.
- Chapter 3 assesses the past and present environmental status of a transplanting site; examines the differences between the storage capacity of natural and transplanted meadows and dead matte; reconstructs the changes in geochemical and pollutant inputs occurred in the area over the last century.

# Chapter 1

## Factors determining the variability in carbon and nitrogen stocks in seagrass sediments along a hydrodynamic gradient in a coastal marine ecosystem.

### Abstract

Despite the importance of seagrass beds as blue carbon ecosystems and natural filters, little is known about which factors affect their ability to store organic and inorganic carbon, and nitrogen. In this study, we determined the environmental factors affecting the ability of two Mediterranean species, *Cymodocea nodosa* (Ucria) Ascherson and *Posidonia oceanica* (L.) Delile, to sequester carbon and nitrogen. We compared the stocks and accumulation rates of organic and inorganic carbon and nitrogen at five sites within a semi-enclosed basin (Stagnone di Marsala, Italy) characterized by different habitats (*P. oceanica*, *C. nodosa*, bare sediment) and connection to the open sea. Partial least squares analysis showed that the variability of organic carbon and nitrogen stocks in seagrass sediments was primarily related to the mud content, the percentage contribution of autochthonous carbon to the sediment organic carbon pool, and the total biomass of seagrass meadows. Inorganic carbon stocks were primarily related to hydrodynamics and were significantly higher in the outermost station, suggesting that carbonate deposition in seagrass ecosystems is mainly from allochthonous sources and not produced in situ. Looking at the stations covered by *C. nodosa*, the Kruskal-Wallis test revealed a significantly higher organic carbon content in the station with the lowest hydrodynamics. Overall, the *C. nodosa* sediments are important sinks for organic carbon (100.36-156.24 Mg C<sub>org</sub> ha<sup>-1</sup> in 1 m) and nitrogen (9.04-10.05 Mg N<sub>tot</sub> ha<sup>-1</sup> in 1 m), especially compared to the adjacent unvegetated sediments (7.44 Mg C<sub>org</sub> ha<sup>-1</sup>; 2.25 Mg N<sub>tot</sub> ha<sup>-1</sup> in 1 m). Inorganic carbon stocks in the top 1 meter of *C. nodosa* sediment ranged from 247.69 Mg C<sub>inorg</sub> ha<sup>-1</sup> to 688.31 Mg C<sub>inorg</sub> ha<sup>-1</sup>, following the hydrodynamic gradient. Mean stocks of C<sub>org</sub>, N<sub>tot</sub> and C<sub>inorg</sub> in the top 1 m of sediment were higher in *P. oceanica* (334.31 ± 4.44 Mg C<sub>org</sub> ha<sup>-1</sup>, 47.30 ± 10.47 Mg N<sub>tot</sub> ha<sup>-1</sup>, 629.47 Mg C<sub>inorg</sub> ha<sup>-1</sup> ± 346.17).



## **Keywords**

Blue carbon, seagrass meadows, marine sediment, organic carbon, inorganic carbon, nitrogen, storage, mitigation of climate change, Mediterranean Sea

## **Highlights**

- Organic carbon and total nitrogen sequestration increase with mud content, autochthonous contribution, and seagrass total biomass.
- Organic carbon content is significantly higher in the station with the lowest hydrodynamics.
- Inorganic carbon sequestration increases with hydrodynamics and exposure.
- *C. nodosa* is a significant carbon sink.

## Introduction

Seagrass meadows are among the most productive aquatic ecosystems on Earth and provide a wide range of ecosystem services such as support of biodiversity and fisheries, improvement of water quality, coastal protection, and culture preservation (Nordlund et al., 2018). In addition, seagrass meadows perform the important ecological function of storing carbon in their underlying sediment (Fourqurean et al., 2012). Although their extension corresponds to less than 0.2% of the oceans, it is estimated that, globally, they bury up to  $27.4 \text{ Tg C}_{\text{org}} \text{ y}^{-1}$ , which corresponds to about 10% of the organic carbon buried annually in the oceans (Duarte et al., 2005; Fourqurean et al., 2012). For this reason, seagrass ecosystems, along with the other coastal Blue Carbon (BC) ecosystems (i.e. saltmarshes and mangroves), have gained international interest as their conservation and restoration represents a nature-based solution for climate change mitigation (Peter I. Macreadie et al., 2021).

Apart from the ability of seagrass meadows to sequester organic carbon, these ecosystems bury significant amounts of  $\text{CaCO}_3$ , the concentration of which exceeds that of organic carbon in seagrass sediment (Mazarrasa et al., 2015). As calcification processes lead to the emission of  $\text{CO}_2$ , there was concern that  $\text{CaCO}_3$  production in seagrass ecosystems represents a source of  $\text{CO}_2$  to the atmosphere, counteracting their role as Blue Carbon ecosystems. However, it has been demonstrated that the  $\text{CaCO}_3$  stored in seagrass meadows mainly originates from allochthonous sources, so that seagrass ecosystems can be considered as net carbon sinks (Saderne et al., 2019). Seagrass meadows are also recognised as nutrient-filtering habitats (Piehler & Smyth, 2011; Kindeberg et al., 2018; Saderne et al., 2020), mainly because they remove nitrogen from the water column and store it in their sediment. In addition, several biogeochemical processes characterize the nitrogen dynamics in seagrass ecosystems, such as nitrogen fixation and dissimilatory nitrate reduction to ammonium, the former providing a source of nitrogen and the latter cycling rather than losing nitrogen. When denitrification or anaerobic ammonium oxidation are the main processes instead, seagrass beds are nitrogen sinks and play an important role in mitigating coastal eutrophication (Welsh et al., 2001; Salk et al., 2017; Hoffman et al., 2019).

The amount and accumulation rate of carbon and nitrogen in the sediment are influenced by both abiotic and biotic factors. Generally, literature data focus on the capacity of the different seagrass species to accumulate organic carbon and on the environmental factors that promote or hinder this process, while less attention has been paid to the factors that determine the storage of inorganic carbon and total nitrogen in seagrass sediment (Gullström et al., 2018; Kinderberg et al., 2018; Martins et al., 2022; Leiva-Dueñas et al., 2023). Abiotic factors such as exposure, hydrodynamics, wave height and depth have been shown to influence organic carbon (Lavery et al., 2013; Serrano et al., 2014;

Samper-Villarreal et al., 2016; Mazarrasa et al., 2018, 2021) with meadows located at shallower depth, subjected to lower level of exposure and slower currents, showing the highest stocks. Sediment grain size is another variable to consider, with higher content of mud being indicative of higher organic carbon amount in seagrass sediment (Dahl et al., 2016; Röhr et al., 2016; Samper-Villarreal et al., 2016). The biological traits of the seagrass species influence the organic carbon stock as it is strictly related to the productivity of the species (Kennedy et al. 2022), and species with higher structural complexity and greater leaf canopy have greater capacity to attenuate flow and retain particles (Terrados & Duarte, 2000; Hendriks et al., 2008). Inorganic carbon has been shown to be negatively related to sediment density and shoot density, while canopy height has a positive relationship (Gullstrom et al., 2018). Nitrogen sequestration appears to be positively affected by mud content (Kinderberg et al., 2018; Leiva-Dueñas et al., 2023) and negatively affected by flow velocity (Martins et al., 2022).

In the Mediterranean Sea much of our knowledge on seagrass stocks is based on studies on *Posidonia oceanica* (L.) Delile, the iconic endemic species of the region (Serrano et al., 2016; Mazarrasa et al., 2017; Pergent-Martini et al., 2021; Apostolaki et al., 2019, 2022; Monnier et al., 2022). There is limited information on the storage capacity of the Mediterranean native species *Cymodocea nodosa* (Ucria) Ascherson (Apostolaki et al., 2019; Piñeiro-Juncal et al., 2021; Wesselmann et al., 2021, Fern et al., 2020), a pioneer species, widespread throughout the Mediterranean and adjacent Atlantic coasts, characterized by lower primary production and structural complexity, but also by faster growth (Guidetti et al., 2002; Hendriks et al., 2022) than *P. oceanica*. Early information supported that *C. nodosa* may be less susceptible to global change than *P. oceanica* (Chefaoui et al., 2016) being able to occupy newly available spaces resulting from the regression of *P. oceanica* (Cancemi et al., 2002; Montefalcone et al., 2006, 2007, Boudouresque et al. 2009). However, other studies showed the significant negative impact that water temperature rise may pose on the populations of *C. nodosa* (Olsen et al., 2012; Chefaoui et al., 2018). In coastal areas where these two seagrass species coexist under the same environmental conditions and stressors, it becomes possible to compare their storage capacity and to infer on changes in the services they provide. Semi-enclosed marine basins, in particular, represent model ecosystems where the ecological consequences of climate change are anticipated and exacerbated, due to their shallow depth, limited connection to the open sea and prolonged water renewal time (Lloret et al., 2008; Brito et al., 2012; Angus, 2017).

This paper aimed at identifying the abiotic and biotic factors determining the ability of *C. nodosa* meadows to sequester organic and inorganic carbon and nitrogen and compare it with bare sediment and coexisting *P. oceanica*. For this purpose, we compared sediment characteristics in three sites within a semi-enclosed basin (Stagnone di Marsala, Sicily, Italy) characterised by a different level of

connection to the adjacent open-sea and, hence, by different environmental and biological settings (i.e., hydrodynamics, seawater salinity and temperature, sediment granulometry, seagrass detritus contribution to the stocks). In the central area of this basin, extensive and spreading meadows of *C. nodosa* coexist with patchy *P. oceanica*, which is, however, under a marked regression (Calvo and Frada Orestano, 1984; Tomasello personal communication), seemingly because of extreme values of climate-relevant variables (e.g., temperature and salinity) this climax seagrass species is experiencing. This allowed conclusions to be drawn about whether and how blue carbon ecosystems might change their capacity to store elements under climate change if the climax species *P. oceanica* is replaced by the less sensitive seagrass *C. nodosa*, which follows *P. oceanica* along a regressive series.

## Materials and methods

### Study Site

The study was carried out in the Stagnone di Marsala (Fig.1, 137° 52' N; 12° 26'), a semi-enclosed basin on the westernmost coast of Sicily (Italy) with an area of about 20 km<sup>2</sup> and an average depth of 1.5 m. The basin is separated from the open sea by a calcareous platform (Isola Grande), while two inlets, the Bocca di San Teodoro in the northern area (400 m wide, 0.3-0.4 m deep) and the Bocca Grande in the southern area (2.9 km wide with an average depth of 1.5 m), allow water exchange. Hydrodynamics is mainly driven by tides and wind (Sarà & Mazzola, 1999; de Marchis et al., 2012) and was measured in a previous work (La Loggia et al., 2004) using the mean intertidal dispersion coefficient (MDC), an index that integrates data on current velocity, wind shear stress, and fetches. The MDC (m<sup>2</sup>/s) decreases from the south (26.9 m<sup>2</sup>/s) to the centre (12.6 m<sup>2</sup>/s), reaching the lowest values in the northern region (9.7 m<sup>2</sup>/s). In recent decades, the connection to the open sea has been further reduced due to bottom uplift and heavy sedimentation near the northern channel, resulting in very little water exchange between the north-central area of the basin and the sea (Agnesi et al., 1993; de Marchis et al., 2012). The whole area is oligotrophic, characterized by sandy–muddy sediments and entirely colonized by dense *C. nodosa* meadows, while *P. oceanica* patches are present in the central-southern sector and have undergone a significant decline in recent decades (Calvo and Frada Orestano, 1984; Tomasello personal communication). There are no freshwater inputs. The Stagnone di Marsala has a great naturalistic value, even if embedded in a highly anthropized area, and is included in the list of Sites of Community Importance (Directive 92/43/CEE; ITA010026).



Fig. 1 Map of Stagnone di Marsala with sampling stations.

### Sampling strategy

Sampling was conducted in 2017 at five stations characterized by different connectivity to the sea and different hydrodynamics (Fig. 1). Three stations were characterized by the presence of *C. nodosa* and hereafter called ‘*C. nodosa* North’ (37°53’53’’ N; 12°27’44’’ E), ‘*C. nodosa* Centre’ (37° 52’29’’N; 12° 27’ 28’’ E), and ‘*C. nodosa* South’ (37° 52’ 29’’ N; 12° 27’ 28’’E). In the central area a station characterized by the presence of *P. oceanica* (37°52’29’’ N; 12°28’02’’ E) was also selected. As there are no large unvegetated areas within the basin, a station with unvegetated sediment, ‘Bare sediment’, was sampled in the northern area bordering the open sea (37° 54’ 22’’ N; 12° 27’ 44’’ E).

Salinity and water temperature were measured at the same time of the day once per month for one year, in the northern, central, and southern area of the basin. At each vegetated station, above- and below-ground plant material was collected in triplicate using quadrats (20x20cm) that were randomly dropped onto the meadows.

For the granulometry analysis, sediment samples were collected using Plexiglas cores (25 cm long and Ø 5 cm) in one replicate per station. For the chemical analysis (nutrient stocks and isotopic composition), sediment samples were collected using PVC cores (100 cm long and Ø 8 cm) in two replicates per station, with the exception of Bare sediment, where only one core was sampled. The compression factor was measured by considering the outer, the inner, the total length of the core, and the observed length of sediment inside the core.

### **Analytical procedures**

In the laboratory, the first 10 cm of each core collected for granulometry analysis were homogenized and left in an H<sub>2</sub>O<sub>2</sub> solution (3-10%) to remove organic material. Subsequently, the sediment fractions (gravel > 2 mm, sand 2 mm - 63 mm, silt/clay < 63 mm) were oven dried at 60°C, separated by dry sieving using a set of sieves up to 63 µm, and weighed.

For chemical analyses, cores were cut into 1 cm thick layers along their entire actual length using a stainless-steel hand saw, and the decompressed thickness of each layer was corrected by dividing the observed thickness by the compression factor. Each layer was freeze-dried and pulverized for determination of dry bulk density, elemental concentration, and isotopic composition of carbon and nitrogen. Dry bulk density (DBD, g cm<sup>-3</sup>) was estimated by dividing the dry weight of the sediment by the volume of the wet samples. Total carbon (C<sub>tot</sub> %) and nitrogen (N<sub>tot</sub> %) concentration and the isotopic composition of carbon (δ<sup>13</sup>C ‰) and nitrogen (δ<sup>15</sup>N ‰) were determined by weighing sedimentary aliquots into tin capsules and analysing them with an isotope ratio mass spectrometer (Thermo IRMS Delta Plus XP) coupled to an elemental analyser (Thermo EA -1112). δ<sup>13</sup>C was determined after acidification with HCl (2N) to remove carbonates. Organic carbon (C<sub>org</sub>) was determined by acidifying a fraction of each sediment sample in silver capsules with HCl (18%) to eliminate carbonates before analysis in the EA. The concentration of inorganic carbon (C<sub>inorg</sub>) was calculated as the difference between the concentration of C<sub>tot</sub> and C<sub>org</sub>.

Sediment accumulation rates were determined using the <sup>210</sup>Pb dating technique. <sup>210</sup>Pb activity was determined through the analysis of <sup>210</sup>Po by alpha spectrometry after addition of <sup>209</sup>Po as an internal tracer and digestion in acid media using an analytical microwave, following Sanchez-Cabeza et al., 1998. Concentrations of excess <sup>210</sup>Pb used to build the age models were determined as the difference between total <sup>210</sup>Pb and <sup>226</sup>Ra (supported <sup>210</sup>Pb). Gamma spectrometric measurements were made in

selected samples from different depths along each core. Supported  $^{210}\text{Pb}$  was taken as the concentrations at depth and/or from gamma spectrometry analyses that allowed determining the concentrations of  $^{226}\text{Ra}$  conducted in selected samples of each core.

The total number of shoots collected in the quadrats was counted, and the plant material was cleared of debris and epiphytes, dried, and weighed to determine above- and belowground biomass.

### Calculations and Data Analysis

$^{210}\text{Pb}$  dating technique has been widely used to determine the rate of sediment and, therefore, element accumulation in coastal vegetated habitats (Arias-Ortiz et al., 2018). This technique is limited to sedimentary deposits less than 120 years old (dating horizon), after which  $^{210}\text{Pb}_{\text{excess}}$  decays to negligible or undetectable activities.  $^{210}\text{Pb}$  is a naturally occurring radionuclide with a half-life of 22.3 years; the accumulation of sediments over time ideally generates a decreasing distribution of  $^{210}\text{Pb}$  activity as a function of depth, due to the decay of  $^{210}\text{Pb}$ . Dating is based on determination of the vertical distribution of  $^{210}\text{Pb}$  derived from atmospheric fallout ( $^{210}\text{Pb}_{\text{excess}}$ ) and the known decay rate of  $^{210}\text{Pb}$  (Appleby and Oldfield, 1992). In this study, mass and sediment accumulation rate (MAR,  $\text{g cm}^{-2} \text{ yr}^{-1}$  and SAR,  $\text{cm y}^{-1}$ ) were calculated from  $^{210}\text{Pb}$  data using the Constant Flux:Constant Sedimentation CF:CS model (Krishnaswami et al., 1971). This model assumes constant  $^{210}\text{Pb}$  depositional flux and constant MAR. Following the CF:CS model, the sedimentation rate was calculated by plotting the natural logarithm of the  $^{210}\text{Pb}_{\text{excess}}$  activity against depth and determining the least-squares fit. MAR and SAR accumulation rates cannot be determined for *C. nodosa* North, *C. nodosa* Centre and Bare sediment, because sediments were mixed or  $^{210}\text{Pb}_{\text{ex}}$  concentrations were very low, indicating negligible net sedimentation. The stocks of  $C_{\text{org}}$ ,  $C_{\text{inorg}}$  and  $N_{\text{tot}}$  were estimated as the cumulative product of their elemental concentration, decompressed DBD and decompressed sediment slice thickness in the first 50 cm of sediment depth, as this is the length of the shortest vegetated core, whereas the results for the stocks of Bare sediments refer to 44 cm, the actual length of this core. Stocks were then standardized to 1 meter depth, to allow comparison, by fitting a linear regression of cumulative stock per slice against sediment depth and expressed as  $\text{Mg}\cdot\text{ha}^{-1}$ .

Vertical average down-core profiles and age profiles of sediment characteristics were visualized. Since the replicates of the cores within the same station had different compression and thus different decompressed length and thickness of the layers, average values and standard deviations for each variable were measured in five-centimetre (decompressed) intervals to a maximum depth of 100 cm.

Pearson's correlation analysis was performed to assess changes in geochemical variables with depth after checking for normality through Shapiro-wilk test; when the distribution was not normal, Spearman's correlation was used.

The Kruskal-Wallis test was performed to detect significant differences between stations in DBD,  $C_{org}$ ,  $N_{tot}$  and  $C_{inorg}$  content,  $\delta^{13}C$  and  $\delta^{15}N$ , considering the upper 50 cm of depth for the vegetated stations and the upper 44 cm for Bare sediment. Pairwise comparison using Wilcoxon rank sum test with Bonferroni correction allowed to understand which station showed differences.

Mixing models were used to determine the origin of organic carbon in seagrass sediments and to assess the contribution of autochthonous (seagrasses) and allochthonous (suspended particulate organic matter-POM and algae) organic material.  $\delta^{13}C$  values of the end-members were retrieved from Vizzini et al. (2006, 2013): POM  $\delta^{13}C$  was  $-20.0 \pm 2.3$  ‰ and this value was used for all the stations; algae  $\delta^{13}C$  values used for the northern and the central areas were  $-16.7 \pm 3.3$  ‰ (represented by the mean value  $\pm$  sd of *Caulerpa prolifera*, *Cladophora* sp., *Cystoseira* spp., *Dictyota* sp., *Laurencia obtusa*, *Polysiphonia* sp., *Rytiphalea tinctoria* and seagrass epiphytes),  $-16.1 \pm 2.8$  ‰ in the southern area (represented by the mean value  $\pm$  sd of *C. prolifera*, *Cystoseira* spp., *Dictyota* sp., *R. tinctoria* and epiphytes); seagrass  $\delta^{13}C$  were  $-9.5 \pm 0.4$ ‰ and  $-8.6 \pm 0.7$ ‰ respectively in the northern and southern areas (represented by *C. nodosa* leaves) and  $-9.7 \pm 0.5$ ‰ in the central area for both *C. nodosa* Center and *P. oceanica* Center stations (representing the mean value of  $\delta^{13}C$  of *C. nodosa* and *P. oceanica* leaves). T-test was used to infer significant differences between the end-members. POM  $\delta^{13}C$  showed non-significant differences with algae, therefore these sources were combined, obtaining 'POM + algae' and 'seagrass leaves' as end-members.

Because diagenesis processes may have occurred in the deeper layers after deposition potentially altering  $\delta^{13}C$  values (Kelleway et al., 2022), mixing models were applied only to surficial sediment slices (first 5 cm). The R package *simmr: Stable Isotope Mixing Models in R* was used (Parnell et al., 2013).

### **Factors driving storage**

Partial least squares (PLS) regression multivariate analysis was used to assess the influence of different types of factors on  $C_{org}$ ,  $C_{inorg}$  and  $N_{tot}$  stocks in the first 50 cm (Carrascal et al., 2009; Gullström et al., 2018; Rohr et al., 2018; Lima et al., 2020). The explanatory variables considered were mean dispersion coefficient - MDC (La Loggia et al., 2004), mud content, DBD,  $C_{org}/N_{tot}$ , seagrass contribution (outcome of mixing models), salinity (annual maximum), water temperature



(annual maximum), shoot density, total seagrass biomass (see Tab. 2). The leave-one-out cross-validation was used for each model. The best number of PLS components was chosen based on the best trade-off between lower RMSE and lower model complexity. Jack-Knifing method was used to compute confidence interval for testing if the coefficients are statistically different from zero. Furthermore, principal component analysis (PCA) was performed to visualize how the different stations are related to the explanatory variables that showed significant contribution on the response one ( $C_{org}$ ,  $C_{inorg}$  and  $N_{tot}$  stocks).

PLS models were computed using the *mdatools* R package (Kucheryavskiy, 2020). A p-value < 0.05 was considered as significant. All the analyses were performed using the R (4.2.2) statistical software.

## Results

### Elemental stocks

Overall, *C. nodosa* stations in the upper 50 cm had 14-21 times higher  $C_{org}$  stocks (on average  $6.28 \pm 1.27$  kg  $C_{org}$   $m^{-2}$ ) and 3 times higher  $N_{tot}$  stocks ( $0.47 \pm 0.02$  kg  $N_{tot}$   $m^{-2}$ ) than in the upper 44 cm at Bare sediment station ( $0.36$  kg  $C_{org}$   $m^{-2}$  and  $0.17$  kg  $N_{tot}$   $m^{-2}$ ). Furthermore, in the upper 50 cm *C. nodosa* stations had 2-3 times lower  $C_{org}$  stocks and 3 times lower  $N_{tot}$  stocks than *P. oceanica* station ( $16.22 \pm 1.36$  kg  $C_{org}$   $m^{-2}$  and  $1.39 \pm 0.14$  kg  $N_{tot}$   $m^{-2}$ ). *C. nodosa* North station had higher  $C_{org}$  stock ( $7.66 \pm 2.70$  kg  $C_{org}$   $m^{-2}$ ) than *C. nodosa* Centre and *C. nodosa* South ( $5.15 \pm 0.83$  kg  $C_{org}$   $m^{-2}$ ;  $6.03 \pm 1.47$  kg  $C_{org}$   $m^{-2}$ , respectively).  $C_{inorg}$  stock was 2-8 times higher in *C. nodosa* stations (on average  $19.05 \pm 13.73$  kg  $C_{inorg}$   $m^{-2}$ ) than in Bare sediment ( $3.82$  kg  $C_{inorg}$   $m^{-2}$ ). *C. nodosa* South is the station with the highest  $C_{inorg}$  stock ( $33.89 \pm 1.67$  kg  $C_{inorg}$   $m^{-2}$ ), 5 times higher than *C. nodosa* North ( $6.79 \pm 3.22$  kg  $N_{tot}$   $m^{-2}$ ) and 2 times higher than *C. nodosa* Centre and *P. oceanica* stations ( $16.49 \pm 0.82$  kg  $N_{tot}$   $m^{-2}$ ;  $14.71 \pm 1.39$  kg  $N_{tot}$   $m^{-2}$ , respectively) (Fig. 2).

Mean stocks extrapolated to the uppermost metre of sediment at *C. nodosa* stations ranged from  $100.36 \pm 3.98$  Mg  $C_{org}$   $ha^{-1}$  to  $156.24 \pm 38.90$  Mg  $C_{org}$   $ha^{-1}$ , from  $9.04 \pm 4.53$  Mg  $N_{tot}$   $ha^{-1}$  to  $10.05 \pm 3.48$  Mg  $N_{tot}$   $ha^{-1}$ , and from  $247.69 \pm 132.11$  Mg  $C_{inorg}$   $ha^{-1}$  to  $688.31 \pm 2.84$  Mg  $C_{inorg}$   $ha^{-1}$  (Table 1). Mean stocks of *P. oceanica* station were  $334.31 \pm 4.44$  Mg  $C_{org}$   $ha^{-1}$ ,  $47.30 \pm 10.47$  Mg  $N_{tot}$   $ha^{-1}$  and  $629.47$  Mg  $C_{inorg}$   $ha^{-1}$   $\pm 346.17$ , while in Bare sediment they were  $7.44$  Mg  $C_{org}$   $ha^{-1}$ ,  $2.26$  Mg  $N_{tot}$   $ha^{-1}$  and  $79.31$  Mg  $C_{inorg}$   $ha^{-1}$ .

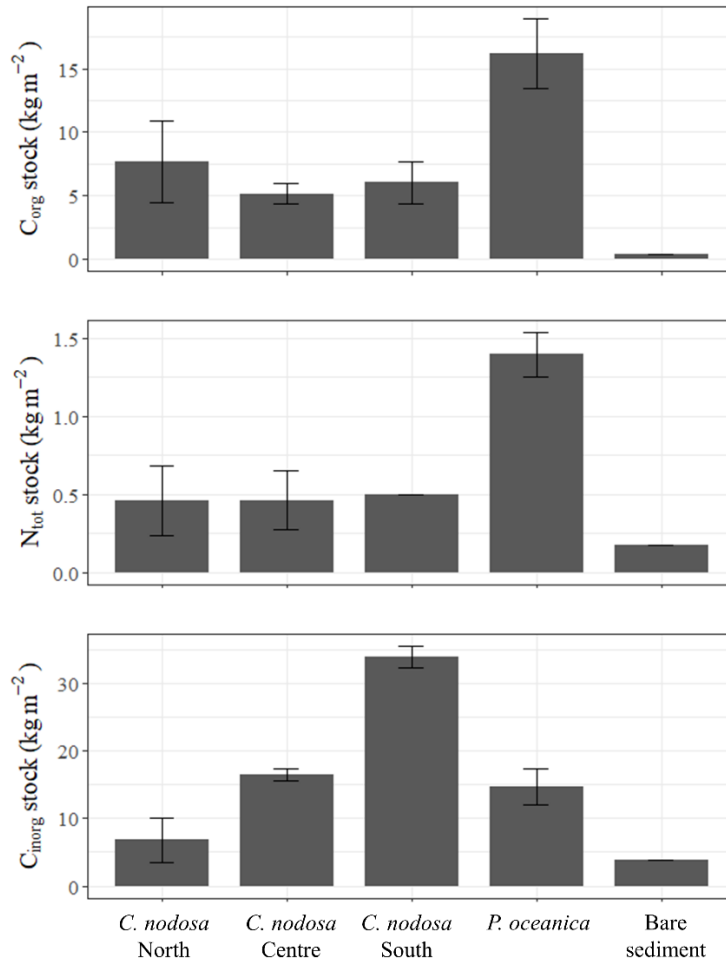


Fig. 2 Mean and STDEV of  $C_{org}$ ,  $N_{tot}$  and  $C_{inorg}$  stocks in the top 50 cm (maximum common length of cores) of the sediment at each vegetated station. Bare sediment stocks are at the top 44 cm, the maximum length of the core for this station.

Tab. 1 Mean  $\pm$  STDEV of  $C_{org}$ ,  $N_{tot}$  and  $C_{inorg}$  stocks at top meter of sediment at each station.

	$C_{org}$ stock (Mg ha <sup>-1</sup> ) at 1 m	$N_{tot}$ stock (Mg ha <sup>-1</sup> ) at 1 m	$C_{inorg}$ stock (Mg ha <sup>-1</sup> ) at 1 m
<i>C. nodosa</i> North	156.24 $\pm$ 38.90	9.04 $\pm$ 4.53	247.69 $\pm$ 132.11
<i>C. nodosa</i> Centre	128.97 $\pm$ 21.61	9.45 $\pm$ 2.05	286.98 $\pm$ 7.56
<i>C. nodosa</i> South	100.36 $\pm$ 3.98	10.05 $\pm$ 3.48	688.31 $\pm$ 2.84
<i>P. oceanica</i>	334.31 $\pm$ 4.44	47.30 $\pm$ 10.47	629.47 $\pm$ 346.17
Bare sediment	7.44	2.25	79.31

### **Pb dating and accumulation rates**

SAR and MAR were  $0.11 \pm 0.03 \text{ cm y}^{-1}$  and  $0.13 \pm 0.03 \text{ g cm}^{-2} \text{ y}^{-1}$ , respectively, for *C. nodosa* South, whereas they were  $0.35 \pm 0.02 \text{ cm y}^{-1}$  and  $0.15 \pm 0.01 \text{ g} \cdot \text{cm}^{-2} \cdot \text{yr}^{-1}$ , respectively, for *P. oceanica*. Over the last 100 years, the rate of accumulation of  $C_{\text{org}}$ ,  $N_{\text{tot}}$  and  $C_{\text{inorg}}$  was lower in *C. nodosa* South ( $12.91 \pm 2.22 \text{ g } C_{\text{org}} \text{ m}^{-2} \text{ y}^{-1}$ ,  $1.20 \pm 0.25 \text{ g } N_{\text{tot}} \text{ m}^{-2} \text{ y}^{-1}$ ,  $68.61 \pm 10.68 \text{ g } C_{\text{inorg}} \text{ m}^{-2} \text{ y}^{-1}$ ) than in *P. oceanica* ( $120.14 \pm 10.84 \text{ g } C_{\text{org}} \text{ m}^{-2} \text{ y}^{-1}$ ,  $9.34 \pm 0.24 \text{ g } N_{\text{tot}} \text{ m}^{-2} \text{ y}^{-1}$ ,  $92.62 \pm 3.00 \text{ g } C_{\text{inorg}} \text{ m}^{-2} \text{ y}^{-1}$ ).

### **Factors driving storage**

The average annual water temperature was similar at the different stations ( $22.0 \pm 6.3 \text{ }^{\circ}\text{C}$ ,  $22.0 \pm 7.2^{\circ}\text{C}$ , and  $19.5 \pm 6.2 \text{ }^{\circ}\text{C}$  in the northern, central, and southern areas, respectively). Average annual water salinity was  $38.5 \pm 1.8 \text{ psu}$  in the northern,  $42.1 \pm 6.5 \text{ psu}$  in the central area and  $37.7 \pm 3.5 \text{ psu}$  in the southern.

The maximum values of water temperature and salinity at each station were recorded in summer and were higher in the central area of the basin ( $34.2 \text{ }^{\circ}\text{C}$ ,  $52.5 \text{ psu}$ ) than in the northern ( $30.8 \text{ }^{\circ}\text{C}$ ,  $41.44 \text{ psu}$ ) and southern ( $29.7 \text{ }^{\circ}\text{C}$ ,  $43.18 \text{ psu}$ ) areas (Table 2).

Shoot density (Table 2) was higher at *C. nodosa* South ( $1029.33 \pm 236.59 \text{ shoots m}^{-2}$ ) than at *C. nodosa* North ( $642.66 \pm 153.60 \text{ shoots m}^{-2}$ ) and *C. nodosa* Centre ( $538.66 \pm 62.92 \text{ shoots m}^{-2}$ ). The lowest shoot density was recorded at the *P. oceanica* station ( $228.33 \pm 32.53 \text{ shoots m}^{-2}$ ).

Total seagrass biomass (Table 2) was similar among *C. nodosa* stations and was  $344 \pm 17.0 \text{ g DW m}^{-2}$  at *C. nodosa* North,  $417 \pm 12.0 \text{ g DW m}^{-2}$  at *C. nodosa* Centre, and  $385 \pm 12.0 \text{ g DW m}^{-2}$  at *C. nodosa* South. *P. oceanica* showed the highest total seagrass biomass ( $1105 \pm 46.6 \text{ g DW m}^{-2}$ ).

Granulometry analysis (Table 3) indicated that sediments at *C. nodosa* stations were mainly sandy, reaching 91%, 85%, and 93% at *C. nodosa* North, *C. nodosa* Centre and *C. nodosa* South, respectively. The proportion of gravel and mud was low at these stations: gravel accounted for 3%, 10%, and 2% at *C. nodosa* North, *C. nodosa* Centre, and *C. nodosa* South, respectively, while mud accounted for 5-6% at all stations. At *P. oceanica* station, mud content was highest at 48%, while gravel and sand constituted 12% and 40%, respectively. Bare sediment was entirely composed by sand.

Tab. 2 Mean  $\pm$  STDEV of environmental and seagrass variables measured at each station.

Variable	Station				
	<i>C.nodosa</i> North	<i>C. nodosa</i> Centre	<i>C. nodosa</i> South	<i>P. oceanica</i>	Bare sediment
Depth (m)	0.45	0.5	1.2	0.5	1.5
Water salinity annual maximum (psu)	41.4	52.5	43.2	52.5	-
Water temperature annual maximum (°C)	30.8	34.2	29.7	34.2	-
MDC (m <sup>2</sup> s <sup>-1</sup> )	9.7	12.6	26.9	12.6	9.7
Seagrass density (shoots m <sup>-2</sup> )	642.66 $\pm$ 153.60	538.66 $\pm$ 62.92	1029.33 $\pm$ 236.59	228.33 $\pm$ 32.53	
Seagrass biomass (g DW m <sup>-2</sup> )	344 $\pm$ 17.0	417 $\pm$ 12.0	385 $\pm$ 12.0	1105 $\pm$ 46.6	

Tab. 3 Mean  $\pm$  STDEV of the sediment variables over the top 50 cm of sediment per station. Granulometry variables refer to the top 10 cm of sediment.

Variable	Station				
	<i>C. nodosa</i> North	<i>C. nodosa</i> Centre	<i>C. nodosa</i> South	<i>P. oceanica</i>	Bare sediment
Gravel (%)	3	10	2	12	0
Sand (%)	91	85	93	40	100
Mud (%)	6	5	5	48	0
DBD (g cm <sup>-3</sup> )	0.91 $\pm$ 0.22	1.06 $\pm$ 0.11	1.18 $\pm$ 0.16	0.77 $\pm$ 0.13	1.38
C <sub>org</sub> (%)	1.71 $\pm$ 0.66	0.97 $\pm$ 0.23	1.03 $\pm$ 0.27	4.26 $\pm$ 1.69	0.06 $\pm$ 0.01
C <sub>inorg</sub> (%)	1.45 $\pm$ 0.69	3.16 $\pm$ 0.98	5.74 $\pm$ 0.75	3.64 $\pm$ 1.16	0.63 $\pm$ 0.36
$\delta^{13}\text{C}$ (‰)	-13.2 $\pm$ 0.8	-12.6 $\pm$ 0.9	-12.2 $\pm$ 1.2	-12.2 $\pm$ 0.8	-24.1
N <sub>tot</sub> (%)	0.10 $\pm$ 0.05	0.08 $\pm$ 0.04	0.08 $\pm$ 0.02	0.36 $\pm$ 0.07	0.03 $\pm$ 0.07
$\delta^{15}\text{N}$ (‰)	2.6 $\pm$ 0.5	0.8 $\pm$ 0.4	3.9 $\pm$ 1.5	2.1 $\pm$ 0.5	-

The correlation of sediment variables with depth highlighted differences among stations (Fig. 3). Overall DBD was positively correlated with depth at all stations, with the exception of *C. nodosa* Centre where the correlation was negative and Bare sediment where correlation did not occur. The correlation of  $C_{org}$  with depth was positive at *C. nodosa* Centre station and negative at *C. nodosa* South station, where also  $N_{tot}$  was negatively correlated.  $C_{inorg}$  vertical profiles showed a positive correlation with depth at both *C. nodosa* North and *P. oceanica* stations.  $\delta^{15}N$  vertical profiles at *C. nodosa* North station showed significant positive correlation with depth, while  $\delta^{13}C$  was correlated negatively at Bare sediment station.

The mean values of DBD,  $C_{org}$ ,  $C_{inorg}$  and  $N_{tot}$  content,  $\delta^{13}C$  and  $\delta^{15}N$  along the sediment interval studied differed significantly among stations (Tables 3 and 4).  $C_{org}$  content was significantly higher at the *P. oceanica* station, followed by *C. nodosa* stations and Bare sediment station. Considering only the *C. nodosa* stations, the highest organic carbon content was recorded at the station with the lowest hydrodynamics (*C. nodosa* North).  $C_{inorg}$  content was significantly higher at *C. nodosa* South than at all other stations.  $N_{tot}$  content was higher at *P. oceanica* station than at *C. nodosa* stations, which did not differ each other and had higher  $N_{tot}$  values than bare sediment station.  $\delta^{13}C$  was not different between *C. nodosa* South, *C. nodosa* Centre and *P. oceanica*, while all these stations had higher values than *C. nodosa* North and Bare sediment stations.  $\delta^{15}N$  was higher at *C. nodosa* South than at the other stations, with the lowest value recorded at *C. nodosa* Centre station.

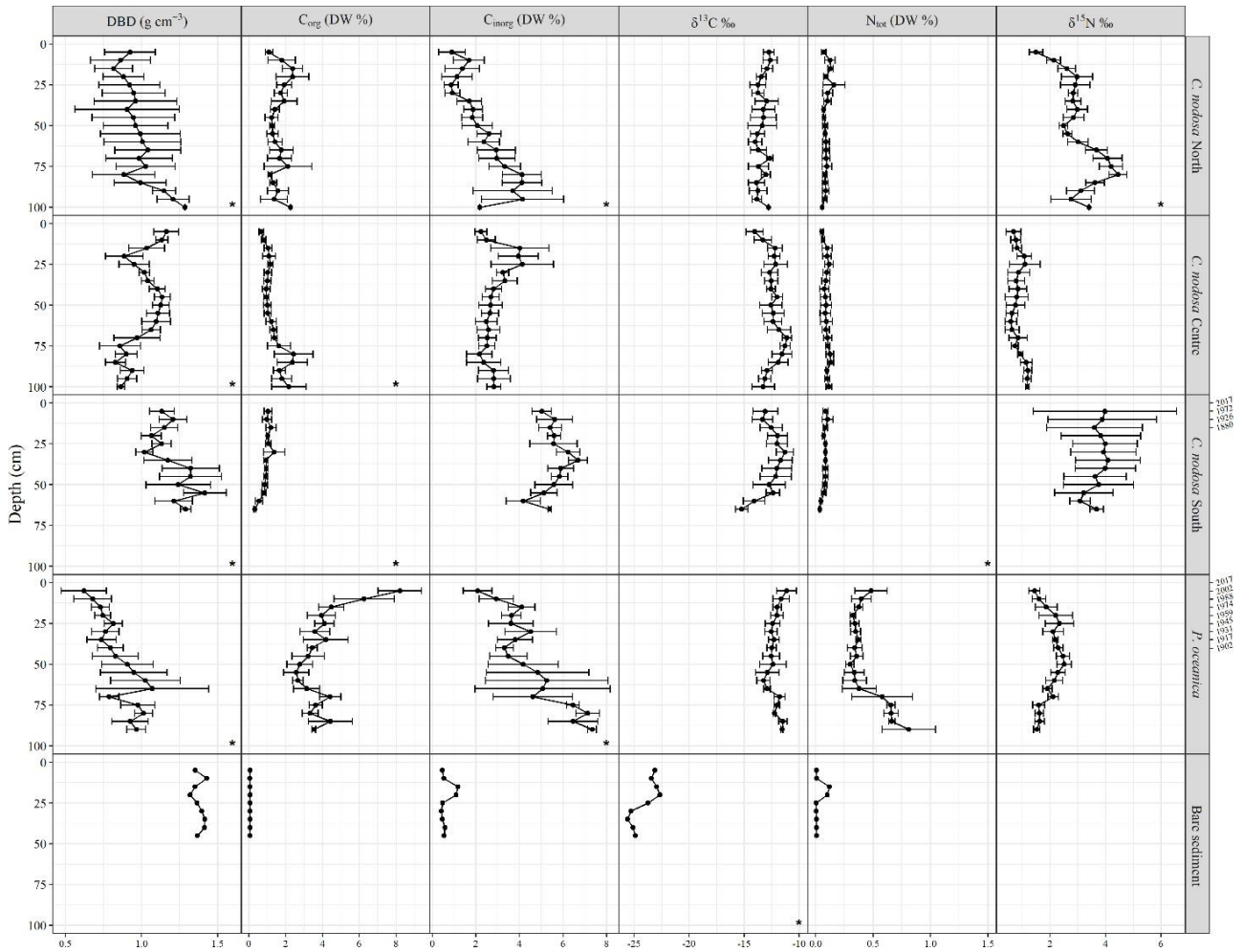


Fig. 3 Vertical average down-core profiles of DBD ( $\text{g cm}^{-3}$ ),  $C_{\text{org}}$  (DW %),  $C_{\text{inorg}}$  (DW %),  $\delta^{13}\text{C}$  (‰),  $N_{\text{tot}}$  (%),  $\delta^{15}\text{N}$  (‰). Averages for each variable were calculated in five centimetres intervals to a maximum depth of 100 cm. Temporal trend for the last 100 years are provided for *C. nodosa* South and *P. oceanica*. Asterisks indicate significant correlation between variable and sediment depth.

Based on the outcome of mixing models, overall, the contribution of seagrasses (i.e. autochthonous material) at each station was higher than that of allochthonous sources accounting for 65%, 52%, 60% and 79% at respectively *C. nodosa* North, *C. nodosa* Centre, *C. nodosa* South and *P. oceanica*.

Table 4. Statistical analysis results of the sediment variables standardised at the top 50 cm of sediment between stations.

Variable	Kruskal-Wallis Rank sum test			Pairwise Wilcoxon Rank Sum Test
	DF	Chi-squared	p-value	
DBD (g cm <sup>-3</sup> )	4	214.97	< 0.01	<i>C. nodosa</i> South > <i>C. nodosa</i> Centre > <i>P. oceanica</i> > <i>C. nodosa</i> North > Bare sediment
C <sub>org</sub> (%)	4	296.22	< 0.01	<i>P. oceanica</i> > <i>C. nodosa</i> North > <i>C. nodosa</i> Centre = <i>C. nodosa</i> South > Bare sediment
C <sub>inorg</sub> (%)	4	321.79	< 0.01	<i>C. nodosa</i> South > <i>P. oceanica</i> > <i>C. nodosa</i> Centre > <i>C. nodosa</i> North > Bare sediment
δ <sup>13</sup> C (‰)	4	153.92	< 0.01	<i>P. oceanica</i> = <i>C. nodosa</i> South = <i>C. nodosa</i> Centre > <i>C. nodosa</i> North > Bare sediment
N <sub>tot</sub> (%)	4	209.33	< 0.01	<i>P. oceanica</i> > <i>C. nodosa</i> North = <i>C. nodosa</i> Centre = <i>C. nodosa</i> South > Bare sediment
δ <sup>15</sup> N (‰)	4	243.4	< 0.01	<i>C. nodosa</i> South > <i>C. nodosa</i> North > <i>P. oceanica</i> > <i>C. nodosa</i> Centre



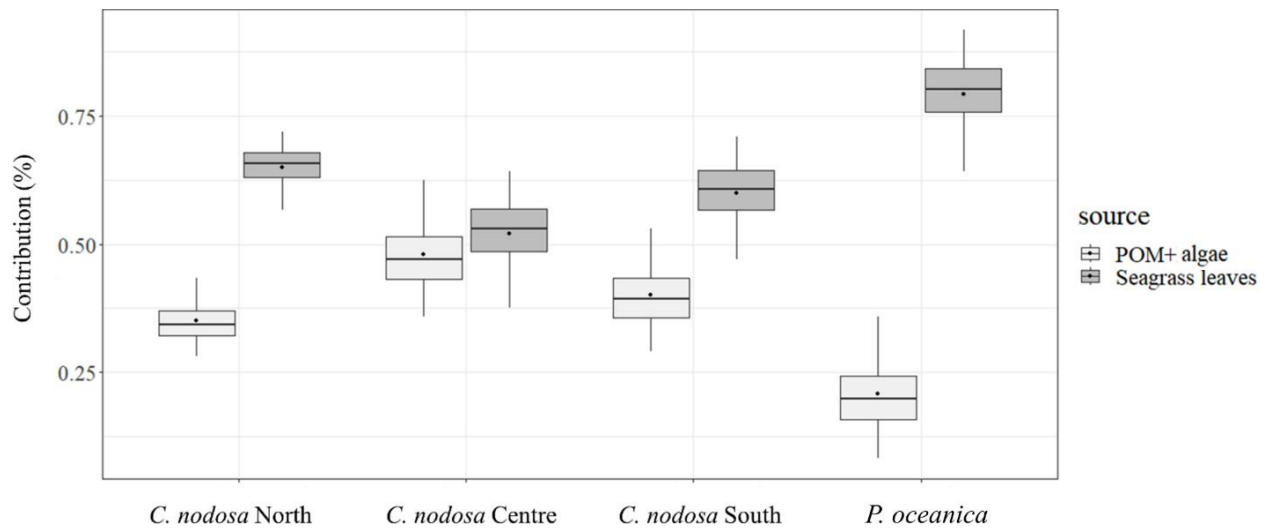


Fig. 4 Boxplot of the percentage contribution of end-members (POM + algae, Seagrass leaves) to organic carbon of the top 5 cm of sediment at the three different habitats. Each box contains 50 % of the data, black lines inside the boxes represent the medians, black points inside the boxes represent the means, tails represent 2.5 % and 97.5 % intervals.

All PLS models showed a significant effect of explanatory variables to stock variability (Fig. 5). Sediment mud content, seagrass contribution and total seagrass biomass had a positive effect on  $C_{org}$  and  $N_{tot}$  stocks, while shoot density had a negative effect on  $C_{org}$  stock (Fig. 5, A and B). When  $C_{org}$  was considered as the response variable, the first two components of PCA explained 93% of the observed variability (Fig. 6, A). When  $N_{tot}$  was considered as the response variable, the first two components explained 97% of variability (Fig. 6, B). In both PCA *P. oceanica* stations are positively associated to the explanatory (mud, seagrass contribution and total biomass) and response variables ( $C_{org}$  stock or  $N_{tot}$  stock) and are clustered separately from *C. nodosa* stations. MDC and total biomass showed a significant and positive effect on  $C_{inorg}$  stock (Fig. 5, C). Considering  $C_{inorg}$  as the response variable the first two components of the PCA explained 99% of variability (Fig. 6, C). The relationship between  $C_{inorg}$  stock and the explanatory variables was not consistent among sites, and *C. nodosa* South grouped separately from the other stations and was positively related to MDC and  $C_{inorg}$  stock.

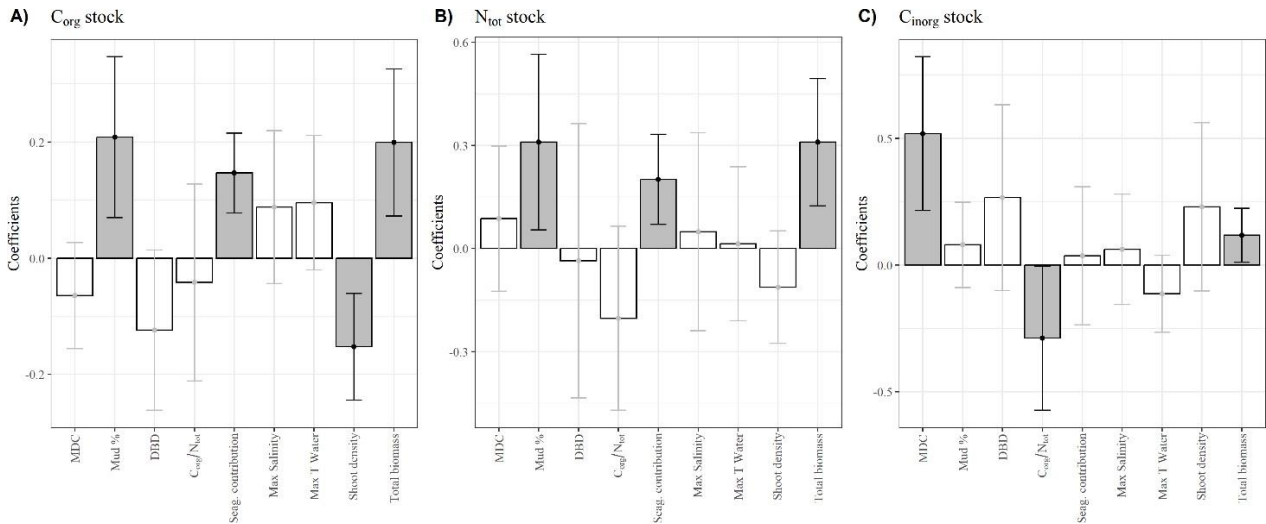


Fig. 5 Coefficient plots of partial least squares (PLS) regression models of  $C_{org}$  (A),  $N_{tot}$  (B) and  $C_{inorg}$  (C) stocks at 50 cm of sediment depth. Grey bars represent significant variables, white bars represent not significant variables. Segments represent 95% confidence intervals.

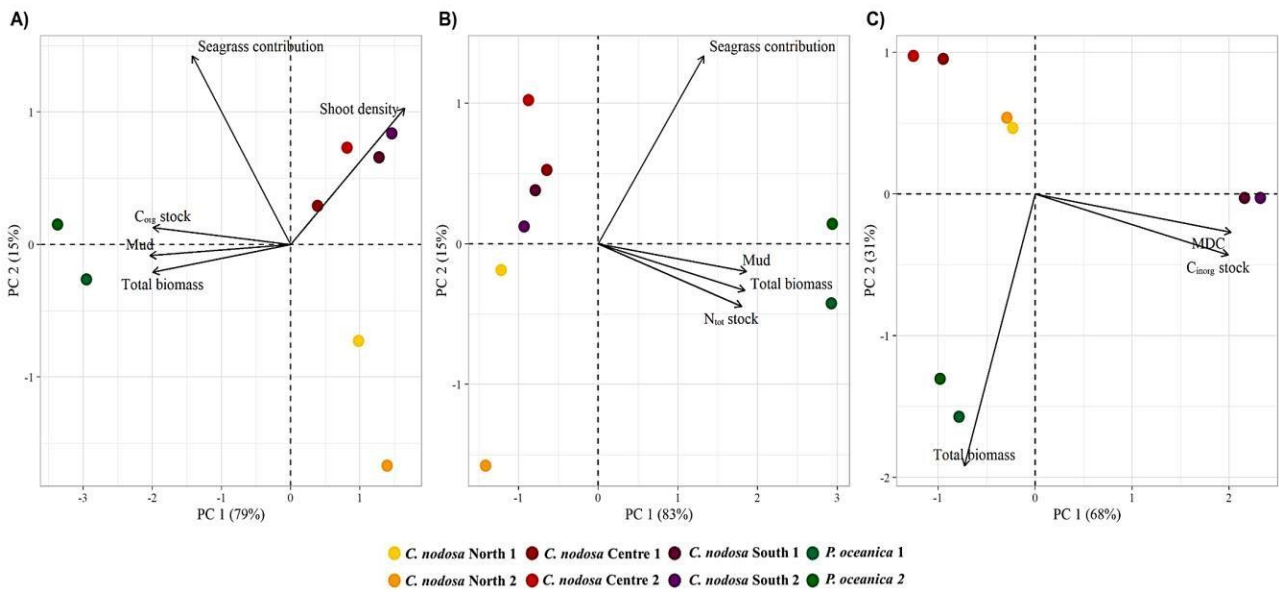


Fig. 6 Biplot of Principal component analysis among variables significantly associated with  $C_{org}$  stock (A),  $N_{tot}$  stock (B) and  $C_{inorg}$  stock (C).

## Discussion

Our data analysis revealed that *C. nodosa* sediments are a significant sink for organic carbon and total nitrogen, as shown by comparison with the unvegetated sediment, although the highest stocks were observed in *P. oceanica*. Seagrass traits, such as total biomass, explain a large part of the variability in organic carbon and nitrogen stocks. The accumulation of organic carbon and nitrogen appeared to be increased in meadows that occupy less exposed areas, where sediment erosion and export of seagrass detritus are limited, while fine sediment accumulation is promoted. More exposed areas, on the other hand, promote large inorganic carbon sequestration, suggesting that inorganic carbon in seagrass ecosystems comes mainly from allochthonous sources. These results show how important it is to consider both the characteristics of seagrasses and their environment when evaluating the functionality of these ecosystems and to understand which areas are crucial as carbon and nitrogen sinks. As reported elsewhere (Miyajima et al., 2017; Serrano et al., 2016; Mazarrasa et al., 2021), both *C. nodosa* and *P. oceanica* meadows in this study had higher stocks than the adjacent unvegetated sediment. Organic carbon and nitrogen stocks of *C. nodosa* were higher than those reported in other studies in Greece, Cyprus, and Spain (21-72 Mg C<sub>org</sub> ha<sup>-1</sup> in the upper 1 meter; 0.3 ± 0.1 kg m<sup>-2</sup> C<sub>org</sub> in the upper 10 cm; 3-9 Mg N<sub>tot</sub> ha<sup>-1</sup>; Apostolaki et al., 2019; de los Santos et al., 2022; Wesselmann et al., 2021). Compared to other species of the same genus, organic carbon stocks of *C. nodosa* in our study were in the range of those reported for *C. rotundata* (95-300 Mg C<sub>org</sub> ha<sup>-1</sup> in the upper 1 m; 3 kg m<sup>-2</sup> in the upper 50 cm; Gullström et al., 2018, Juma et al., 2020) and within the range of values reported for *C. serrulada* (10 ± 20 Mg C<sub>org</sub> ha<sup>-1</sup> in the upper 1 m; 110 ± 50 Mg C<sub>org</sub> ha<sup>-1</sup> in the upper 50 cm; 3 kg m<sup>-2</sup> in the upper 50 cm; Juma et al., 2020; Gullström et al., 2018; Omollo et al., 2022). Overall, inorganic carbon stocks in *C. nodosa* meadows were lower than those reported in the literature for *Cymodocea* species (771 Mg C<sub>inorg</sub> ha<sup>-1</sup>, 760 Mg C<sub>inorg</sub> ha<sup>-1</sup>, in the upper 1 m, 10 kg C<sub>inorg</sub> m<sup>-2</sup> in the upper 50 cm, Apostolaki 2019; Mazarrasa et al., 2015, Gullstrom et al., 2018), especially for *C. nodosa* North and *C. nodosa* Centre. The organic carbon stock at *P. oceanica* was within the range of previous studies (47–755 Mg C<sub>org</sub> ha<sup>-1</sup>; in the upper 1 m; Romero et al., 1994; Serrano et al., 2014; Monnier et al., 2022, Mazzarasa et al., 2015). The total nitrogen stock of *P. oceanica* was higher than the values reported for Greece and eastern Sicily (3 Mg N<sub>tot</sub> ha<sup>-1</sup> in the upper 1 m, Apostolaki et al., 2019, 2022). The inorganic carbon stock of *P. oceanica* from our results appeared to be higher than previously reported values (3-580 Mg C<sub>inorg</sub> ha<sup>-1</sup> in the upper 1 m; Mazzarasa et al., 2015, Monnier et al., 2022; Apostolaki et al., 2019, 2022). Organic carbon and total nitrogen accumulation rates in *C. nodosa* South were within the range reported in the literature (4 to 44 g C<sub>org</sub> m<sup>-2</sup> y<sup>-1</sup>; 0.99 to 5 g N<sub>tot</sub> m<sup>-2</sup> y<sup>-1</sup> Duarte et al., 2013, Apostolaki et al., 2019; de los Santos et

al., 2022), while inorganic carbon accumulation rates were lower than previously reported results (281 g C<sub>inorg</sub> m<sup>-2</sup> y<sup>-1</sup>, Apostolaky et al., 2019). The element accumulation rate in *P. oceanica* was within the range of previous studies (6-198 g C<sub>org</sub> m<sup>-2</sup> y<sup>-1</sup>; 0.99-13 g N<sub>tot</sub> m<sup>-2</sup> y<sup>-1</sup>; 47-1147 g C<sub>inorg</sub> m<sup>-2</sup> y<sup>-1</sup>, Romero et al. 1994; Pedersen et al., 1997; Gacia et al., 2002; Barrón et al., 2006; Serrano et al., 2014; Apostolaki et al., 2022).

As highlighted in other studies (Dahl et al., 2016; Kindeberg et al., 2018; Mazarrasa et al., 2021) mud content is a strong predictor of organic carbon stocks. Indeed, sediments with an elevated content of fine fractions have a larger specific surface area that can favour organic matter sorption to the sediment matrix (Bergamaschi et al., 1997; Thabit et al., 2023). Furthermore, a greater proportion of mud reduces pore water exchange and oxygen diffusion, favouring the establishment of anoxic conditions, limiting the rate of bacterial decomposition and, therefore, supporting organic matter preservation (Serrano et al., 2016). The amount of organic carbon in the sediment is also influenced by the balance between the rate of burial and remineralization of these elements (Macreadie et al., 2014; Martins et al., 2022), which depends on a variety of biotic and abiotic factors that include the quality of the organic material stored. Allochthonous organic carbon sources such as macroalgae, microalgae, and POM represent labile organic sources, while seagrass tissue represents recalcitrant material (Mazarrasa et al., 2018, Kaal et al., 2018). The recalcitrant plant tissues and detritus produced could lead to a slower microbial activity and thus, slower remineralization processes, particularly in a shallow, enclosed and muddy environment, where hypoxic conditions are likely to be established (Costa et al. 2019).

The distribution of carbon sources is influenced both by the biological characteristics of seagrass species (Mazarrasa et al., 2021), as large species have a higher contribution from seagrass detritus, and by the geomorphological setting, as low hydrodynamics and exposure reduce the input of organic matter from nearby allochthonous sources (Leiva-Dueñas et al., 2023).

The difference in total biomass between our stations is species-specific, and the associated difference in stocks is expected, as *P. oceanica* is already known to be the most effective species in fixing and storing carbon and nutrients due to its highest primary production and ability to form mattes (Forqurean 2012; Pergent-Martini 2021). The greater is the aboveground biomass the higher is the capacity to filter out particles from the water column and store them in sediment (Hendriks et al., 2008). In addition, higher below-ground biomass contributes to carbon storage, as below-ground tissues are characterized by a high content of decay-resistant lignin, which slows down the degradation processes of organic matter (Trevathan-Tackett et al., 2017). Furthermore, these tissues

grow directly into the sediment pool, which means a direct input of organic matter into the sediment (H. Kennedy et al., 2022).

The same factors that have a positive effect on the storage of organic carbon are responsible for the burial and preservation of nitrogen in sediments. The correlation between mud and nitrogen content has also been shown in other studies (Kinderberg et al., 2018; Casal-Porrás et al., 2022; Leiva-Dueñas et al., 2023), as well as the relationship between recalcitrant tissue and nitrogen content (Leiva-Duenas et al., 2023) or between nitrogen burial and net primary production, which reflects the autochthonous organic matter produced by the seagrass community (Eyre et al., 2016).

Notwithstanding the decline of *P. oceanica* meadows in the studied basin, highlighted in previous studies, the chronostratigraphy of the organic carbon and nitrogen content from *P. oceanica* sediments is coherent during the last century. Recently, it has been shown that loss of seagrass cover alone does not necessarily lead to changes in sediment organic carbon, while significant erosion occurs in association with high hydrodynamics (Salinas et al., 2020). In shallow environments characterized by low hydrodynamics, continuous sediment accumulation can occur in the absence of mechanical damage such as moorings, even when the mat is dead (Apostolaki et al., 2022). In the basin studied, the potential loss of organic carbon and nitrogen after *P. oceanica* regression must have been limited by the low hydrodynamics and exposure associated with the *P. oceanica* canopy, which also resulted in the highest deposition of mud and autochthonous material in its sediment. The slight change in the organic carbon content in *C. nodosa* Centre may be considered within the natural temporal variability of seagrass sediments (Hilary Kennedy et al., 2010). However, the *C. nodosa* meadows in the centre of the Stagnone di Marsala basin are exposed to the same environmental stresses that cause the decline of *P. oceanica*, such as the extreme salinity of the water and the temperatures reached in summer. Although *C. nodosa* is a seagrass species that can tolerate salinity fluctuations better than *P. oceanica*, a significant change in the photosynthetic physiology of *C. nodosa* and a marked reduction in carbon assimilation under hypersaline stress were observed (Piro et al., 2015; Fernández-Torquemada & Sánchez-Lizaso, 2011). Despite the role of *C. nodosa* meadows as carbon and nutrient sinks, and despite the lack of apparent loss of organic carbon due to the decline of *P. oceanica*, further increases in global temperatures could exacerbate the consequences of the confinement characteristic of the basin under study, leading to higher evaporation rates, temperatures, and salinities. In this scenario, the ability of *C. nodosa* to store elements and protect sediment stocks previously accumulated by *P. oceanica* could also be threatened, at least in the central parts of the basin.

In the southern station, the simultaneous increase in organic carbon and total nitrogen content in the upper sediment and the decrease in dry bulk density indicate a decrease in organic matter degradation processes in this area. In fact, bulk density is one of the factors influencing the oxygen concentration in the sediment and thus the microbial degradation rates of organic matter, with lower bulk density being associated with lower oxygen concentration and high organic carbon content (Avnimelech et al., 2001; Dahl et al., 2016; Ward & Joyce, 2020). The northern sector covered by *C. nodosa* has experienced a past increase in sediment uplift processes, leading to a decrease in water exchange with the open sea and a decrease in hydrodynamics (de Marchis et al., 2012), which could be related to the decrease in inorganic carbon content found in this sector. The low particle transport in the inner parts of the basin, which has decreased over time, could explain the very low inorganic carbon content in the sediment of the inner *C. nodosa* meadows. Conversely, the high particle transport that characterizes the southern part of the basin could enhance the input of allochthonous inorganic carbon, explaining the higher carbonate content in the southern sediments.

Higher levels of hydrodynamics and water exchange could also provide greater oxygenation of the water column, allowing the proliferation of a larger community of calcifying benthic organisms that, generally, characterize seagrass meadow fauna and promote the deposition of  $\text{CaCO}_3$  (van der Heide et al. 2012; Mazarrasa et al., 2015). The spread of calcifying benthic communities may instead be limited in the innermost stations because these communities are sensitive to hypoxia (Gray et al., 1992). As our results also show, the amount of inorganic carbon buried in the sediments may depend on seagrass biomass due to the afore-mentioned ability to intercept particles from the water column resulting from thicker leaf coverage. Furthermore, seagrass allow the precipitation of  $\text{CaCO}_3$  because their photosynthetic use of  $\text{CO}_2$  alters the pH of the surrounding water (Enríguez & Schubert, 2014) and increases the availability of dissolved carbonate ions, which promotes calcification (Hendriks et al., 2015). Higher pH leads to higher levels of  $\text{CO}_3^{2-}$  in seawater, which is important for calcifying organisms to form vital calcium carbonate structures. Instead, seawater acidification poses a limit and a threat to calcifying marine organisms. pH variation has been linked to biomass levels and plant species (Buapet et al., 2013), with meadows characterized by higher biomass leading to higher pH during the most active hours, which may partially explain why total seagrass biomass is positively associated with inorganic carbon stocks in our study.

Similar inorganic carbon stocks between *P. oceanica* and *C. nodosa* South, but different values of inorganic carbon stocks between stations covered by *C. nodosa*, however, suggest that inorganic carbon accumulation is not exclusively from calcification within the meadow and is not strictly related to the species, as environmental factors and geomorphological features may play an important role in favouring carbonate precipitation and accumulation from allochthonous sources.

## **Conclusion**

This study expands our knowledge of the factors that determine the extent and variability of organic carbon, nitrogen, and inorganic carbon storage in seagrass systems.

Accurate knowledge of what factors positively or negatively affect the ability of coastal vegetation to store carbon and nutrients can help manage restoration and protection projects.

The result also confirms the overall high capacity of coastal basins to store organic carbon and nutrients and the need of conservation actions to protect and foster these natural carbon sinks.

## Chapter 2

### Microplastic pollution in seagrass ecosystems from a coastal marine area in the western Mediterranean Sea

#### Abstract

Microplastic (MPs) pollution is widespread in the marine environment and poses a new threat to marine life. The aim of this study was to determine the environmental factors that influence the composition, abundance and distribution of MPs in marine sediment and seawater samples and to investigate how the resulting distribution affects the uptake of microplastics by fish. Sediment, water and fish samples were collected in a semi-enclosed coastal basin in the western Mediterranean Sea (the Stagnone di Marsala, Italy), in sectors characterised by different hydrodynamics and exposure to the open sea. MPs were found in the sediment ( $58 \pm 35$  MPs  $\text{kg}^{-1}$ ) in the water ( $30 \pm 186$  MPs  $\text{m}^{-3}$ ), in all resident fish species (*Aphanius fasciatus*, *Atherina boyeri*, *Syngnathus abaster*;  $0.16 \pm 0.07$  MPs/ind.;  $0.20 \pm 0.11$  MPs/ind.;  $0.16 \pm 0.08$  MPs/ind, respectively) and in both transient species studied (*Diplodus annularis*, *D. vulgaris*; 0.2 MPs/ind and 0.4MPs/ind, respectively). In total 21 MPs were found in 20 of the 106 fish analysed (19%).  $\mu$ -FTIR analysis allowed to identify the following polymers: acrylic, acrylic resin, PE, PET, polyester, PP, PU PVC, nylon, rayon. The abundance of MPs in the sediment was two orders of magnitude higher than the abundance of MPs in the water. Pearson correlation analysis revealed a significant correlation between the abundance of MPs in the water column and the number of microplastics ingested by resident fish species. A negative correlation was found between hydrodynamics and the number of MPs ingested by the fish. No significant difference was found in Fulton's condition factor between individuals of the same species that had and had not ingested MPs. No correlation was found between fish species trophic position and the number of MPs ingested. Significantly narrower  $\delta^{13}\text{C}$  and  $\delta^{15}\text{N}$  range were observed in *A. boyeri*, *A. fasciatus* and *Diplodus spp.* individuals that ingested MPs. This is one of the first studies to use a holistic approach, considering both environmental parameters and the trophic ecology of the biota, to assess which factors most influence the ingestion of MPs by fish.

#### Keywords

Microplastics, seagrass, marine sediment, marine water, marine vertebrates, Mediterranean Sea



## Highlights

- MPs were found in sediment, water and in all the fish species analysed.
- MPs abundance in seagrass sediment was three orders of magnitude higher than in the water column.
- MPs ingestion by fish was positively related to MPs abundance in the water column, negatively related to hydrodynamics and to water depth.

## Introduction

Among the current emerging issues related to the development of human society, microplastic pollution is of greatest interest and accounts for two-thirds of all articles published between 2020 and 2022 (Zhou et al., 2022). The increasing demand for plastics has led to a continuous annual growth in global production, which has risen from 2 million tons in 1950 to more than 390 million tons in 2021 (Plastic Europe 2022). Globally, 94% of the plastic produced annually ends up in the natural environment (Xu et al., 2020) and between 4.8 and 12.7 million tons have been disposed in the oceans, and it has been predicted that this amount will increase by an order of magnitude by 2025 (Jambeck et al., 2015). Plastics consist of long polymer chains composed of chemical monomers derived from fossil fuels. Since microorganisms that can degrade these chains are not widespread, plastic polymers are highly resistant to biodegradation. Although its lightness and incredibly durable molecular bonds make plastic a desirable material useful for numerous applications, these same properties make it a widespread and persistent threat to human and ecosystem health (Azoulay et al., 2019). After disposal, plastic breaks down into microscopic particles due to UV irradiation, frictional forces, abiotic degradation and photo-oxidation (Gewert et al., 2015; Andrady, 2017), creating what is known as 'secondary microplastics'. Intentionally and industrially produced microplastics are referred to as 'primary microplastics', usually in the form of microbeads added to personal care products or industrial abrasives (Friot & Boucher, 2017), but their presence and impact in the environment is of lesser importance (Duis & Coors, 2016). The presence of MPs in the ocean was first demonstrated by Thompson et al. (2004) and they are now considered a major component of "marine debris" (Cole et al., 2011). MPs have been found in all marine habitats and biota around the world (Cincinelli et al., 2017; Jamieson et al., 2019; Bergmann et al., 2022). The Mediterranean Sea is considered the sixth hotspot in the world for marine litter accumulation due to its semi-enclosed configuration, the collection of water from various rivers and the proliferation of various tourist and industrial activities along the coasts (Lebreton et al., 2012; Cozar et al., 2015). Overall, a large proportion of marine microplastics originates from land-based sources, including beach litter (Andrady, 2011; Khalid et

al., 2021). Recently, coastal vegetated ecosystems, such as seagrass meadows, have been found to be hotspots for microplastic accumulation (Huang et al., 2020). Seagrass meadows are known for slowing down water currents, intercepting and trapping particles and preventing sediments from settling in the water. They act as a sink for organic and inorganic particles, including microplastics (de Smit et al., 2021; Jones et al., 2020; de los Santos et al., 2022). Microplastics have some intrinsic properties, such as density, that can influence their distribution in the water column or their accumulation in marine sediment (Li et al., 2023), and, although much of the plastic is buoyant (Cózar et al., 2014) and should not sink, biofouling has been shown to be a process that alters this behaviour (Halsband, 2022). In addition, vertical currents and circulations are among the most important environmental factors driving the transfer of microplastics to aquatic habitats (Soto-Navarro et al., 2020). Considering and understanding the environmental processes that influence the fate and transport of microplastics in the aquatic environment can be useful for monitoring and pollution management, which is necessary given the proven ecotoxicological damage that microplastics cause to marine life. Indeed, due to the small size of microplastics, ranging from 0.01 mm to 5 mm (Frias et al., 2018), these particles are of particular concern to the marine environment as they can be similar in size to prey or particles that marine organisms feed on. Their toxic effects on marine organisms, from invertebrates to fish, marine mammals and turtles, have been reported by several authors (Barboza et al., 2018; Messinetti et al., 2018; Di Renzo et al., 2021; Fossi et al., 2012) and include oxidative stress (Pérez-Albaladejo et al., 2020), endocrine disruption (Rochman et al., 2014), liver stress (Rainieri et al., 2018), cell necrosis (Zhang et al., 2023) and metabolic changes (Gardon et al., 2018). In addition, ingestion of microplastics can cause physical injuries such as intestinal perforation, ulcer formation and blockage of the digestive tract (Ahrendt et al., 2020; Kim et al., 2022). Additives such as phthalates, colorants and flame retardants, which are usually added to plastics during manufacturing, as well as PAHs or other hydrophobic organic pollutants and metals that are sorbed to the surface of plastics once they enter the aquatic environment, pose an additional threat to marine organisms (Hermabessiere et al., 2017; Zhang et al., 2022). It has been shown that mussels ingest microplastics to a greater extent when the amount of microplastics in the environment is higher (Qu et al., 2018), while this relationship has not always been proven for fish (McNeish et al., 2018; Agharokh et al., 2022). Some studies have also investigated the relationship between MPs intake and the biological and functional traits of fish, such as body size, feeding strategies and foraging (Covernton et al., 2021; B. Li et al., 2021; Justino et al., 2021). However, the results regarding these relationships and the intake of MPs are controversial and some come to opposite conclusions (Mueller, 2021). Moreover, most of these studies do not use isotopic analysis and do not take into account the diet of the species studied by representing their actual isotopic and trophic niche.

The aims of this study were:

- to evaluate the influence of environmental factors on the composition, abundance and distribution of MPs in coastal areas;
- to investigate how environmental factors and MPs distribution influence their ingestion by fish species;
- to investigate whether the trophic and biological characteristics (trophic position, isotopic niche width, body condition) of the studied species influence the occurrence of MP ingestion.

To this end, we investigated the occurrence and abundance of MPs in water and sediment samples in a semi-enclosed coastal basin in the southwestern Mediterranean Sea (Stagnone di Marsala, Sicily) from different sectors characterized by different hydrodynamics and exposure to the open sea. We investigated the occurrence and abundance of MPs in the gastrointestinal tract of 3 resident fish species (*Aphanius fasciatus*, *Atherina boyeri*, *Syngnathus abaster*) and 2 transient commercial fish species (*Diplodus annularis*, *D. vulgaris*).

## Materials and Methods

### Study area

The study was carried out in the Stagnone di Marsala basin (Fig.1; 37° 52' N; 12° 26'), a semi-enclosed area in the westernmost coast of Sicily (Italy) with a surface area of about 20 km<sup>2</sup>, and an average depth of 1.5 m. The basin is separated from the open sea by a limestone platform (Isola Grande), while two inlets allow water flow within the basin. The Bocca di San Teodoro inlet is located in the northern area, which is about 400 m wide and has an average depth of 0.3-0.4 m, while the Bocca Grande inlet is located in the southern area, which is about 2.9 km wide and has an average depth of 1.5 m. Hydrodynamics is mainly driven by the tides and the wind and differ between the northern, the central and the southern areas within the basin, being higher in the south and reaching its lowest values on the central east coast (Mazzola & Sarà, 1995; La Loggia et al., 2004; de Marchis et al., 2012). The substrate is mainly composed of fine sediments and the whole area is colonised by meadows of *Cymodocea nodosa* (*Ucria*) *Asch.*, which are generally associated with macroalgae, forming a habitat that supports a great diversity of biological communities. *Aphanius fasciatus* Valenciennes 1821 (Cyprinodontidae), *Atherina boyeri* Risso (Atherinidae) and *Syngnathus abaster* Risso (Syngnathidae) are among the main resident fishes, while Sparidae and Mugilidae are the most common transient fishes (Scilipoti, 1998). There are no industrial activities nearby, but the area is urbanised, and tourist infrastructures and recreational activities such as kitesurfing attract tourism to the basin. There is no freshwater supply, although 1.3 km north of the mouth of the Bocca di San

Teodoro the Birgi watercourse flows into the sea, coming from areas characterised by arable farming and the presence of a civil and military airport. The Stagnone di Marsala is included in the list of Sites of Community Importance (Directive 92/43/CEE; ITA010026).



Fig. 1 Map of Stagnone di Marsala. Squares indicate the sampling sites (North, Centre, South). Grey arrows indicate the water flux at the three sampling sites, based on Mazzola & Sarà 1995. The two inlets (Bocca San Teodoro, Bocca Grande) and the Birgi River mouth are showed.

### Field sampling

Sediment, water column and fish samples were collected in summer 2021 at 3 sites characterised by different connectivity to the open sea and different hydrodynamics: North, Centre and South (Fig. 1). The mean water depth was  $20 \pm 8$  cm in the North,  $16 \pm 8$  cm in the Centre and  $33 \pm 11$  cm in the South. The hydrodynamics in these sites was inferred in a previous work by La Loggia et al. (2004), through the intertidal dispersion coefficient (IDC,  $\text{m}^2 \text{s}^{-1}$ ), which allows to describe the water exchange in a given sector. The mean IDC (MDC,) is  $9.7 \text{ m}^2 \text{ s}^{-1}$  in the North,  $7.5 \text{ m}^2 \text{ s}^{-1}$  in the Centre,  $26.9 \text{ m}^2 \text{ s}^{-1}$  in the South. At each sampling site, seagrasses and macroalgae were collected in three random replicates, using a  $20 \times 20$  cm quadrat, to estimate the biomass of submerged vegetation. At

each site 3 cores (10 cm Ø) of the first 5 cm of sediment were collected randomly and stored in 1 L glass jars. 18 L of water were sampled from each site, using 1 L glass bottles. Resident fish (*Aphanius fasciatus*, *Atherina boyeri*, *Syngnathus abaster*) were captured with a small trawl-net (length: 3 m; mesh size: 2 mm), promptly euthanized with a solution of clove oil and sea water (0.40 ml/ L) and preserved at -20 °C. In order to collect transient fish species, a fourth sampling site was selected outside the basin, External site, where fish caught by a trawl net were obtained by local fisherman, and preserved at -20°C prior to processing.

### **Samples processing, digestion, and MPs extraction**

To remove organic components, the sediment samples were treated with a 20% H<sub>2</sub>O<sub>2</sub> solution for one week, then rinsed several times with ultrapure water (Milli-Q ®), filtered through a metal strainer (63 µm), dried at 60°C for 5 days and weighed. Then, two subsamples of 50 g from each replicate of sediment were used to extract MPs, following two different methods of density separation. Each subsample was firstly sieved using a 1 mm mesh and examined under microscope to visualize the coarser debris. Then, the remaining sediment fractions (< 1 mm) were added to a 500 mL solution, respectively of ZnCl<sub>2</sub> and NaCl, stirred with a magnetic stir for 20 min and allowed to stand for 24 h. The ZnCl<sub>2</sub> (1.5 g cm<sup>-3</sup>) solution was previously prepared by adding 972 g of ZnCl<sub>2</sub> to 1 L of ultrapure water, while the NaCl (1.2 g cm<sup>-3</sup>) solution was previously prepared by adding 337 g of salt to 1 L of ultrapure water (Coppock et al., 2017).

Water samples were filtered by a vacuum pump system using GF/F filters of 0.7 µm (pores size).

Fish were identified to the species level and each species was assigned to habitat and trophic habit categories according to the literature (Tab. 2). Key biometric data were recorded for each specimen: total length (cm), standard length (cm) and total weight (g). The gastrointestinal tract was removed from the oesophagus to the end of the intestine, digested with a 10% KOH solution to allow extraction of the MP particles (Tsangaris et al., 2021) and filtered with a vacuum pump system using cellulose nitrate filters with a pore size of 0.8 µm.

### **Debris visual sorting**

Filters with material extracted from the sediment, water and fish samples were examined using a Leica MZ 16A stereomicroscope connected to a camera. The Leica Application Suite (V4.5.0) was used to take photos and measure all identified particles. Visual identification to detect debris that could be MPs was performed according to the criteria described by Hidalgo-ruz et al. (2012): no

cellular or organic structures should be visible; the fibres should be equally thick; particles should have a homogeneous colour.

The debris particles were classified by colour (transparent, white, yellow, orange, red, pink, green, blue, grey, brown, black, other colour), size (0.02-0.1, 0.1-0.3, 0.3-0.5, 0.5-1, 1-2.5, 2.5-5, 5-25 mm) and shape (fibre, fragment, film, pellet, rope and filament, foam) following Frias et al. (2018). Although monitoring programmes (Frias & Nash, 2019) have reported 100  $\mu\text{m}$  as the lower size limit, due to the small size of the fish species treated in this study, 20  $\mu\text{m}$  was set as the size limit for the qualification and quantification of debris particles. The isolated debris particles were placed in Eppendorf tubes containing ultrapure water and filtered with a vacuum pump system on silica filters to allow  $\mu\text{-FTIR}$  characterization of the polymers. Despite the accuracy or experience of the operator, a certain percentage of the debris particles is lost at this stage, whether due to handling with tweezers, or the fact that particles stick to the glasses and not every step can be performed under the microscope. However, around 65% of particles were successfully recovered for  $\mu\text{-FTIR}$  analysis.

Silica filters were analysed at the Department of physical science, earth and environment of the University of Siena with, the  $\mu\text{-FTIR}$  Nicolet™ iN™ 10 (Thermo Fisher Scientific) in transmittance mode and, when the particles were not sufficiently thin, in reflectance mode and visualized with the imaging section of the Omnic™ Picta™ software. Spectra were compared to a database of reference spectra to establish a list of potential polymer correspondences. Only spectra having more than 70% similarity with the reference spectra were accepted.

### **Quality assurance and quality control**

Measures were taken to minimize contamination of the samples during field collection: the equipment used to store the sediment samples was previously rinsed with ultrapure water and covered; only glass containers and metal tools were used. To minimize contamination of samples during laboratory work, all surfaces used were cleaned before any work was performed; equipment and glassware were rinsed with distilled water; synthetic cloths were avoided, and a 100% cotton lab coat was used; plastic tools were avoided and glass and metal instruments were preferred; the presence of other staff in the room was minimized. A blank sample was taken every three fish samples. A petri dish with a filter was placed at the laboratory workstation to monitor air contamination during fish analysis. For sediment samples analysis, the salt solutions used to extract MPs from the sediment were filtered through 0.8  $\mu\text{m}$  filters before density separation. Three blanks were carried out by filtration of the NaCl solution and three blanks filtering the ZnCl<sub>2</sub> solution. A petri dish with a filter was placed at the laboratory

workstation to monitor air contamination during sediment analysis. For water samples analysis, a filter to evaluate airborne contamination was placed near the workstation for each working day and 1 L of ultrapure water (Milli-Q ®) was filtered for each working day as blank. The analysis of all the blanks and filters for air contamination was carried out at the same time as that of the samples. In case of contamination of blank samples or filters for air contamination, the same typology of microplastics, according to shape, color, size and type of polymer was removed from the results.

### **Stable isotopes analysis**

To determine the isotopic niche of the studied species, the dorsal muscle of each specimen was removed with scalpel and tweezers, freeze-dried and pulverised with a micro-mill. 1 mg of each sample was weighed into tin capsules (5 x 9 mm) and analysed for  $\delta^{13}\text{C}$  and  $\delta^{15}\text{N}$  using an isotope ratio mass spectrometer (Thermo Delta IRMS Plus XP) coupled to an elemental analyzer (Thermo Flash EA1112). The stable isotope ratios of carbon and nitrogen were expressed in  $\delta$ -unit notation as follows:  $\delta X = [(R_{\text{sample}}/R_{\text{standard}}) - 1] \times 10^3$ , where the  $\delta$  notation indicates the deviation from the international reference standards (Pee Dee Belemnite for carbon and atmospheric  $\text{N}_2$  for nitrogen), X stands for  $^{13}\text{C}$  or  $^{15}\text{N}$ , and R is the relative  $^{13}\text{C}/^{12}\text{C}$  or  $^{15}\text{N}/^{14}\text{N}$  ratio. The analytical precision of the measurement was based on the standard deviation of replicates of internal standards (International Atomic Energy Agency IAEA-CH-6 for  $\delta^{13}\text{C}$  and IAEA-NO-3 for  $\delta^{15}\text{N}$ ) and amounted to 0.1‰ for  $\delta^{13}\text{C}$  and 0.2‰ for  $\delta^{15}\text{N}$ , respectively.

### **Calculation and data analysis**

For each species, the results were expressed as frequency of occurrence (%), percentage of individuals examined with ingested plastic items, number of ingested particles per individual for each species. The MPs found in water samples were quantified and compared as number of MPs per litre of water and then converted into MPs per  $\text{m}^{-3}$  to allow comparison with the literature. MPs found in sediment samples were quantified as number of MPs per 50 g dry sediment and then expressed as number of MPs per kg. Conversion to MPs per L was performed to allow comparison with MPs abundance in water samples.

The data were tested for normality using the Shapiro-Wilk test. The chi-square test was used to test for significant differences in the occurrence of MPs characterised by shape, size, colour and material in sediment, water and fish samples between North, Central and South. The Kruskal-Wallis test was

used to determine significant differences in the abundance of microplastics in sediment between sampling site and in water between sampling sites. In addition, the Kruskal-wallis test was also used to test for significant difference in the abundance of microplastics between sediment and water samples. Trophic positions (TP) of fish species were estimated at individual level following (Post, 2002) equation:  $TP_f = [(\delta^{15}N_f - \delta^{15}N_b)/\Delta_n] + \lambda$ .  $\delta^{15}N_f$  and  $\delta^{15}N_b$  are the nitrogen isotopic signatures for the fish and the reference baseline, respectively,  $\Delta_n$  is the trophic enrichment assumed for each trophic level (3.4 ‰, according to Post et al., 2002) and  $\lambda$  is the baseline's trophic position, which is 2 for zooplankton. The mean  $\delta^{15}N$  of zooplankton collected in the Stagnone di Marsala basin (6.5 ‰ (Andolina et al., 2022) was used as baseline for *A. boyeri*, *A. fasciatus*, *S. abaster*. The mean  $\delta^{15}N$  signature of zooplankton collected in the nearby islands of Favignana and Levanzo (3.3 ‰, Vizzini & Mazzola, 2009) was used as baseline for *D. annularis* and *D. vulgaris*.

The relationship between fish trophic position and MPs abundance (items/individual) was evaluated through Pearson correlation analysis, using the fish trophic position as independent variable and abundance in each species as dependent variable.

The trophic niche characteristics of fish that had and had not ingested MPs were calculated for each species using Layman isotopic metrics (Layman & Post, 2008):  $\delta^{13}C$  range (CR),  $\delta^{15}N$  range (NR), mean Distance to Centroid (CD), mean Nearest Neighbour distance (NND) and its Standard Deviation (SDNND). Layman metrics were bootstrapped ( $n = 1000$ ) and their mode was reported along with the 95% credible interval (Jackson et al., 2011, 2012). The corrected standard ellipse area (SEAc) and the Bayesian standard ellipse area (SEAb), used to describe the isotopic niche width (Jackson et al., 2011), were also calculated. Differences in the SEAb and the bootstrapped Layman metrics between groups with and without ingested MPs was tested using a probability test (Jackson et al., 2011).

Fulton's condition factor (K) was calculated using the following equation:  $K = W * 100 * l^{-3}$ , where W is the total weight of the fish (g), l is the standard length (cm) and 100 is a factor used to bring the value close to unity (Fulton, 1904). Differences in Fulton's condition factor between individuals that had and had not ingested MPs were tested for each species through Wilcoxon-Mann-Whitney test.

Pearson correlation analysis was used to determine significant correlation between environmental and biological factors and the abundance of microplastics ingested by fish. The following variables were used as explanatory: mean dispersion coefficient (MDC,  $m^2 s^{-1}$ ), seagrass biomass ( $g m^{-2}$ ), macroalgae biomass ( $g m^{-2}$ ), MPs abundance in water (n MPs/L), MPs abundance in sediment (n MPs/Kg), fish trophic position, fish Fulton's factor and fish  $\delta^{13}C$  (‰). The response variable was the number of MPs



ingested by the different species in the North, Centre and South. Due to the small sample size of the data set, statistical significance was accepted at the 0.1 alpha level.

All the analyses were carried out using R (v.4.1.2). Both SEA and Layman metrics were calculated using the SIBER package (Stable Isotope Bayesian Ellipses in R) (Jackson et al., 2011).

## Results

### Habitats characteristics

The three areas studied are characterised by the presence of *C. nodosa* meadows associated with macroalgae, such as *Caulerpa prolifera*, which was detected at each sampling site, and *Laurencia* spp. in the Centre and South (Tab.1). The northern area had the lowest *C. nodosa* ( $24.2 \pm 18 \text{ g m}^{-2}$ ) and *C. prolifera* ( $5.7 \pm 10.0 \text{ g m}^{-2}$ ) biomass, largely characterised by bare sediment. In the Centre, higher *C. nodosa* biomass ( $123.6 \pm 129.2 \text{ g m}^{-2}$ ) was found in association with *C. prolifera* ( $91.6 \pm 107.5$ ) and *Laurencia* spp. ( $11.9 \pm 20.6 \text{ g m}^{-2}$ ). Rather low *C. nodosa* biomass values ( $33.3 \pm 38.4 \text{ g m}^{-2}$ ) were found in the South, with a high presence of *Laurencia* spp. ( $68.7 \pm 56.5 \text{ g m}^{-2}$ ) and *C. prolifera* ( $62.8 \pm 68.7 \text{ g m}^{-2}$ ).

Tab.1 List of the seagrass and algae species recorded in the sites examined with biomass data ( $\text{g m}^{-2}$ ).

		Sampling site		
		North	Centre	South
Seagrass biomass ( $\text{g m}^{-2}$ )				
<i>Cymodocea nodosa</i>	Mean	24.2	123.6	33.3
	STDEV	18	129.2	38.4
Macroalgae ( $\text{g m}^{-2}$ )				
<i>Caulerpa prolifera</i>	Mean	5.75	91.6	62.8
	STDEV	9.96	107.5	68.7
<i>Laurencia</i> spp.	Mean	-	11.9	68.7
	STDEV	-	20.6	56.5

### Contamination control

The blank filters used in the water analysis were clean. The following fibers were identified by  $\mu$ -FTIR in the filters used to control air contamination: 1 red acrylic, 1 red rayon, 3 black rayon, 7 black

cellulose, 1 blue cellulose, 5 black cotton. Black and red rayon fibers were also found in water samples and removed from the count. No red acrylic fibers were found in water samples.

Five black cotton fibers and 1 black wool fiber were identified by  $\mu$ -FTIR in the blanks for sediment analysis. The filters used to control air contamination during sediment analysis were clean.

The following fibers from the blank samples used in the analysis of *A. boyeri*'s guts were identified by  $\mu$ -FTIR: 11 celluloses, 3 cotton fibers, 1 mineral fiber, 1 transparent PET, and 1 black rayon fiber. Rayon fibers were also found in *A. boyeri* and removed from the count. 3 black cotton fibers, 3 black cellulose fibers, 1 black wool fiber and 1 black rayon fiber were found in *S. abaster* blanks. Rayon fibers were also found in *S. abaster* and removed from the count. For the samples of *A. fasciatus* and *Diplodus* spp. no black rayon contamination was found in the corresponding blanks. 1 black acrylic fiber was found in the blanks analyzed for *Diplodus* spp. and since this was also found in the gut of *Diplodus* spp. black acrylic fibers were removed from the count. Filter for air contamination were clean.

### **MPs abundance and % occurrence in sediment**

After density separation with NaCl and visual sorting, 117 particles of debris were isolated from sediment samples and 69 % of them was recovered for  $\mu$ -FTIR analysis: 19 % of the particles analysed were microplastics, 10 % were semisynthetic items (rayon), 40% were cellulose, 14 % were cotton, 14 % were wool, 2 % were organic and 1 % were mineral. After density separation with ZnCl<sub>2</sub> and visual sorting, 138 particles of debris were isolated and 65% of them was recovered for  $\mu$ -FTIR analysis: 18% of the particles analysed were microplastics, 7% were semisynthetic items (rayon), 44% were cellulose, 20% were cotton, 9 % were wool and 2% were organic. No significant difference was found in the abundance of microplastics extracted from sediments through density separation with NaCl and ZnCl<sub>2</sub> (Tab.2) . MPs abundance in sediment was the following  $40 \pm 18$  MPs kg<sup>-1</sup> d.w. at North,  $72 \pm 50$  MPs kg<sup>-1</sup> at Centre and  $70 \pm 26$  MPs kg<sup>-1</sup> at South (Fig. 2). Although the abundance of microplastics in sediment was higher in the sampling areas (Centre, South) with higher seagrass and macroalgae biomass, among site differences were not significant (chi-squared = 2.5, df = 2, p-value = 0.28). Considering the overall basin, averaged MPs abundance in sediment was  $58 \pm 35$  MPs kg<sup>-1</sup>.

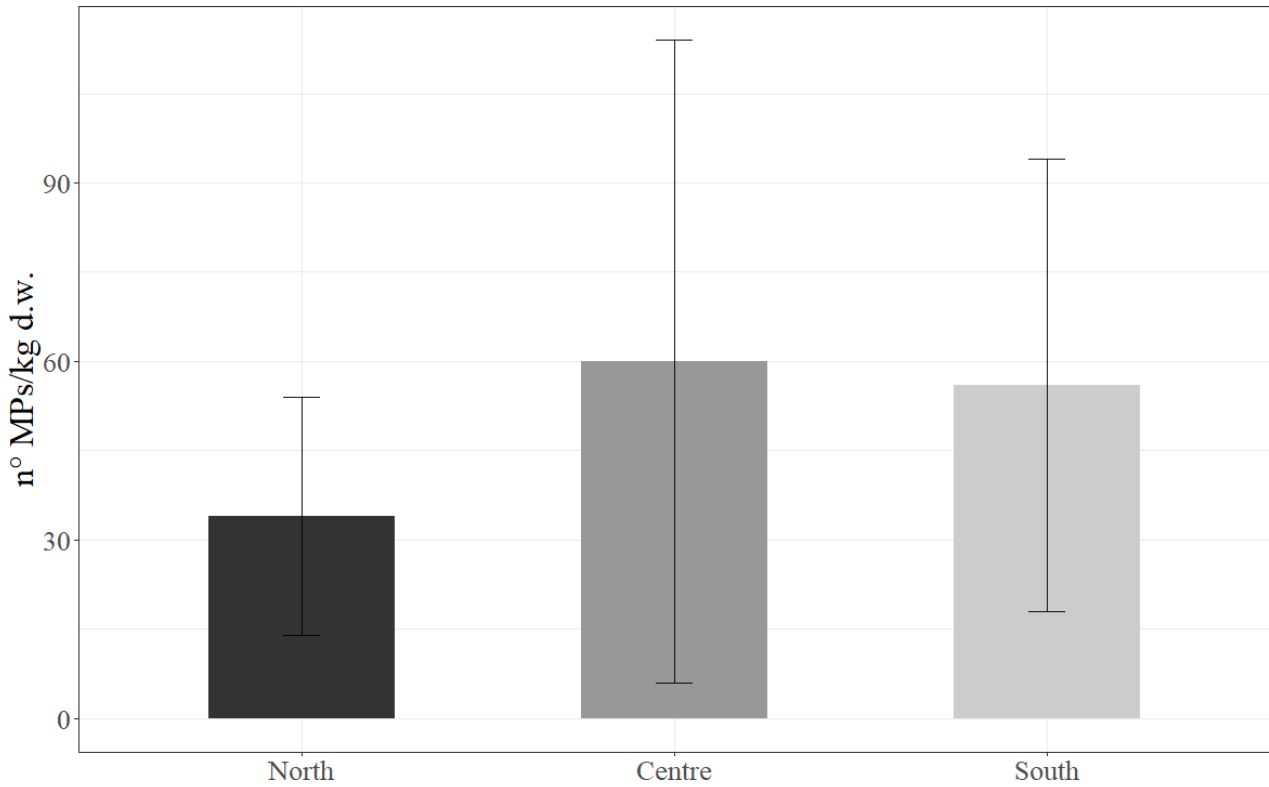


Fig. 2 Mean and STDEV of microplastics and rayon abundance (MPs kg<sup>-1</sup> of dry sediment) per sampling site.

$\mu$ -FTIR analysis on items extracted by NaCl allowed to identify the following polymers (Fig. 3a): rayon (35 %), acrylic (22 %), polyurethane (PU, 17 %), polyester (13 %), polyethylene terephthalato (PET, 9%) and polypropylene (PP, 4%).  $\mu$ -FTIR analysis on items extracted by ZnCl<sub>2</sub> allowed to identify the following polymers (Fig. 3b): rayon (24%), PU (24 %), PET (24 %), PP (14 %), PE (polyethylene, 5 %), PVC (polyvinyl chloride, 5 %), polyester (5%).

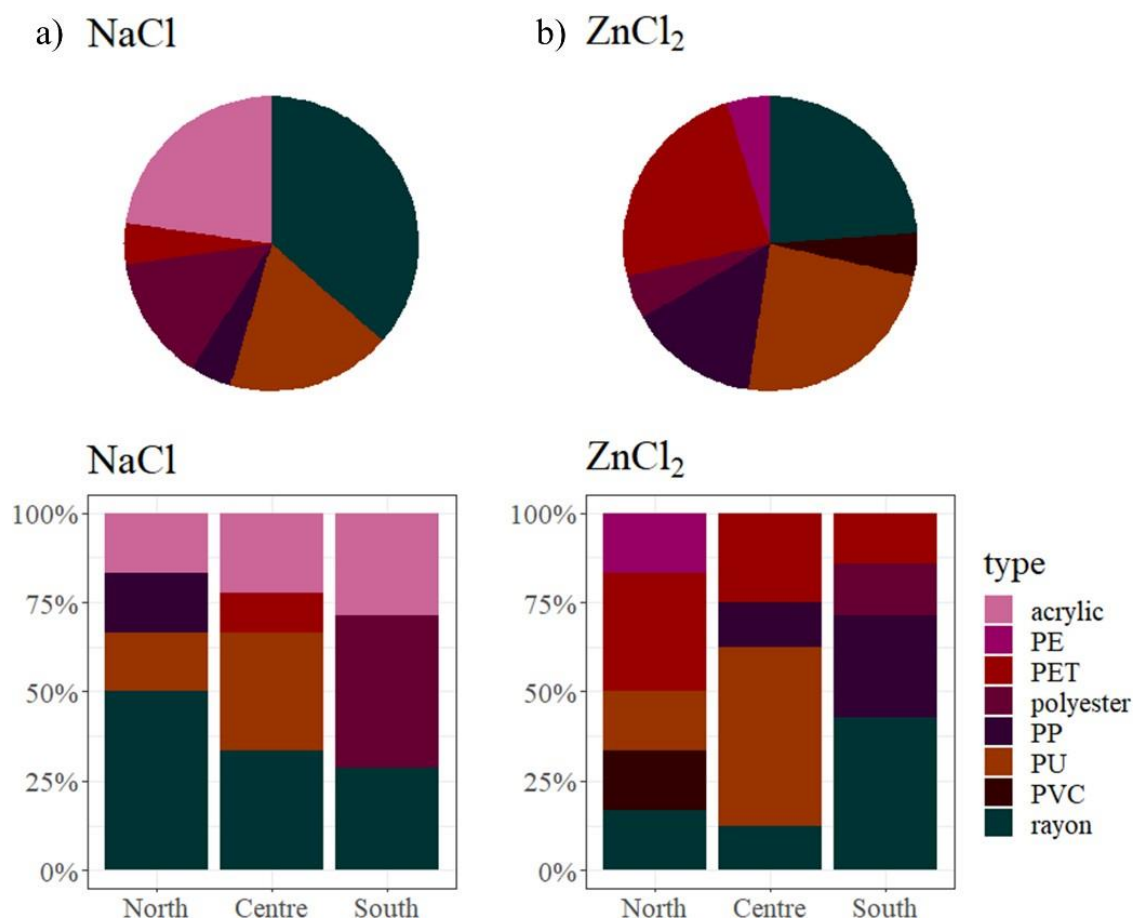


Fig. 3 Polymer composition, revealed by  $\mu$ -FTIR, of the MPs recovered from the sediment samples, through NaCl density separation method (a) and ZnCl<sub>2</sub> density separation method (b) overall and by site.

Overall, the size of the isolated particles (Fig. 4b) ranged from 0.04 to 9.40 mm and, except for only one item, all the particles found were smaller than 5 mm. The most common size classes were 0.5-1 (30%), 0.1-0.3 (30%) and 0.02-0.1 (18 %). Concerning the shape of the particles analysed (Fig. 4c) the only types detected were fibres (57 %), fragments (41 %) and films (2 %). The colours found (Fig. 4) were blue (43%), black (39%), red (11%) and green (7%). The photographs of some polymers with the relative  $\mu$ -FTIR spectra are shown in Fig. 5.

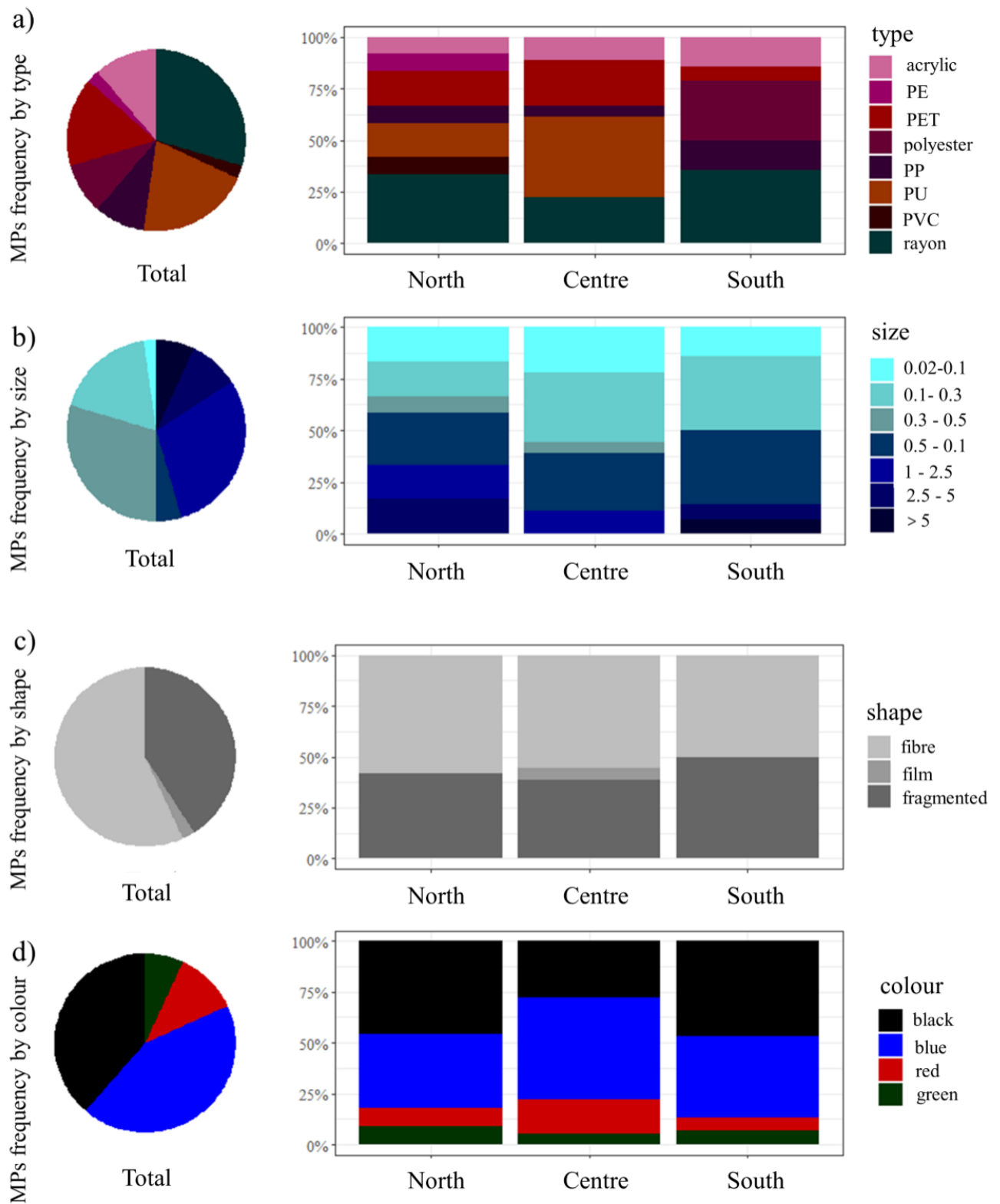
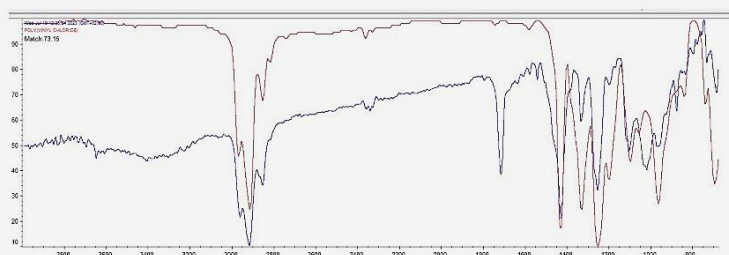
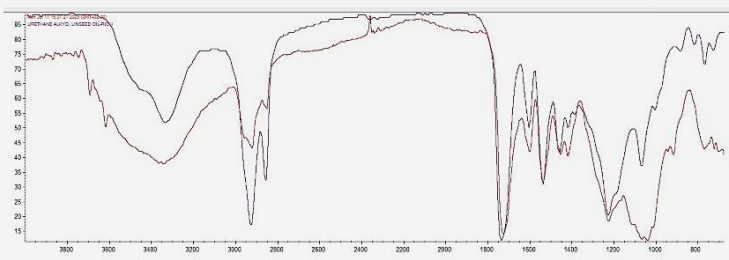
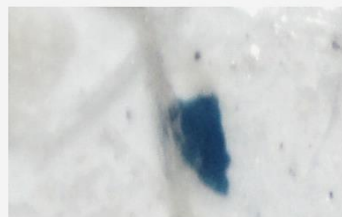


Fig. 4 Type of polymer (a), size range (b), shape (c) and colour (d) of the MPs recovered from the sediment samples, overall and by site.

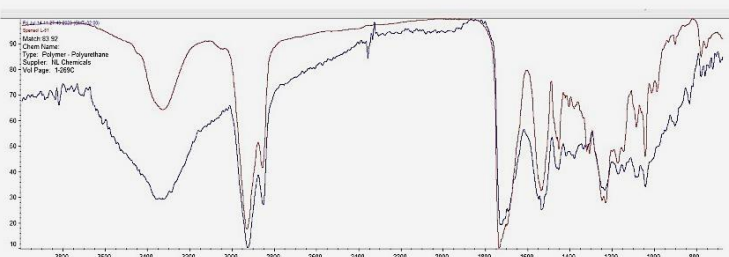
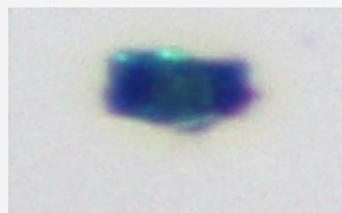
**Polyvinyl chloride (PVC)** Match 74 %  
Range size 0.1 -0.3 mm



**Urethane alkyd (PU)** Match 76 %  
Range size 0.1-0.3 mm



**Spensol L-51 (PU)** Match 84 %  
Range size 0.02 -0.1 mm



**Alkyd resin (Polyester)** Match 81 %  
Range size 0.1 - 0.3 mm



**Polyethylene terephthalate (PET)**  
Match 81 %  
Range size 0.1 -0.3 mm

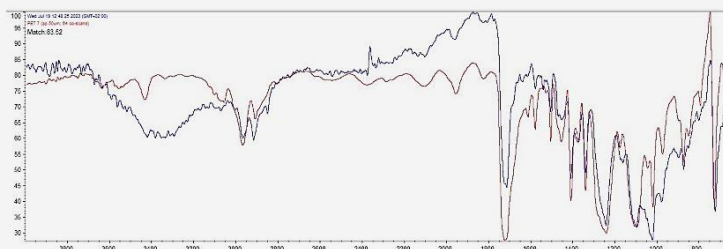


Fig. 5 Examples of polymers identified by  $\mu$ -FTIR in sediment samples and relative spectra.

Chi-squared test (Tab. ) revealed that MPs found in sediment did not differ significantly between the three sampling sites in terms of size, shape and colour, while a significant difference was found in terms of type of material, with PET and PU being more abundant in the Centre and polyester only in the South, indicating different sources of pollution at the three sites.

Tab. 2 Chi-squared test, difference in the abundance of MPs recovered through NaCl and ZnCl<sub>2</sub>; difference in MPs shape, size, colour and material between sampling sites.

	<b>North</b> <i>N=12</i>	<b>Centre</b> <i>N=17</i>	<b>South</b> <i>N=14</i>	<b>p.overall</b>
salt used:				0.982
NaCl	6 (50.0%)	9 (52.9%)	7 (50.0%)	
ZnCl <sub>2</sub>	6 (50.0%)	8 (47.1%)	7 (50.0%)	
shape:				1.000
fibre	7 (58.3%)	9 (52.9%)	8 (57.1%)	
film	0 (0.00%)	1 (5.88%)	0 (0.00%)	
fragment	5 (41.7%)	7 (41.2%)	6 (42.9%)	
size:				0.579
0.02-0.1	2 (16.7%)	4 (23.5%)	2 (14.3%)	
0.1-0.3	2 (16.7%)	6 (35.3%)	5 (35.7%)	
0.3-0.5	1 (8.33%)	0 (0.00%)	0 (0.00%)	
0.5-1	3 (25.0%)	5 (29.4%)	5 (35.7%)	
1-2.5	2 (16.7%)	2 (11.8%)	0 (0.00%)	
2.5-5	2 (16.7%)	0 (0.00%)	1 (7.14%)	
>5	0 (0.00%)	0 (0.00%)	1 (7.14%)	
colour:				0.826
black	5 (41.7%)	4 (23.5%)	7 (50.0%)	
blue	5 (41.7%)	9 (52.9%)	5 (35.7%)	
green	1 (8.33%)	1 (5.88%)	1 (7.14%)	
red	1 (8.33%)	3 (17.6%)	1 (7.14%)	
material:				0.045
acrylic	1 (8.33%)	1 (5.88%)	2 (14.3%)	
PE	1 (8.33%)	0 (0.00%)	0 (0.00%)	
PET	2 (16.7%)	4 (23.5%)	1 (7.14%)	
polyester	0 (0.00%)	0 (0.00%)	4 (28.6%)	
PP	1 (8.33%)	1 (5.88%)	2 (14.3%)	
PU	2 (16.7%)	7 (41.2%)	0 (0.00%)	
PVC	1 (8.33%)	0 (0.00%)	0 (0.00%)	
rayon	4 (33.3%)	4 (23.5%)	5 (35.7%)	

## MPs abundance and % occurrence in water samples

After visual sorting, debris was found in 15 (83%), 10 (55%) and 12 (66%) samples out of the 18 samples collected respectively in North, Centre and South sites.

A total of 115 particles were isolated, 64% of which was successfully recovered for  $\mu$ -FTIR analysis. Considering the particles analysed, 32% were microplastics, 31% were cellulose, 18% were rayon, 11% were organic or mineral items, 8% were cotton. Any rayon black or red fibres were removed from subsequent analyses, as they were found in the filters placed to monitor the airborne, while procedural blanks resulted clean. The highest abundance was recorded in the North ( $0.49 \pm 1.53$  MP L<sup>-1</sup>), followed by the Centre ( $0.35 \pm 0.7$  MP L<sup>-1</sup>) and the South ( $0.12 \pm 0.5$  MP L<sup>-1</sup>) (Fig. 6) and significantly differed between sampling sites (chi-squared=26.963, df=2, p-value = < 0.01). Taking the entire basin into account, an average abundance of  $320 \pm 186$  MP m<sup>-3</sup> was recorded. The following plastic polymers were identified (Fig. 7a): 42 % PP, 25 % alkyd resin, 16 % PET, 4% polyester, 4 % PU, 4 % PVC, 4 % acrylic and 4 % nylon.

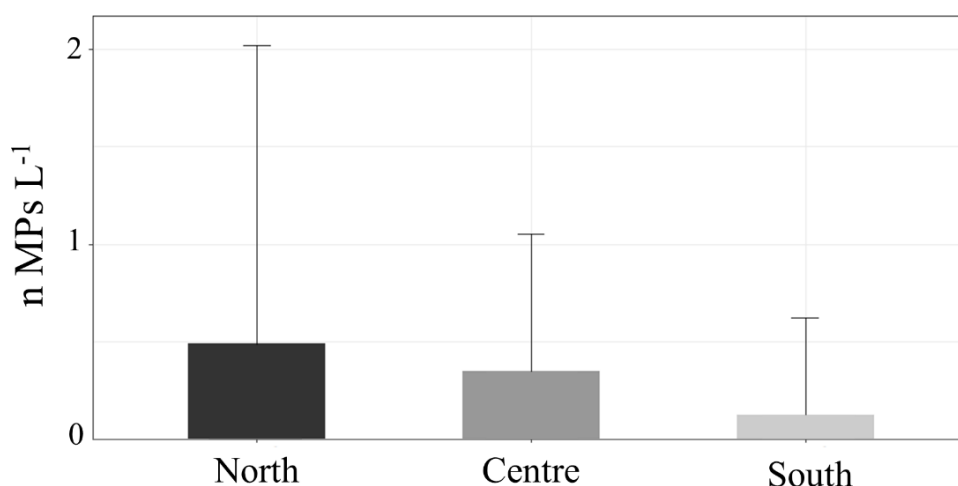


Fig. 6 Mean and STDEV of microplastics abundance in water (MPs L<sup>-1</sup>) per sampling site.

The size of the isolated MP particles ranged from 0.08 mm to 2 mm. The most common size classes (Fig. 7b) were 0.3-0.5 mm (29%), 0.1-0.3 mm (25%), 0.5-1 mm (21%) and 1-2.5 mm (21%). Concerning the shape of the particles analysed (Fig. 7c) the only types detected were fragments (42%), films (37%) and fibres (21%). The colours found (Fig. 7d) were black (72 %), blue (12 %), transparent (12%) and red (4 %). The photographs of some polymers with the relative  $\mu$ -FTIR spectra are shown in Fig. 8.



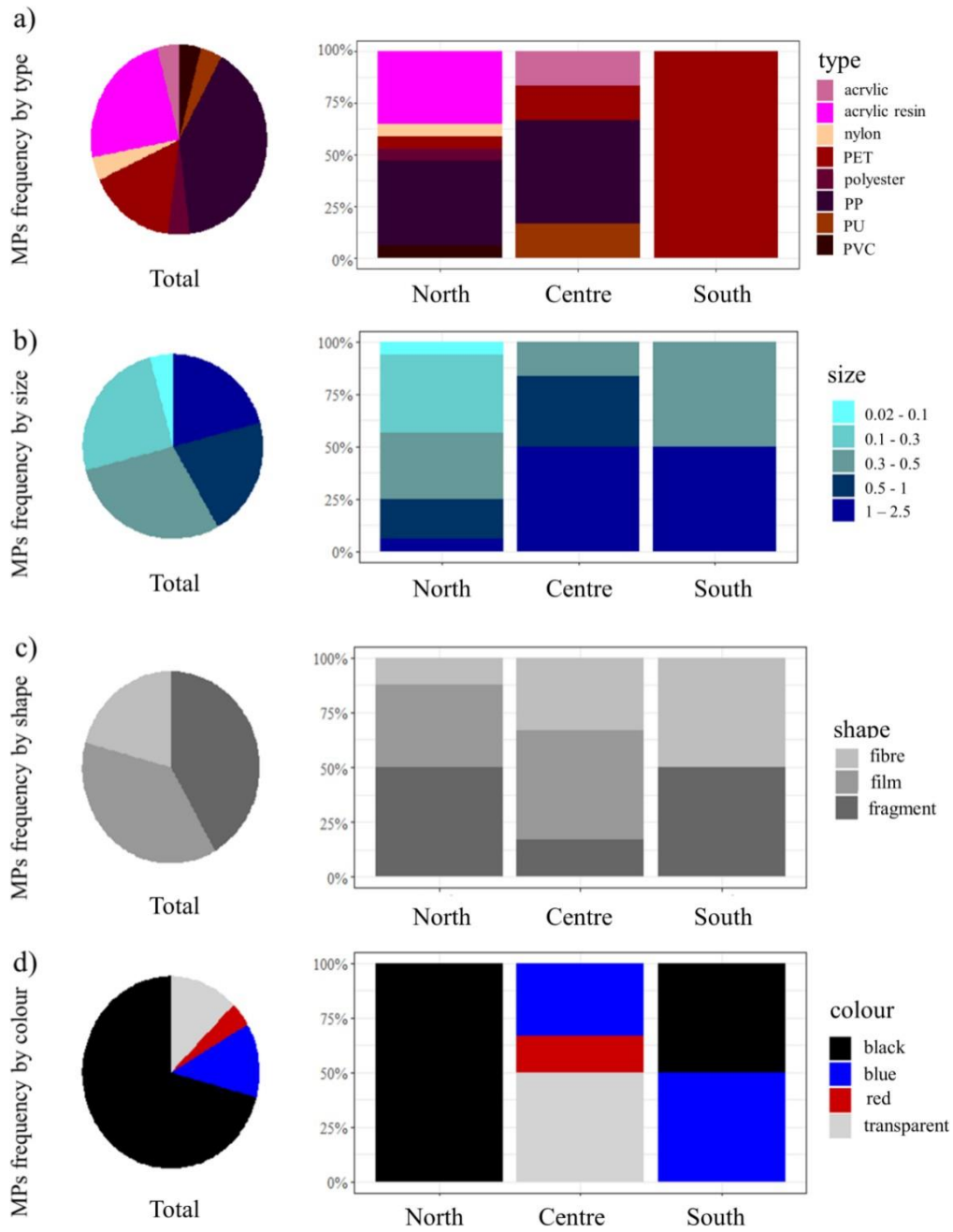


Fig. 7 MPs occurrence (%) in water, overall (on the left) and considering the sampling sites (on the right), categorized by type of polymer (a), size (b), shape (c), and colour (d).

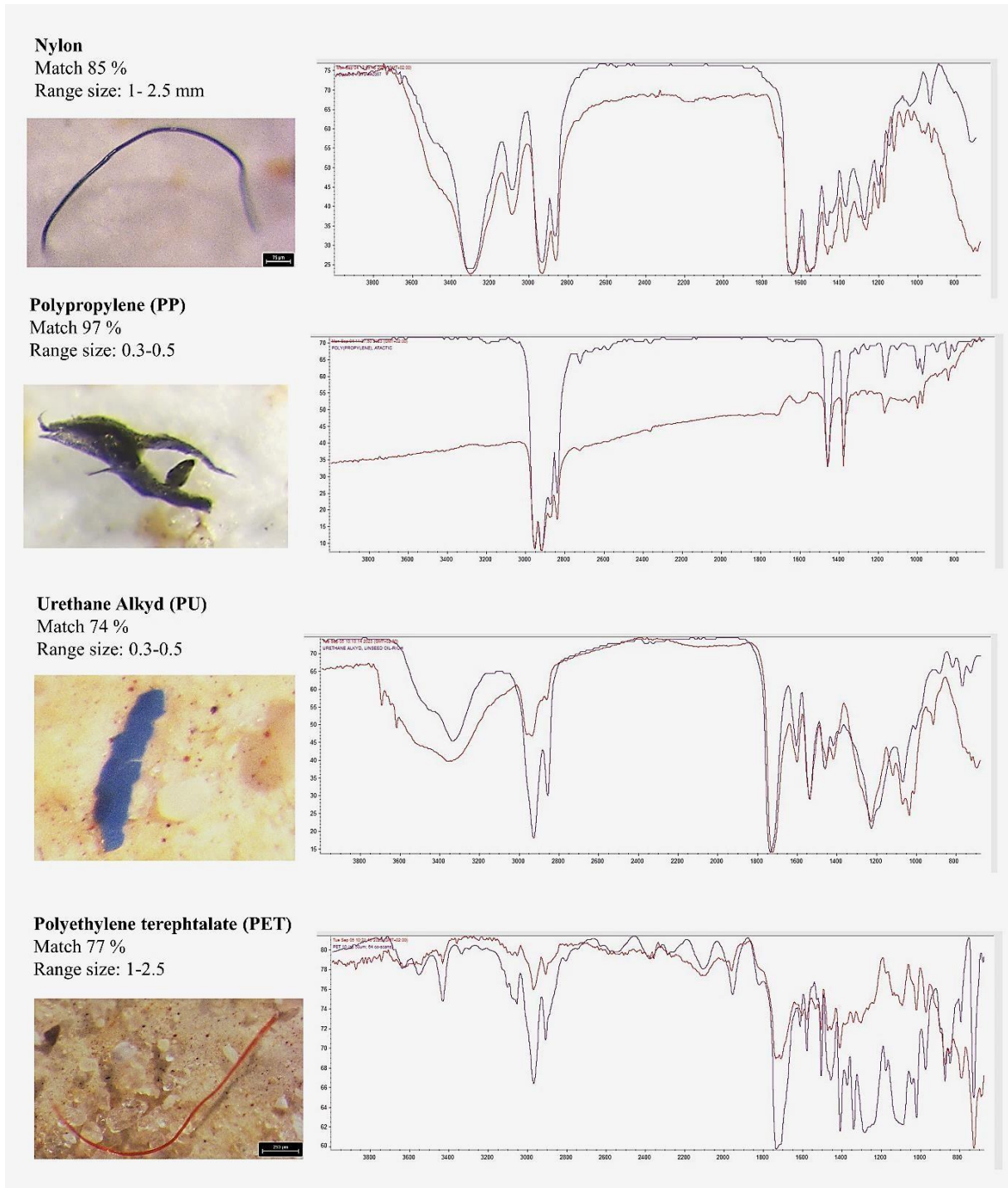


Fig. 8 Examples of polymers identified by  $\mu$ -FTIR in water samples and relative spectra

Chi-squared test (Tab.3) revealed that the MPs found in the water did not differ significantly between sampling sites in terms of size, shape and material, while their colour showed significant differences, with more black items found in the North, while red and transparent pieces were only found in the Centre, indicating different sources of pollution.

The Kruskal-Wallis test revealed significant differences in the abundance of MPs between the sediment and water samples overall (p-value= <0.001) and at each sampling site (p-value= 0.005, 0.006, 0.006, at North, Centre and South respectively). Overall, mean MPs abundance per litre of dry sediment was two orders of magnitude higher than mean MPs abundance in water.

Tab. 3 Chi-squared test, difference in shape, size, colour and material in the water samples, between sites

	North	Centre	South	p.overall
shape:				0.516
fibre	3 (17.6%)	2 (33.3%)	1 (50.0%)	
film	6 (35.3%)	3 (50.0%)	0 (0.00%)	
fragment	8 (47.1%)	1 (16.7%)	1 (50.0%)	
size:				0.316
0.02-0.1	1 (5.88%)	0 (0.00%)	0 (0.00%)	
0.1-0.3	6 (35.3%)	0 (0.00%)	0 (0.00%)	
0.3-0.5	5 (29.4%)	1 (16.7%)	1 (50.0%)	
0.5-1	3 (17.6%)	2 (33.3%)	0 (0.00%)	
1-2.5	2 (11.8%)	3 (50.0%)	1 (50.0%)	
colour:				<0.001
black	17 (100%)	0 (0.00%)	1 (50.0%)	
blue	0 (0.00%)	2 (33.3%)	1 (50.0%)	
red	0 (0.00%)	1 (16.7%)	0 (0.00%)	
transparent	0 (0.00%)	3 (50.0%)	0 (0.00%)	
material:				0.062
acrylic	0 (0.00%)	1 (16.7%)	0 (0.00%)	
nylon	1 (5.88%)	0 (0.00%)	0 (0.00%)	
PET	1 (5.88%)	1 (16.7%)	2 (100%)	
polyester	1 (5.88%)	0 (0.00%)	0 (0.00%)	
PP	7 (41.2%)	3 (50.0%)	0 (0.00%)	
PU	0 (0.00%)	1 (16.7%)	0 (0.00%)	
PVC	1 (5.88%)	0 (0.00%)	0 (0.00%)	
Alkyd resin	6 (35.3%)	0 (0.00%)	0 (0.00%)	

### **MPs abundance and % occurrence in fish**

A total of 106 fish specimens were collected throughout the study sites. *Atherina boyeri* individuals showed a mean total length of  $4.70 \pm 0.54$  cm, a mean standard length of  $3.96 \pm 0.47$  and an average weight of  $0.80 \pm 0.25$  g (Table 4). *A. boyeri* Fulton's factor was on average  $0.73 \pm 0.08$ . *Syngnathus abaster* individuals showed a mean total length of  $9.50 \pm 1.40$  cm, a mean standard length of  $9.40 \pm 1.51$  cm and an average weight of  $0.34 \pm 0.21$  g. *S. abaster* Fulton's factor was on average  $0.04 \pm 0.01$ . *Aphanius fasciatus* individuals showed a mean total length of  $3.20 \pm 1.02$  cm, a mean standard length of  $2.57 \pm 0.82$  cm and an average weight of  $0.60 \pm 0.63$  g. *A. fasciatus* Fulton's factor was on average  $1.17 \pm 0.24$ . *Diplodus annularis* individuals showed a mean total length of  $14.90 \pm 1.28$  cm, a mean standard length of  $11.69 \pm 0.82$  cm and an average weight of  $59 \pm 7.9$  g. *D. annularis* Fulton's factor was on average  $1.80 \pm 0.26$ . *Diplodus vulgaris* individuals showed a mean total length of  $14.2 \pm 1.08$  cm, a mean standard length of  $10.8 \pm 0.96$  cm and an average weight of  $48.5 \pm 10.3$  g. *D. vulgaris* Fulton's factor was on average  $1.67 \pm 0.15$ .

Tab. 4 List of the analysed species with sample size (n-number of individuals analysed), mean  $\pm$  standard deviation of the main biometric variables (total and standard length, cm; total weight, g; Fulton's condition factor, K; MPs and rayon occurrence, % of analysed individuals with ingested plastic and rayon items; total abundance of microplastic particles ingested, n). Ecological and feeding groups are also indicated according to Franco et al. (2006). Ecological groups are: ER, estuarine resident and MM-MS, marine migrants-marine stragglers. Feeding groups are HZ, hyperbenthivores/zoobenthivores; Bmi, microbenthivores; OV, omnivores.

Family	Species	Acronym	Ecological group	Feeding group	n	Total length (cm)	Total weight (g)	Fulton's condition factor (K)	MPs-rayon occurrence (%)	Total MPs and rayon (n)
Atherinidae	<i>Atherina boyeri</i>	ABO	ES	HZ	29	4.70 $\pm$ 0.54	0.80 $\pm$ 0.25	0.73 $\pm$ 0.08	21	6
Syngnathidae	<i>Syngnathus abaster</i>	SAB	ES	Bmi	24	9.50 $\pm$ 1.40	0.34 $\pm$ 0.21	0.04 $\pm$ 0.01	17	4
Cyprinodontidae	<i>Aphanius fasciatus</i>	AFA	ES	OV	28	3.20 $\pm$ 1.02	0.60 $\pm$ 0.63	1.17 $\pm$ 0.24	14	4
Sparidae	<i>Diplodus annularis</i>	DAN	MM	OV	14	14.2 $\pm$ 1.08	48.5 $\pm$ 10.30	1.67 $\pm$ 0.15	20	3
Sparidae	<i>Diplodus vulgaris</i>	DVU	MM	OV	11	14.9 $\pm$ 1.28	59.00 $\pm$ 7.90	1.80 $\pm$ 0.26	40	4

After visual sorting, debris was found in 76% digestive tracts from *A. boyeri*, 56% digestive tracts from *S. abaster*, 36% digestive tracts from *A. fasciatus*, 66% digestive tracts from *D. annularis* and 72% digestive tracts from *D. vulgaris*. A total of 204 debris particles were counted and 65% of debris samples was recovered and analysed by  $\mu$ -FTIR: 9% were microplastics, 10% semisynthetic items (rayon), 52% cellulose, 19% cotton, 5% wool, 5% organic or mineral. Considering both MPs and rayon, a total of 21 items were found in 20 out of the 106 fish analysed (19%). Taking into account the resident species *A. boyeri* and *S. abaster*, the highest occurrence of ingestion was in the North and in the Centre (Fig. 9a). *A. boyeri* ingested  $0.2 \pm 0.1$  MPs ind<sup>-1</sup>, with an occurrence of 21%. *S. abaster* ingested  $0.16 \pm 0.08$  MPs ind<sup>-1</sup>, with an occurrence of 17%. *A. fasciatus* ingested  $0.16 \pm 0.07$  MPs ind<sup>-1</sup>, with an occurrence of 14%. *D. annularis* ingested 0.2 MPs ind<sup>-1</sup>, while *D. vulgaris* ingested 0.4 MPs ind<sup>-1</sup> (Fig. 9b), with an occurrence of 20% and 40%, respectively.

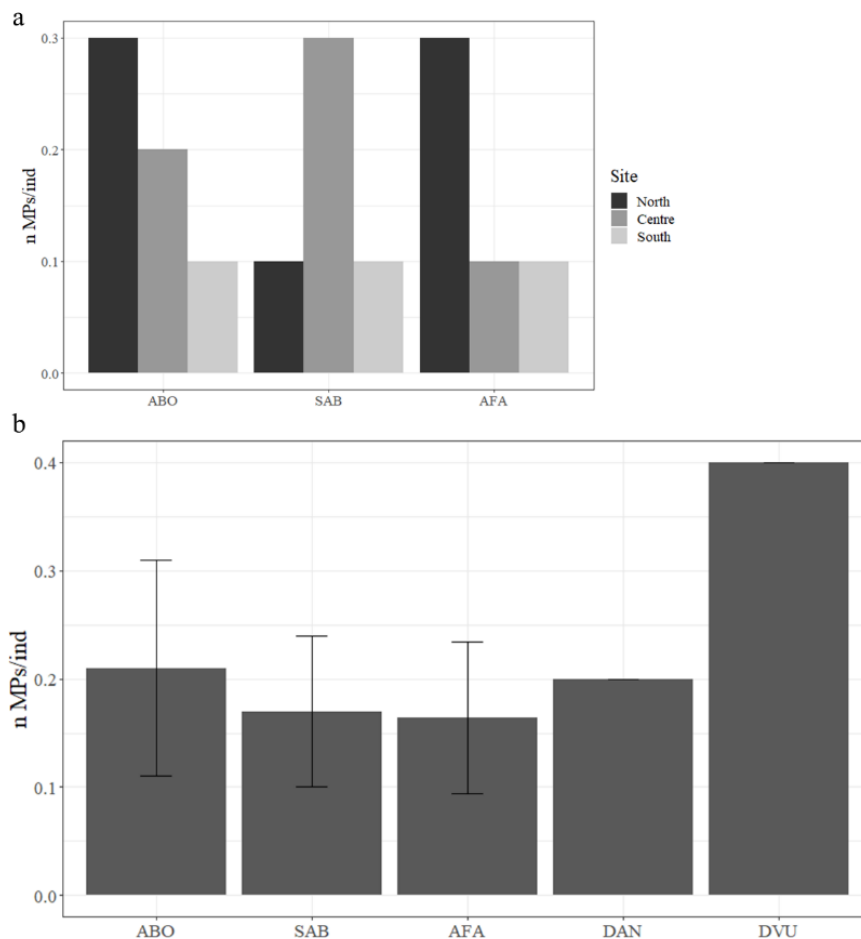


Fig. 9 a) Number of MPs ingested per species in each sampling site. b) Mean ( $\pm$  s.d.) number of MPs ingested per species, overall. For species acronyms see Table 4.

The following polymers were identified in fish samples (Fig. 10a): rayon (48%), PP (14%), acrylic (14%), PET (9.5%), polyester (9.5%), nylon (5%) (Fig. 8a). The size of the isolated particles (Fig. 10b) ranged from 0.05 to 8.30 mm, however, all the particles found, except for two, were microplastics (< 5 mm). Considering both microplastic and rayon particles, high variability in size was detected in *A. boyeri*, for which the most common size class was 0.3-0.5 mm (33%). In *S. abaster* the most common size class was 1-2.5 mm (50%), while *A. fasciatus* showed equal percentage of 2.5-5 mm and >5 mm particles. The particles isolated from *D. annularis* and *D. vulgaris* ranged from 0.5 to 5 mm, and the most represented size class was 2.5-5 mm (43%). Overall, concerning the shape of the particles analysed (Fig. 10c), the only types detected in all species were fibres (81%) and fragments (19%). Considering both microplastic and rayon particles, the colours found (Fig. 10d) were black (38%), red (19%), transparent (14%), green (14%), blue (10%) and yellow (5%). The photographs of some polymers with the relative  $\mu$ -FTIR spectra are shown in Fig. 12. Chi-squared test revealed no significant difference in the abundance of MPs ingested, considering individuals of the same species collected at the three inner sites (Tab. 5), nor significant differences in the MPs abundance of MPs ingested, comparing the species overall (Tab. 6). No significant difference was detected in the MPs characteristics (shape, size, colour, material) comparing the species overall (Tab. 7).

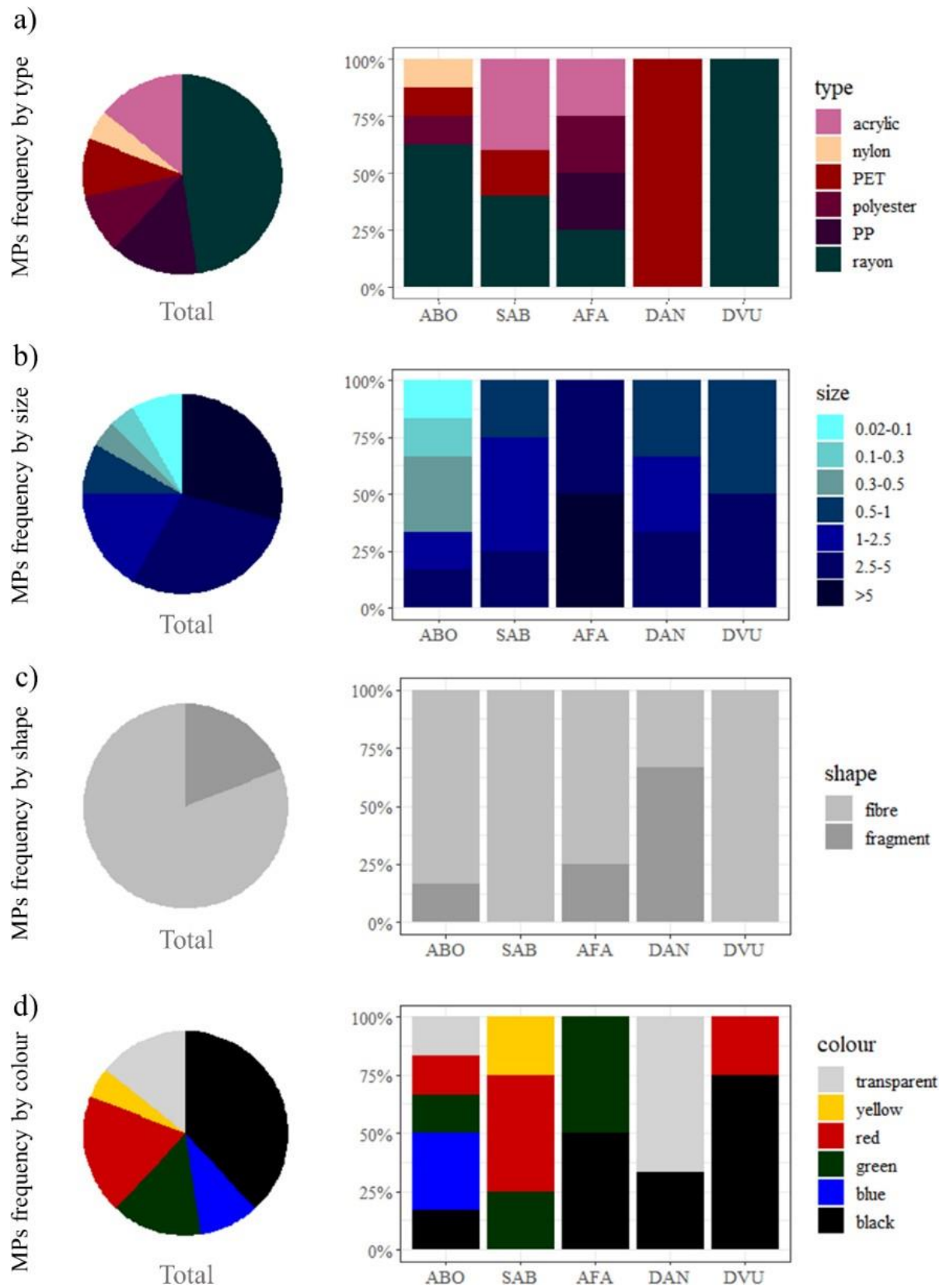


Fig. 10 MPs occurrence (%) in fish, overall (on the left) and considering the investigated species (on the right), categorized by type (a), size (b), shape (c), and colour (d). For species acronyms see Table 2.



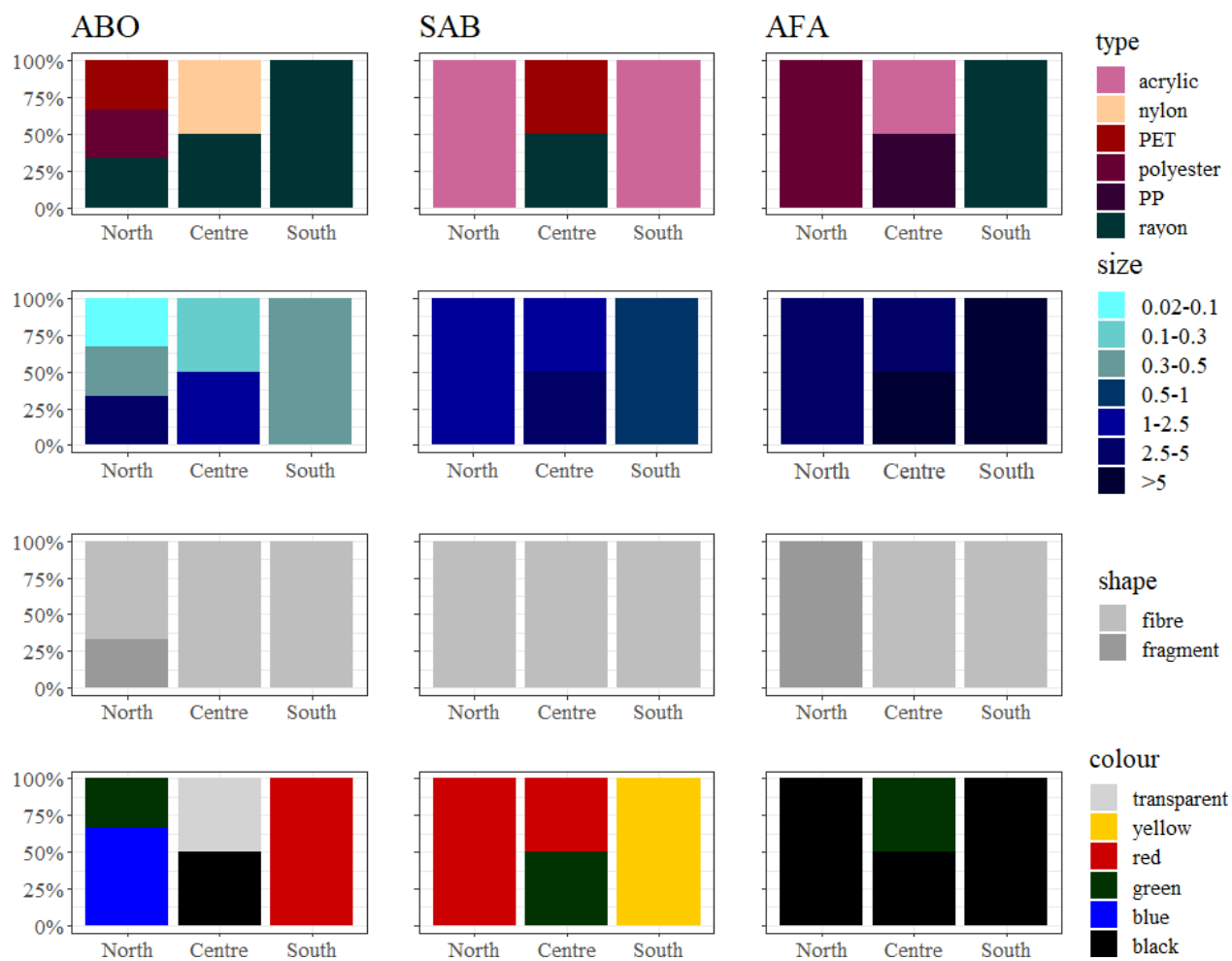


Fig. 11 MPs occurrence (%) in the investigated resident species (ABO, SAB, AFA) per sampling site, categorized by type, size, shape, and colour.

Tab. 5 Chi-squared test, abundance of ingested MPs in resident fish species, difference by site.

	MPs - n= 23	MPs + n= 6	p.overall
<i>A. boyeri</i>	Station:		0.642
	North	7 (30%)	3 (50%)
	Centre	7 (30%)	2 (33%)
	South	9 (39%)	1 (17%)

	MPs - n= 20	MPs + n= 4	p.overall
<i>S. abaster</i>	Station:		0.810
	North	6 (30%)	2 (50%)
	Centre	6 (30%)	1 (25%)
	South	8 (40%)	1 (25%)

	MPs - n= 24	MPs + n= 4	p.overall
<i>A. fasciatus</i>	Station:		0.800
	North	3 (12%)	1 (25%)
	Centre	12 (50%)	2 (50%)
	South	9 (37%)	1 (25%)

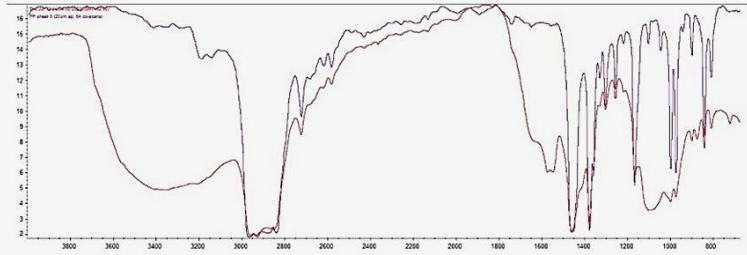
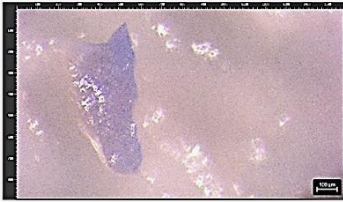
Tab. 6 Chi-squared test, abundance of ingested MPs, difference between species.

	MPs - n = 86	MPs + n = 20	p.overall
Species:			0.607
<i>A. boyeri</i>	23 (27 %)	6 (30 %)	
<i>S. abaster</i>	20 (23 %)	4 (20 %)	
<i>A. fasciatus</i>	24 (28%)	4 (20 %)	
<i>D. annularis</i>	12 (14 %)	2 (10 %)	
<i>D. vulgaris</i>	7 (8 %)	4 (20 %)	

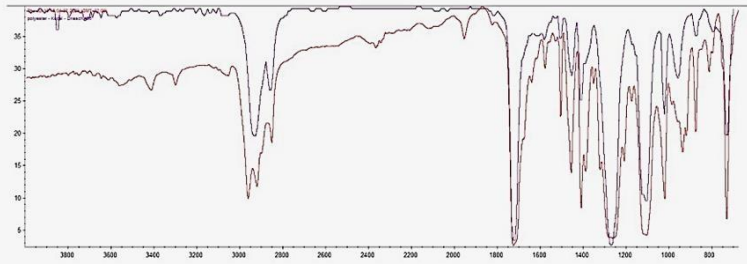
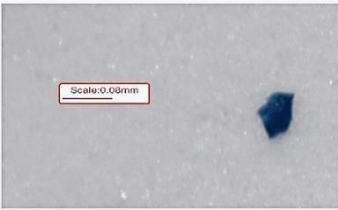
Tab. 7 Chi-squared test, difference in MPs shape, size, colour, and material between fish species.  
For species acronyms see Table 4.

	<b>ABO</b> n = 6	<b>SAB</b> n = 4	<b>AFA</b> n = 4	<b>DAN</b> n = 2	<b>DVU</b> n = 4	p.overall
<b>shape:</b>						0.075
fibre	5 (83.3%)	4 (100%)	3 (75.0%)	0 (0.00%)	4 (100%)	
fragment	1 (16.7%)	0 (0.00%)	1 (25.0%)	2 (100%)	0 (0.00%)	
<b>size:</b>						0.332
>5	0 (0.00%)	0 (0.00%)	2 (50.0%)	0 (0.00%)	0 (0.00%)	
0.02 - 0.1	1 (16.7%)	0 (0.00%)	0 (0.00%)	0 (0.00%)	0 (0.00%)	
0.1 - 0.3	1 (16.7%)	0 (0.00%)	0 (0.00%)	0 (0.00%)	0 (0.00%)	
0.3- 0.5	1 (16.7%)	0 (0.00%)	0 (0.00%)	0 (0.00%)	0 (0.00%)	
0.3-0.5	1 (16.7%)	0 (0.00%)	0 (0.00%)	0 (0.00%)	0 (0.00%)	
0.5-1	0 (0.00%)	0 (0.00%)	0 (0.00%)	0 (0.00%)	2 (50.0%)	
0.5 - 1	0 (0.00%)	1 (25.0%)	0 (0.00%)	1 (50.0%)	0 (0.00%)	
1-2.5	1 (16.7%)	2 (50.0%)	0 (0.00%)	0 (0.00%)	0 (0.00%)	
2.5 - 5	1 (16.7%)	1 (25.0%)	2 (50.0%)	1 (50.0%)	2 (50.0%)	
<b>colour:</b>						0.088
black	1 (16.7%)	0 (0.00%)	3 (75.0%)	0 (0.00%)	3 (75.0%)	
blue	2 (33.3%)	0 (0.00%)	0 (0.00%)	0 (0.00%)	0 (0.00%)	
green	1 (16.7%)	1 (25.0%)	1 (25.0%)	0 (0.00%)	0 (0.00%)	
red	1 (16.7%)	2 (50.0%)	0 (0.00%)	0 (0.00%)	1 (25.0%)	
transparent	1 (16.7%)	0 (0.00%)	0 (0.00%)	2 (100%)	0 (0.00%)	
yellow	0 (0.00%)	1 (25.0%)	0 (0.00%)	0 (0.00%)	0 (0.00%)	
<b>material:</b>						0.108
acrylic	0 (0.00%)	2 (50.0%)	1 (25.0%)	0 (0.00%)	0 (0.00%)	
nylon	1 (16.7%)	0 (0.00%)	0 (0.00%)	0 (0.00%)	0 (0.00%)	
PET	1 (16.7%)	1 (25.0%)	0 (0.00%)	0 (0.00%)	0 (0.00%)	
polyester	1 (16.7%)	0 (0.00%)	1 (25.0%)	0 (0.00%)	0 (0.00%)	
PP	0 (0.00%)	0 (0.00%)	1 (25.0%)	2 (100%)	0 (0.00%)	
rayon	3 (50.0%)	1 (25.0%)	1 (25.0%)	0 (0.00%)	4 (100%)	

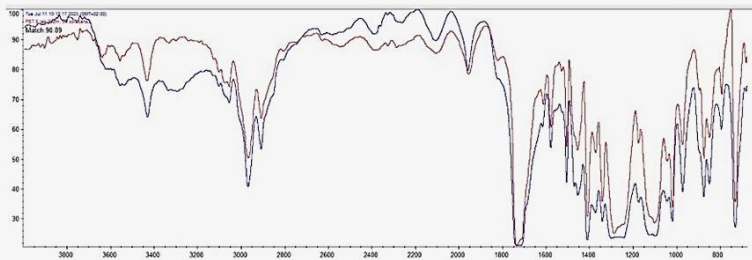
**Polypropylene (PP)**  
Match 88 %  
Range size: 0.5 - 1mm



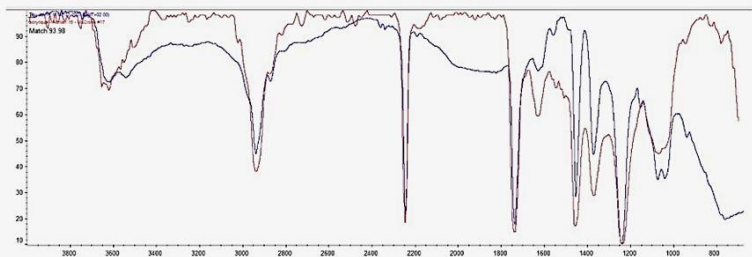
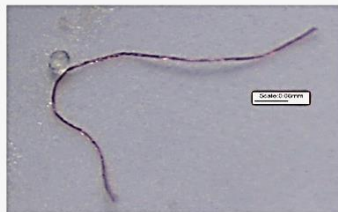
**Polyester (PES)**  
Match 82 %  
Range size: 0.02 – 0.1 mm



**Polyethylene terephthalate (PET)**  
Match 91 %  
Range size: 0.3 – 0.5 mm



**Acrylic**  
Match 94 %  
Range size : 1 – 2.5 mm



**Nylon**  
Match 88 %  
Range size: 0.1- 0.3 mm

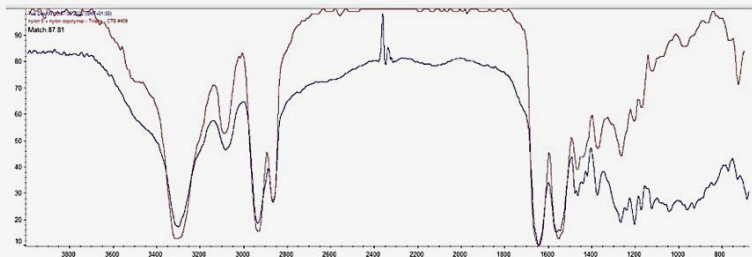
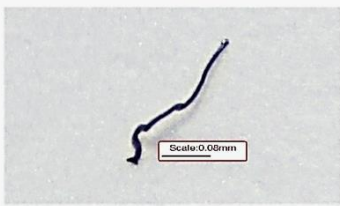


Fig. 12 Examples of polymers identified by  $\mu$ -FTIR in fish and relative spectra.

## Relationship between fish traits, trophic niche metrics and MPs ingestion

Although the Fulton's condition factor was lower in *D. annularis* and *D. vulgaris* specimens that had ingested MPs, the Wilcoxon-Mann-Whitney test revealed no significant differences between individuals of the same species which had ingested and had not ingested MPs (Fig. 13).

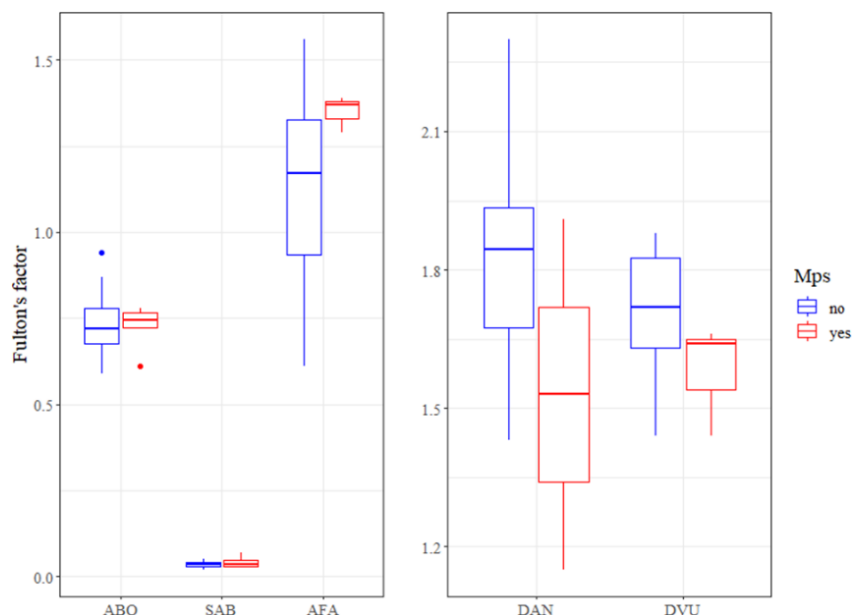


Fig. 13 Fulton's condition factor per species: specimens without ingested microplastics are represented in blue, specimens that ingested microplastics in red. For species acronyms see Table 4.

*A. boyeri*  $\delta^{13}\text{C}$  values ranged from  $-13.4\text{‰}$  in the Centre to  $-12.6\text{‰}$  in the South, while  $\delta^{15}\text{N}$  ranged from  $7.8\text{‰}$  in the North to  $12.2\text{‰}$  in the South. *S. abaster*  $\delta^{13}\text{C}$  values ranged from  $-13.6\text{‰}$  in the Centre to  $-11.5\text{‰}$  in the North, while  $\delta^{15}\text{N}$  ranged from  $6.8\text{‰}$  in the North to  $10.3\text{‰}$  in the South. *A.fasciatus*  $\delta^{13}\text{C}$  values ranged from  $-12\text{‰}$  in the North to  $-11.2\text{‰}$  in the South, while  $\delta^{15}\text{N}$  values ranged from  $9.1\text{‰}$  in the North to  $11.7\text{‰}$  in the South. Overall, an enrichment in  $\delta^{15}\text{N}$  values was recorded from North to South for all resident species. Compared to the resident species, the transient species resulted depleted in both  $\delta^{13}\text{C}$  and  $\delta^{15}\text{N}$ . *D. annularis*  $\delta^{13}\text{C}$  and  $\delta^{15}\text{N}$  averages were  $-14.3 \pm 1.4\text{‰}$  and  $7.9 \pm 1.3\text{‰}$  respectively, while *D. vulgaris*  $\delta^{13}\text{C}$  and  $\delta^{15}\text{N}$  averages were  $-13.3 \pm 0.9\text{‰}$  and  $9.7 \pm 1.7\text{‰}$ , respectively (Tab. 8).

*D. vulgaris* had the highest trophic position ( $3.7 \pm 0.2$ ), followed by *D. annularis* ( $3.4 \pm 0.4$ ), *A. fasciatus* ( $3.2 \pm 0.4$ ), *A. boyeri* ( $3.1 \pm 0.6$ ) and *S. abaster* ( $2.7 \pm 0.6$ ). The Pearson correlation analysis revealed not significant ( $p\text{-value} = 0.6$ ) correlation between the average TP of the fish species and the number of MPs ingested (Fig. 14).

Tab. 8 Mean  $\pm$  STDEV and range of  $\delta^{13}\text{C}$  and  $\delta^{15}\text{N}$  (‰) of the different species, per sampling site.

	$\delta^{13}\text{C}$	$\delta^{15}\text{N}$
<b><i>Atherina boyeri</i></b>	<b>-13.0 <math>\pm</math> 0.9</b>	<b>10.4 <math>\pm</math> 2.2</b>
North	-13.1 $\pm$ 1.1	7.8 $\pm$ 0.7
Centre	-12.6 $\pm$ 0.7	11.1 $\pm$ 0.8
South	-13.4 $\pm$ 0.5	12.2 $\pm$ 1.4
<b><i>Syngnathus abaster</i></b>	<b>-12.5 <math>\pm</math> 1.3</b>	<b>8.9 <math>\pm</math> 1.9</b>
North	-13.6 $\pm$ 1.0	6.8 $\pm$ 1.7
Centre	-11.5 $\pm$ 1.1	9.8 $\pm$ 0.5
South	-12.3 $\pm$ 1.2	10.3 $\pm$ 0.6
<b><i>Aphanius fasciatus</i></b>	<b>-11.9 <math>\pm</math> 0.8</b>	<b>11.0 <math>\pm</math> 1.3</b>
North	-11.2 $\pm$ 0.4	9.1 $\pm$ 0.0
Centre	-11.9 $\pm$ 0.7	10.7 $\pm$ 1.0
South	-12.0 $\pm$ 1.0	11.7 $\pm$ 1.1
<b><i>Diplodus annularis</i></b> (External)	<b>-14.3 <math>\pm</math> 1.4</b>	<b>7.9 <math>\pm</math> 1.3</b>
<b><i>Diplodus vulgaris</i></b> (External)	<b>-13.3 <math>\pm</math> 0.9</b>	<b>9.7 <math>\pm</math> 1.7</b>

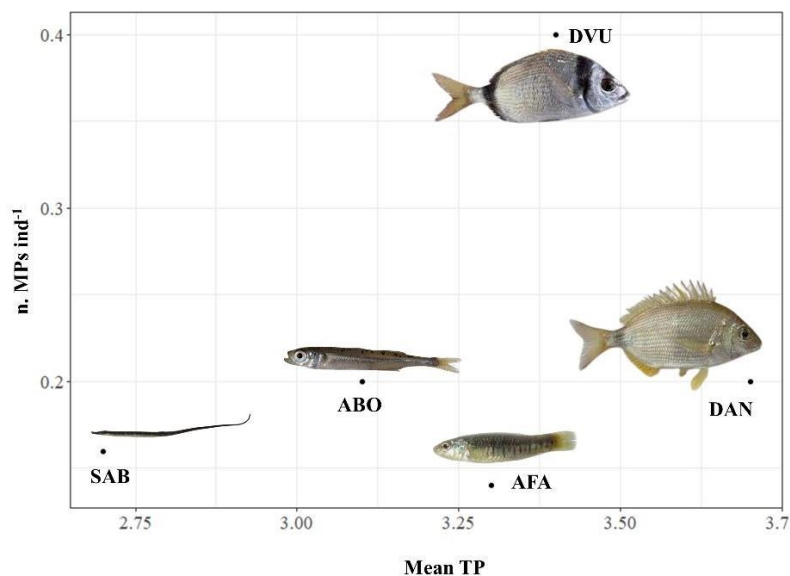


Fig. 14 Mean trophic level (mean TP) calculated through nitrogen isotope analysis and number of MPs ingested by each fish species.

The difference in the isotopic niche width (SEAc and SEAb) between individuals that had and had not ingested MPs was not significant, considering all species. Nitrogen and carbon range (NR and CR) were significantly lower for fish that ingested MPs, compared to those that had not, considering

*A. boyeri*, *A. fasciatus* and *Diplodus spp.* Difference in the distance from the centroid (CD), redundancy (NND) and evenness (SNND) between fish that had and had not ingested MPs was not significant, considering all species (Tab. 9).

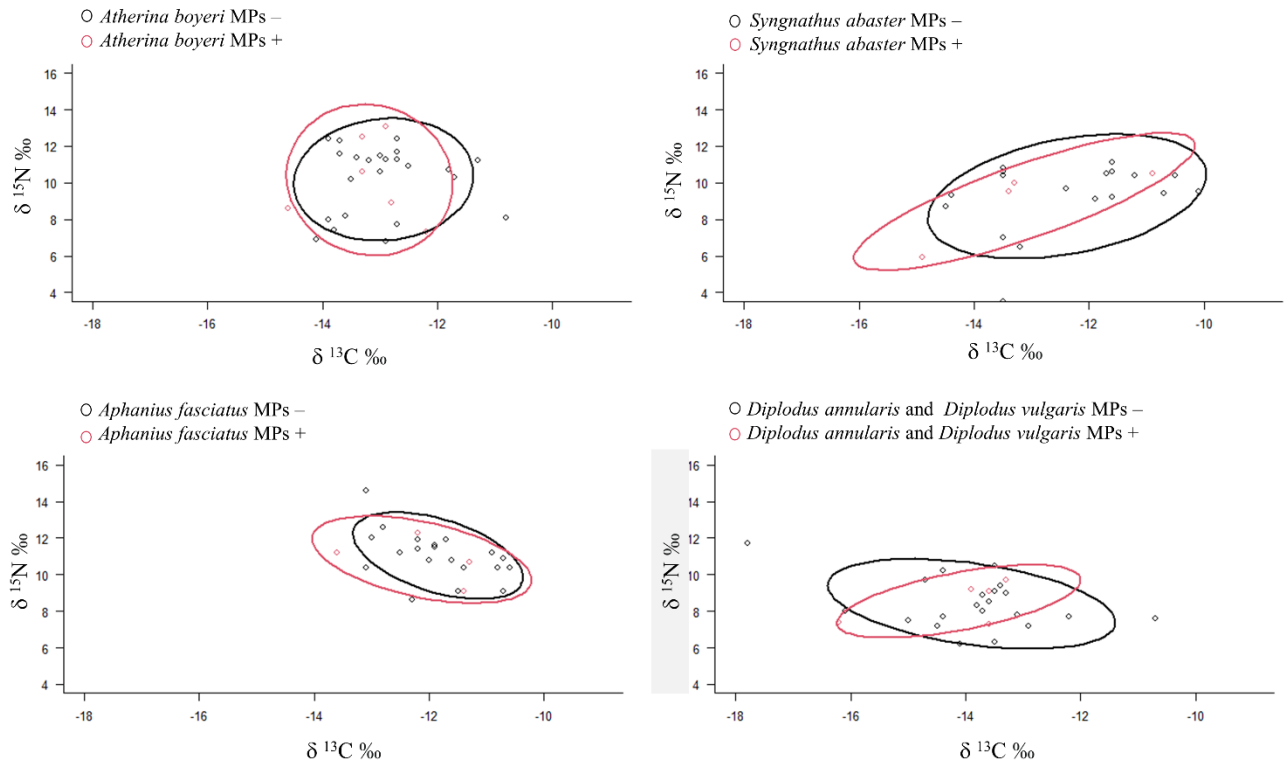


Fig. 15 Standard ellipse areas (SEAc) of fish species. Specimens of each species are differentiated according to the presence (MPs +, red dots) or absence (MPs -, blue dots) of ingested microplastics.

Tab. 9 Mean SEAc, SEAb and bootstrapped (b) Layman metrics along with 95% credible intervals:  $\delta^{13}\text{C}$  range (CR),  $\delta^{15}\text{N}$  range (NR), mean Distance to Centroid (CD), mean Nearest Neighbour distance (NND) and its Standard Deviation (SDNND). Data are reported pergroups of specimens of each fish species that had and had not ingested MPs (+ and -). \*Indicates significant differences between groups that had and had not ingested MPs.

Species	MPs and n° samples	SEAc	SEAb	$\delta^{13}\text{C}$ range	$\delta^{15}\text{N}$ range	CD	MNND	SDNND
<i>Atherina boyeri</i>	-(23)	5.33	5.30 (3.73 - 7.41)	<b>2.94 (2.20-3.30)*</b>	5.42 (4.70 - 5.60)	1.77 (1.29 - 2.13)	0.27 (0.13-0.40)	0.42 (0.25 - 0.60)
	+(6)	7.25	7.03 (3.34 -13.20)	<b>1.61 (0.50 - 2.40)*</b>	4.62 (2.00 - 5.80)	1.76 (1.02 - 2.48)	0.9 (0.14 - 1.55)	1.02 (0.08 - 1.84)
<i>Syngnathus abaster</i>	-(20)	8.01	8.02 (5.31 - 11.78)	4.04 (3 - 4.4)	6.09 (2.04 - 7.6)	1.89 (1.33 - 2.51)	0.37 (0.14 - 0.63)	0.66 (0.26 - 1.30)
	+(4)	9.27	11.24 (4.29 - 25.81)	2.27 (0.0 - 4.0)	2.67 (0 - 4.6)	1.57 (0.0 -2.71)	0.82 (0.0 - 2.71)	1.54 (0.0 - 3.52)
<i>Aphanius fasciatus</i>	-(24)	3.15	3.18 (2.13 - 12.25)	<b>2.41 (2.20 - 2.50)*</b>	<b>4.84 (2.9 -6.00)*</b>	1.24 (0.92 -1.58)	0.28 (0.13- 0.45)	0.45 (0.24 - 0.70)
	+(4)	5.86	5.58 (2.13 - 12.25)	<b>1.46 (0.0 - 2.30)*</b>	<b>1.9 (0.0 -3.20)*</b>	1.08 (0.0 -1.57)	1.15 (0.0 -2.20)	0.88 (0.0 -1.90)
<i>Diplodus</i> spp.	-(20)	5.76	5.82 (3.99 - 8.17)	<b>5.5 (2.30 -7.10)*</b>	<b>4.75 (3.30 -5.50)*</b>	1.54 (1.14 -2.01)	0.36 (0.16 -0.58)	0.62 (0.29 - 0.98)
	+(5)	4.43	4.60 (2.02 - 9.41)	<b>1.78 (0.30 - 2.90)*</b>	<b>1.87 (0.10 -2.40)*</b>	1.09 (0.29-1.66)	0.71 (0.0 -1.44)	0.86 (0.0 - 1.48)



Pearson correlation analysis (Fig.10) revealed significant negative correlation between hydrodynamics (MDC) and the abundance of MPs ingested by fish. Significant positive correlation was highlighted between the abundance of MPs in the water column (n MPs/L water) and the number of MPs ingested by fish species. There was no significant correlation between, seagrass biomass, macroalgae biomass, the abundance of microplastics in the sediment, fish trophic position, Fulton's factor, fish  $\delta^{13}\text{C}$  (‰) and the number of microplastics ingested.

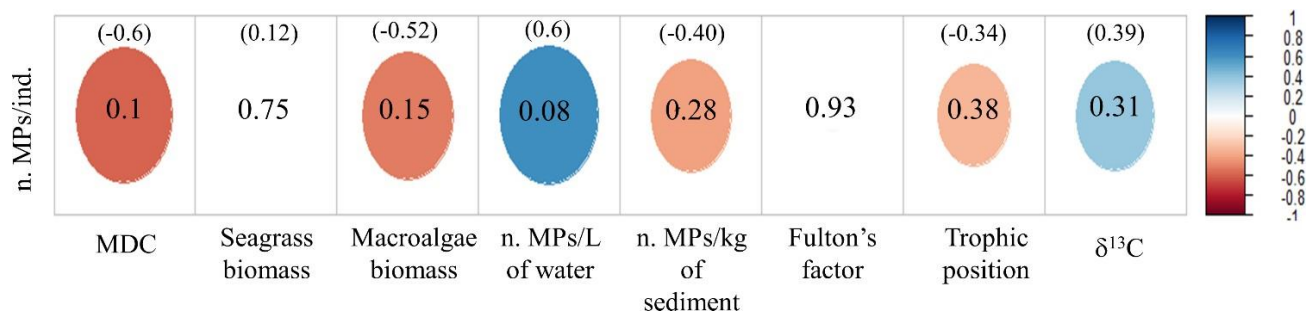


Fig. 10 Pearson correlation coefficients, with the number of microplastics ingested by fish species at the three different sites (n. MPs/ind.) as response variable, while environmental factors (MDC, seagrass biomass, macroalgae biomass, n MPs L<sup>-1</sup> water, n MPs kg<sup>-1</sup> sediment) and fish biological traits (trophic position, Fulton's factor,  $\delta^{13}\text{C}$  (‰)) are the explanatory variables. Red indicates negative correlation while blue indicate positive correlation. Due to the small sample size of the dataset statistical significance was accepted at the 0.1 alpha level (significant level is reported in brackets).

## Discussion

The current study reports on the distribution, abundance, and composition of MPs in different environmental compartments (sediment and water column) in a coastal basin characterized by seagrass beds, at sites differing in terms of hydrodynamics and exposure to the open sea. At the same time, the present study analyzed the ingestion of MPs by different fish species associated to seagrass habitats and compared it between resident and marine migrant species of commercial interest. This is one of the first studies to use a holistic approach, taking into account both environmental parameters and the trophic ecology of the biota, to assess which factors most influence the ingestion of MPs by fish. MPs were found in sediment, water column and in all the fish species analysed.

The abundance of MPs in marine sediment and water varies greatly from region to region but the use of different units to quantify them (*e.g.*,  $n\ m^{-2}$ ,  $n\ m^{-3}$ ,  $n\ kg^{-1}$ ), and different sampling and laboratory methods makes statistical comparison difficult. Regarding sediment in the marine environment, remote areas show lower abundance overall (Kanhai et al., 2017). In a literature review conducted by Harris (2020) the highest median concentrations of MPs in sediments were found in fjords (7000 MPs  $kg^{-1}$  dry sediment), followed by estuarine environments (300 MPs  $kg^{-1}$  dry sediment), beaches and shallow coastal areas (200 MPs  $kg^{-1}$  dry sediment each), the deep sea (80 MPs  $kg^{-1}$  dry sediment) and continental shelf areas (50 MPs  $kg^{-1}$  dry sediment). In general, coasts and seabed are the most important long-term locations for the accumulation of plastic litter. Indeed, the seawater has a specific density of about  $1.027\ g\ cm^{-3}$  and it is assumed that some plastic polymers (PS, PP, LDPE, EVA, HPDE) have a lower density and float, while others (PA, PMMA, PC, PU, PET, PVC, PTFE) have a higher density and sink after entering the water (Frias et., 2018; Simon-Sanchez et al., 2022). However, once microplastics enter the marine environment, they are quickly colonised by bacteria, cyanobacteria and algae (Fazey et al., 2016; Leiser et al. 2020), which form a biofilm that facilitates their sinking (Kaiser et al. 2017). The largest quantities appear to sink near the coast, decreasing towards the open sea (Kaardorp et al. 2020).

The total amount of MPs found in the sediment in this work ( $58 \pm 35$  MPs  $kg^{-1}$  dry sediment) appeared to be lower than expected for shallow coastal areas (Harris et al., 2020), which may be due to the fact that there is no freshwater inflow into the basin, no industrial or port activities on the coast and fishing is officially prohibited within the basin. Sediment samples analysed in this study exhibited MPs abundance two order of magnitude higher than seawater and this is something expected, particularly in a coastal environment characterized by low hydrodynamics and aquatic vegetation, as highlighted in a comprehensive review by Ouyang et al. (2022), who demonstrate that the abundance of plastic in

coastal wetlands sediment is approximately 200 times higher than that in the water column. In addition, in this study a higher occurrence of MPs was found in the central sector, which is characterized by the lowest hydrodynamics and a higher seagrass biomass. Indeed, local hydrodynamics and coastal geomorphology influence the distribution and abundance of MPs in the seabed, with enclosed waters with low hydrodynamics retaining more MPs in their sediments (Wang et al., 2020; Marques Mendes et al., 2021). Furthermore, seagrass beds have been speculated to serve as hotspots for marine MPs, slowing down water currents as a result of drag from the canopy, thus increasing settling and entrapping MPs within their aboveground structures and sediments (Kreitsberg et al., 2021; de los Santos et al., 2021). Seagrass beds exhibit considerably higher abundance of MPs compared to adjacent unvegetated areas (Huang et al., 2021), with an average abundance of  $263.4 \pm 309.2$  n MPs/kg (C. Li et al., 2023).

Literature data on the abundance of MPs in surface waters of the Mediterranean Sea report average concentrations ranging widely from  $0.15 \pm 0.11$  MPs  $m^{-3}$  in the western Mediterranean Sea (western Sardinia, de Lucia et al., 2014) to  $7.68 \pm 2.38$  MPs  $m^{-3}$  in the Aegean-Levantine Sea (van der Hal et al., 2017). Worldwide, the abundance of MPs in water from coastal wetlands ranges from very low concentration as in Anzali Wetland (Iran, 1.77 MPs  $m^{-3}$ ; Rasta et al., 2020), or in Bueng Boraphet Wetland (Thailand, 1.44 MPs  $m^{-3}$ ; Sarin and Klomjek, 2022), to very high concentration as in Hashilan Wetland (Iran, 2000-6000 MPs  $m^{-3}$ ; Abbasi, 2021). The abundance of MPs in the waters of the Stagnone di Marsala ( $320 \pm 186$  MPs  $m^{-3}$ ) was higher than the values reported for other coastal regions of the Mediterranean Sea and within the range of values reported for coastal wetlands worldwide. Notwithstanding the absence of a direct freshwater inflow into the basin, the higher concentration of microplastics in the water of the northern sector compared to the central and southern sectors suggests a contribution from the Birgi River, which is in the north of the basin and may be connected to the basin waters via the northern inlet.

Overall, the occurrence of MPs in the gastrointestinal tract of fish species examined in this study is within the range reported in the literature (between 0.07 MPs  $ind^{-1}$  and 16.33 MPs  $ind^{-1}$ ; Marmara et al., 2023). A study by Cera et al. (2022) reported no evidence of ingestion of MPs by *Atherina boyeri* individuals from Lake Bracciano (Italy), while Shabaka et al. (2020) measured 28 MPs  $ind^{-1}$  for the same species, which is a much higher result than in this study ( $0.20 \pm 0.11$  MPs  $ind^{-1}$ ). To our knowledge, this is the first evidence of MP ingestion by *Syngnathus abaster* and *Aphanius fasciatus*. MP ingestion by another Syngnathidae species (*Syngnathus acus*), studied elsewhere, yielded similar results (0.30 MPs  $ind^{-1}$ , Senturk et al., 2023, vs  $0.16 \pm 0.11$  MPs  $ind^{-1}$  for *S. abaster* in the present study). *D. vulgaris* individuals collected in Portugal showed higher ingestion of MPs

than our samples (3.14 MPs ind<sup>-1</sup>, Bessa et al., 2018 vs 0.40 MPs ind<sup>-1</sup> in the present study), while *D. annularis* individuals from the northwestern Mediterranean Sea showed lower but similar results (0.10 MPs ind<sup>-1</sup>, Constant et al., 2022 vs 0.20 MPs ind<sup>-1</sup> in the present study).

MPs found in sediment and fish gut were predominantly fibres, followed by fragments and, to a very small extent, films. Previous studies have shown that microfibers are the most abundant type of MPs found in the environment (Acharya et al., 2021), and ingested by fish (Marmara et al., 2023). MP fibers originate from synthetic textiles in household laundry and enter the marine environment via wastewater or sewage sludge (Acharya et al., 2021; Li et al., 2023), potentially releasing 210 to 72,000 fibers from one gram of textiles in a single wash (Cai et al., 2020). Fragments, instead, are generally secondary MPs resulting from the breakdown of macroplastics through physical, chemical, and biological degradation (Andrady, 2011). Fragments and films were more common in the water, most of which were made of polypropylene, a polymer characterized by low density and likely to be buoyant in seawater. Black and blue were the most common MP colours found both in water and sediment samples, which is consistent with literature, as blue (26.69–79.03%), transparent (5.65–24.50%), and black (9.60–22.71%) are the most common colours exhibited by MPs found in seagrass environments (Li et al., 2023). MPs ingested by fish were mainly black, and this result agrees with current literature (Marmara et al., 2023). In this study the polymers found both in sediment, water and fish were polyester (PES), polypropylene (PP), polyethylene terephthalate (PET), which according to the literature are also among the major MP polymers found in the marine environment (Chaudhry & Sachdeva, 2021), and acrylic. Forty-five million tonnes of polypropylene are globally produced every year and used for trays, funnels, pails, bottles and clothes (Gazal & Gheewala, 2020; Maddah, 2016). Polyethylene terephthalate is the third most widely diffused polymer, globally produced in 37 million of tonnes each year, exploited in the packaging industry and for the production of bottles/containers of beverages (Gazal & Gheewala, 2020; Nisticò 2020). Polyester is a type of PET with dyes and additives that give the material special properties for use in the textile industry (Palacios-Mateo et al., 2021), and with acrylic and nylon fibers represent 60% of the worldwide production of textile fibers (Mahbub & Shams, 2022). Nylon, which here was found in both fish gut and water samples, is also widely used in fishing gears (Andrady 2011). In this study, microparticles of polyvinylchloride (PVC) and polyurethane (PU) were found both in sediment and water samples, but they were not found in the biota. Polyvinylchloride is the third most demanded polymer in Europe, generally scarcely observed in the marine environment, used for tubes and blood bags for medical applications, clothing, durable applications such as window frames and waterproof goods, industrial applications (pipes, cables) and food packaging (Fernández-González et al., 2022). Polyurethanes can be found in furniture, coatings, adhesives, paddings, paints, synthetic skins, elastomers, and construction materials (Howard, 2002). Alkyd resins, which in this

study were found only in water samples, are used as binders for paints, and films and fragments of them in the marine environment could derive from the abrasive wear of surface coatings (Nolasco et al., 2022). Polyethylene (PE), here found only in sediment samples, is used for plastic bags, netting, drinking straws, milk and juice jugs (Andrady et al., 2011). Rayon was found in both sediments and fish samples. It is a man-made cellulose fiber that is widely used for clothing, interior textiles and hygiene products (Comnea-Stancu et al., 2017) and has been identified as one of the main sources of microplastic litter in the marine environment, even in the deep sea (Woodall et al., 2014).

Physiological condition of fish has been related to MPs ingestion, suggesting a reduction in the number of ingested MPs by fish with a good status because able to avoid useless and inedible items. Contrarily, a worse condition is expected to increase food ingestion even of less profitable sources, thus increasing the likelihood of MPs ingestion. In the literature, the relationship between the condition factor and the ingestion of MPs is controversial, as some authors have demonstrated a lower occurrence of MPs in fish with higher body condition (Filgueiras et al., 2020, Compa et al., 2018), others a positive (Capone et al., 2020) or the absence of relationship (de Vries et al., 2020). According to this last finding, our results show that plastic ingestion by fish was not affected by Fulton's condition factor. MPs appear to be a transient contaminant, as in many cases these particles are simply excreted by the organism after a while (Grigorakis et al., 2017; Kim et al., 2020; Su et al., 2019), which makes it difficult to assess a clear correlation between the presence of MPs and fish characteristics.

Some studies have focused on the relationship between trophic level of marine organisms and MPs ingestion (Garcia et al., 2021; da Silva et al., 2022; Giani et al., 2023) to evaluate the influence of different feeding strategies on the probability of MP uptake and/or to assess the trophic transfer of MPs along the trophic chain. In the present study, there was no significant correlation between the trophic position and the occurrence of MPs in the examined species and this result is consistent with previous studies (Garcia et al., 2021; Hamilton et al., 2021; Covernton et al., 2021), even though some other studies have supported the existence of negative correlation (Giani et al., 2023; Walkinshaw et al. 2020) or the existence of positive correlation (Wanget al., 2021). Intuitively, larger samples size and the sampling of species with trophic positions strongly different should provide clearer information on this relationship.

Several studies indicated that the more varied the diet of an organism is, the greater is the chance of ingesting microplastics. Giani et al. (2023) came to this conclusion analysing the isotopic niche of species at different trophic levels and with different feeding strategies. Mizraji et al. (2017), comparing the MPs abundance among intertidal fish with different feeding type, concluded that omnivorous species ingested higher amount of MPs than herbivores and carnivores, due to their wider

diet sources. Similarly, studying a freshwater ecosystem, Garcia et al. (2020) found a higher intake of MPs in omnivorous fish species, concluding that this feeding behaviour, consisting in the exploitation of a wide variety of resources, may increase the probability of MP ingestion. Not et al. (2020) quantified MPs in four species of mangrove crabs and found that generalist feeders ingested higher amount and diversity of MPs. Although the studies cited above indicate that species that feed on multiple food sources (e.g. generalists, omnivores) have a greater chance of ingesting MPs, contrary results have also been found in the literature (Muller, 2021) while some other studies did not found relationship between feeding strategies and MPs ingestion (Sun et al., 2019; Parker et al., 2022). In this study, there is a general trend that individuals that have ingested MPs have a lower  $\delta^{13}\text{C}$  and  $\delta^{15}\text{N}$  range than individuals that have not ingested MPs. This suggests that individuals with a more selective feeding strategy, based on less variable basal resources and prey of a less variable trophic level, may have a greater chance to ingest MPs. Further studies are needed to investigate the relationship between isotopic niche characteristics and MPs uptake by fish. Increasing the number of species and/or individuals analysed could help to clarify the relationship between feeding ecology and MPs ingestion.

## **Conclusion**

The higher number of MPs found in the sediments, especially in the most enclosed and vegetated area, confirms the great capacity of seagrass systems, supported by the geomorphology and low hydrodynamics of the sheltered coastal environments, to remove pollutants from the water column. Our results suggest that environmental parameters such as hydrodynamics could influence the abundance of MPs in the environment where fish species feed and thus the likelihood of MPs ingestion by different species. The complexity of the food-web and the uncertainties caused by contradictory results in the literature, which are also due to the lack of standardisation of sampling, laboratory and analytical methods, call for a more holistic approach based on the simultaneous analysis of the abundance and properties of microplastics in both biota and the surrounding environment. The quantification of MPs requires rigorous control procedures, in order to avoid contaminations due to the ubiquity of, in particular, microfiber, and polymers verification, for example via  $\mu$ -FTIR.

## Chapter 3

### **Analysis of carbon and nitrogen stocks, stable isotopes, and trace metals from different *Posidonia oceanica* habitats (natural meadow, reforestation, dead matte) from a anthropized coastal area.**

#### **Abstract**

*Posidonia oceanica* meadows offer a variety of benefits to humans but are in decline throughout the Mediterranean Sea. Restoration efforts have increased in recent decades, and transplantation onto dead matte is considered an effective option. Long-term monitoring programs are needed to evaluate the results of a reforestation program. In 2008, following the improvement of water quality, a pilot seagrass reforestation project was carried out on a dead matte in a coastal region previously exposed to high inputs of nutrients and pollutants since the 1950s (Gulf of Palermo, northern Sicily, Italy, Mediterranean Sea). Twelve years after reforestation, the transplanted *P. oceanica* meadows showed structural and functional characteristics comparable to those of the nearby natural meadow, so further transplants were planned in the area. Sediment cores were collected from the naturally growing meadow, the dead matte and the restored meadow, to evaluate the differences between these habitats in terms of carbon, nitrogen and trace metal stocks and to reconstruct the temporal geochemical changes that have occurred at this coastal site. Samples were dated using  $^{210}\text{Pb}$  and analysed for elemental concentrations ( $C_{\text{org}}$ ,  $C_{\text{inorg}}$ ,  $N_{\text{tot}}$ , P), stable isotope ratios ( $\delta^{13}\text{C}$ ,  $\delta^{15}\text{N}$ ) and trace metal concentrations (As, Cd, Co, Cr, Cu, Hg, Ni, Mn, Pb, V and Zn). The vertical and temporal profiles of the geochemical variables and the comparison between the values before and after 1950 indicate an enrichment in  $\delta^{13}\text{C}$  and  $\delta^{15}\text{N}$  as well as an increase in  $N_{\text{tot}}$  and P giving evidence of the past increased nutrient input into the Gulf. Temporal profiles of trace metals showed changes in contaminant concentrations over the past 120 years that are consistent with the history of the Gulf. Low  $^{210}\text{Pb}_{\text{excess}}$  stock and a very low accumulation rate measured in dead matte indicate a reduced sediment trapping capacity of this habitat and the possible occurrence of slight erosion, which in contrast was not observed in the transplanted meadow. This is evidence of the success of the past reforestation project and supports further restoration actions to invert degradation of the coastal area.

## **Keywords**

Blue carbon, nutrient filters, seagrass degradation, restoration, trace metals, seagrass archives, Mediterranean Sea

## **Highlights**

- Trace metals and nutrients increased after 1950 due to coastal development.
- Trace metal concentrations after 1950 did not exceed the Sediment Quality Guidelines.
- Reduced sediment trapping coupled with possible slight erosion were observed in the unvegetated dead matte but not in the transplanted *P. oceanica* meadow.



## Introduction

*Posidonia oceanica* (L.) Delile is a deeply studied marine angiosperm (Magnoliophyta) species (Boudouresque et al., 2012), endemic to the Mediterranean Sea where it occurs up to 45 m depth (Marbà et al., 2014), creating extensive meadows and building up persistent terrace structures formed by rhizomes, roots and sediment, called *matte*. The *matte* of *P. oceanica* can reach several meters in height and, due to the anoxic conditions that characterize its sediment and the stabilization of the sediment it operates on, organic and inorganic carbon and nutrients can remain trapped within this structure for thousands of years (Pergent-Martini et al., 2020). These *matte*s act as significant carbon sinks, storing up to 88 kg C<sub>org</sub> m<sup>-2</sup> in their top meters (Monnier et al., 2021), which is why *P. oceanica* is known as the most efficient seagrass species in storing blue carbon, compared to the others (Lavery et al., 2013; Apostolaki et al., 2022).

*P. oceanica* is a key ecosystem component in the Mediterranean Sea, although it represents barely 1% of the total area of the basin (Boudouresque et al., 2006), as it provides a wide range of ecosystem services, in addition to carbon sequestration, such as protection against coastal erosion, nutrient filtering, support to fishery through its nursery and habitat provision functions, and cultural services, with an annual economic value at the level of the entire Mediterranean basin of 305-553 euros/ha in 2015 (Campagne et al., 2015). Although the *P. oceanica* ecosystem in the Mediterranean Sea is protected by numerous directives (Habitats Directive 1992, Barcellona Convention 1995; Bern Convention 1996) and represents the main priority habitat for which SICs and marine protected areas are proposed in the Mediterranean Sea (Agnesi & Cassese, 2008; Montefalcone et al., 2009), this ecosystem seems to be undergoing an alarming decline throughout the basin (Marbà et al., 2014; Montefalcone et al., 2007, 2009; Boudouresque et al., 2009). The estimated decline in *P. oceanica* meadows extent amounted to 34%, from 1965 to 2015 (Telesca et al., 2015), with a corresponding 11-52% reduction in the carbon sink capacity of the Mediterranean basin (Marbà et al., 2014).

The loss of *P. oceanica* meadows could result in the exposure of the underlying *matte* to aerobic conditions that promote remineralization processes, and to physical disturbance that promote erosion phenomena, causing resuspension of carbon and nutrients (Macreadie et al., 2015). However, dead *matte* can persist also for several years after seagrass loss (Boudouresque et al., 2015) and a recent study has shown that dead *matte* could represent a significant sink even after the death of the meadow (Apostolaki et al., 2022). The main causes of the decline of *P. oceanica* include mechanical disturbance of the seabed by trawling, grounding of hulls, anchoring, dredging, coastal constructions (Milazzo et al., 2004; Badalamenti et al., 2011), changes in water quality due to an excess of nutrient, organic matter or pollutant inputs, and increasing warming due to climate change (Marbà & Duarte, 2010; Guerrero-Meseguer et al., 2017). *P. oceanica* is one of the slowest-growing (1–7 cm year<sup>-1</sup> for

orthotropic rhizomes and  $< 14 \text{ cm year}^{-1}$  for plagiotrophic rhizomes, Marbà & Duarte, 1998; Boudouresque et al., 2021) plant species in the biosphere (Jordà et al., 2012) and for this reason its natural recovery after disturbance is assumed to be very slow (Duarte et al., 2006) and its functional extinction has been predicted by  $2049 \pm 10$  (Jordà et al., 2012).

The main strategies to prevent the loss of *P. oceanica* throughout the Mediterranean Sea include (i) the regulation of human activities that have caused the greatest impact on the *P. oceanica* ecosystems, (ii) the effective protection of seagrass habitats and the implementation of controls in those areas where protection already exists, (iii) the ecological restoration of *P. oceanica* habitats through transplantation actions (Boudouresque et al., 2009; Marbà et al., 2014; Calvo et al., 2021). Currently, marine habitat restoration is becoming an important management tool (Casoli et al., 2022), but if special precautions and knowledges are not observed during transplantation, restoration could be unsuccessful, as demonstrated by several failures (Cunha et al., 2012; Boudouresque et al., 2021). Seagrass transplantation must be realized after the impacts that caused the decline have ceased and should not alter the original ecosystems, such as sandy bottoms or rocky reef forests, but should be carried out in an area previously characterized by a seagrass ecosystem (Boudouresque et al., 2021). Long-term monitoring programs are needed to evaluate the success of a reforestation intervention, and environmental friendly transplantation methods should be preferred (Calvo et al., 2021; Boudouresque et al., 2021).

The aim of this study was to investigate the role of *P. oceanica* matte in blue carbon storage, nutrient and trace metal accumulation by analysing sediment cores from three different stages: a naturally growing *P. oceanica* meadow, dead matte and a sixteen years old meadow transplanted onto dead matte. The selected habitats belong to the historically polluted coastal area of the Gulf of Palermo (Sicily, Italy) in the Mediterranean Sea. Since the mid-20<sup>th</sup> century, this coastal area has been subjected to increasing pollution due to the illegal dumping of construction materials and the creation of illegal landfills along the coast, as well as the disposal of untreated urban and industrial wastewater (Genchi et al., 1982; Calvo et al., 1994; Calvo et al., 2021). The increase in anthropogenic impact on the area has led to the regression of the *P. oceanica* meadows that previously characterized the seabed, as evidenced by the discovery of extensive dead *matte* formations (Tomasello et al., 2009). In the last decades, however, the quality of coastal waters has gradually improved, due to the requalification of the urban context, the improvement of wastewater treatment and the reclamation of landfills (ARPA Sicilia e Università degli Studi di Palermo, 2006), allowing the start of an experimental restoration project focused on the recovery of *P. oceanica* habitat. In July 2008 a 40 m<sup>2</sup> seabed area (14 m depth) characterized by dead *matte* was chosen for the transplantation of *P. oceanica* shoots (66 shoots/m<sup>2</sup>) from a donor meadow located in a nearby coastal site (Solanto). Twenty grids of galvanized electro

welded iron wire meshes (1x1 m) were anchored to the seabed using iron spikes (~70 cm long) and 20 *P. oceanica* cuttings were fixed on each grid (Calvo et al., 2021). After an initial downward trend during the first three years of monitoring, mainly due to fishing, shoot density of transplanted *P. oceanica* meadows appeared to increase by 16% six years after transplanting (Pirrota et al., 2015). Twelve years after transplantation, transplanted *P. oceanica* meadows showed comparable structural and functional characteristics with the adjacent natural meadow, with an average density five times higher than the original density (Calvo et al., 2021), proving that dead *matte* is a good substrate on which vegetative cuttings of *P. oceanica* can establish and grow in a relatively short time (a decade), compared to the natural recovery (century to millennia). Based on these promising results, a larger-scale transplanting operation (~800 m<sup>2</sup>) was planned to restore the habitat of *P. oceanica* in the Gulf of Palermo, supported by the “Marine Hazard” PON project, which aims to “develop innovative technologies to identify, monitor and mitigate phenomena of natural and anthropogenic pollution of the marine environment”, also through the restoration of *P. oceanica* meadows (<https://www.marinehazard.cnr.it/en/project/>). In December 2021 the transplantation onto dead *matte* in the Gulf of Palermo was made using a new and sustainable support system (Biosurvey s.r.l.) for the fixation of *P. oceanica* cuttings on the seabed, made of biodegradable plastic (MaterBi ©), which dissolves over time until the rooting process is finished (Calvo et al., 2014; Tomasello et al., 2019).

In the present study, temporal trend of carbon and nitrogen content, isotopic ( $\delta^{13}\text{C}$ ,  $\delta^{15}\text{N}$ ) composition, phosphorus and trace metals (As, Cd, Co, Cr, Cu, Hg, Ni, Mn, Pb, V and Zn) concentration were analysed in sediment cores to: a) evaluate the current state of the recently-transplanted meadow; b) investigate differences between natural meadow, transplanted meadow and dead *matte*; c) reconstruct the geochemical changes and contaminant input occurred in the Gulf of Palermo in the last century.

## Materials and methods

### Study area

The Gulf of Palermo (Fig. 1) is an extensive coastal area with a total surface of 250 km<sup>2</sup> (Paradis et al., 2021), on the northwest coast of Sicily (Italy). The gulf is situated close to the urban centre of the city of Palermo, bounded to the west by the promontory of Pellegrino Mountain, composed of calcareous rocks, and to the east by Cape Zafferano, composed of dolomitic rocks (Tranchina et al., 2008). The area hosts an important harbour on the western side, where shipyards for the construction and repair of ships are located. Four rivers flow into the gulf: Oreto, Eleuterio, Kemonia and Papireto.

The Oreto flows into the central part of the gulf, while the Eleuterio flows into the eastern part. Both waters are mixed with industrial and domestic wastewater. In the XVI century, Kemonia and Papireto were canalized and buried, together with urban sewage, and today flow, with limited capacity, into the eastern part of the Gulf of Palermo. Currently, this coast is characterized by beach deposits that alternate with anthropogenic deposits that can also reach a thickness of hundreds of meters (di Leonardo et al., 2009, Agate et al., 1998). The seabed of the studied area (off Bandita beach, Fig. 1) is 14.8-20.8 m deep, irregular, mainly sandy and includes areas of dead *matte*, *P. oceanica* meadows in regression and *P. oceanica* patches detected at 7-16 m depth (Tomasello et al., 2007; Tomasello et al., 2009).

### **Field sampling**

In November 2021, prior to the new transplantation activity, two marine sediment cores per habitat were collected by scuba-divers, with a hand-corer and a PVC tube (100 cm long and Ø 5.8 cm) from three different habitats in the Bandita coastal area, within the Gulf of Palermo (Fig.1) : a naturally growing *P. oceanica* meadow (Natural meadow, 13°25'13'' N; 38°67'4''E), the *P. oceanica* meadow transplanted in 2008 onto dead *matte* (Old reforestation, 13°25'13'' N; 38°68'15'' E), and dead *matte* (Dead *matte*, 13°25'14'' N; 38°67'23''E). In the present study, only one core per habitat was analysed, although it is planned that the results will be integrated after the analysis of the second replicates. Therefore, the results presented here should be considered preliminary. When taking cores, compaction of the sediment layers is quite unavoidable and is generally corrected with a compression factor. In this study, compression was corrected by distributing the spatial discordances proportionally between the expected and the observed soil column layers (Glew et al., 2001). Compression of sediment cores during coring operations averaged  $24 \pm 6\%$ . The lengths of sediment cores recovered ranged from 53 to 65 cm, corrected decompressed depths ranged from 63 to 90 cm. For grain size analysis, further short sediment cores were taken in three replicates at each habitat using PVC corers (30 cm long and Ø 6 cm).

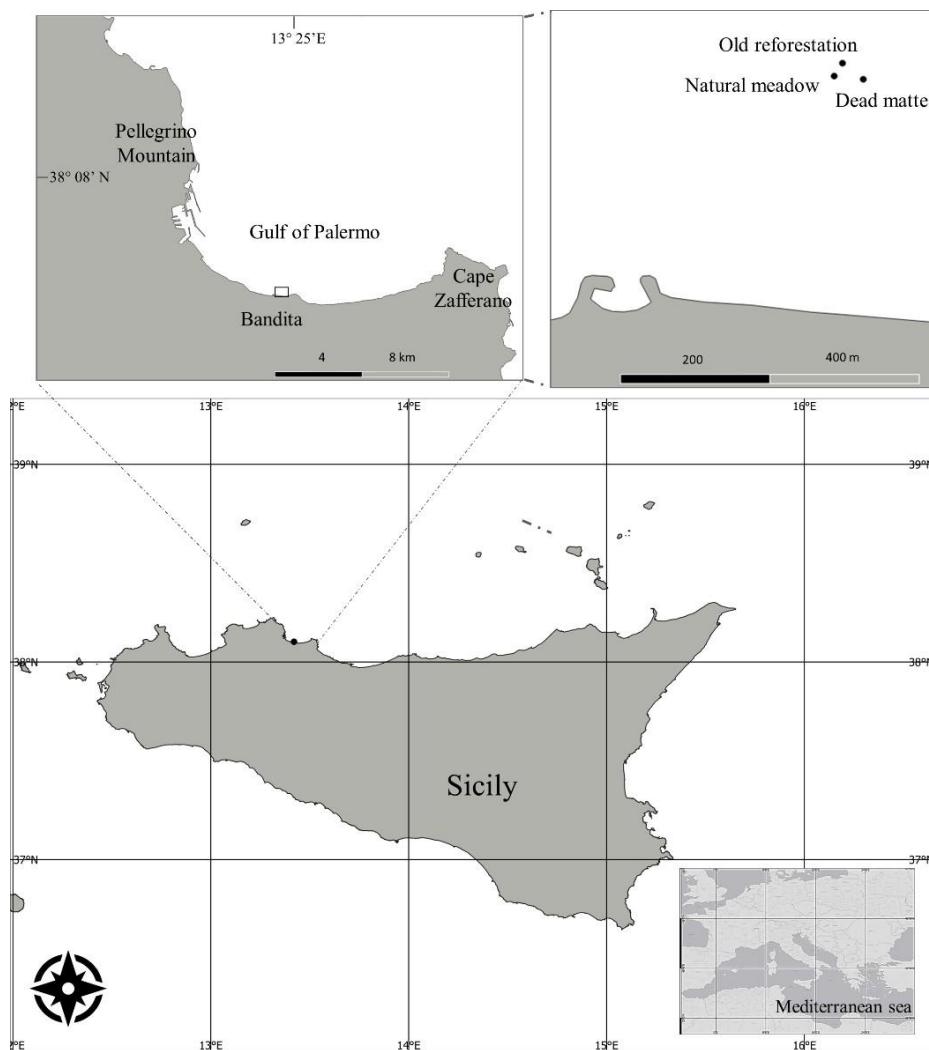


Fig. 1 Map of the Gulf of Palermo and sampling sites at the studied habitats.

## Analytical procedures

### *Elements and isotopes composition*

Once in the laboratory, the sediment cores were immediately frozen at  $-20^{\circ}\text{C}$  vertically in the dark. The cores were cut at regular intervals (1 cm thick layers) along their entire length using a stainless-steel hand saw and then each slice was cut into two halves. A half of each slice was stored in a plastic bag and frozen again at  $-20^{\circ}\text{C}$ , as a backup sample, the other half was analysed. The volume of each half slice was measured with a syringe. Subsequently, all samples were weighed before and after being freeze-dried for 72 hours. After the drying process, the samples were ground to a fine powder and homogenised for elemental concentration, isotopic composition of carbon and nitrogen and trace metals analyses. Organic carbon ( $\text{C}_{\text{org}}$ ) content and  $\delta^{13}\text{C}$  composition of each sample were measured

by weighing  $10 \pm 1$  mg of the sample into a silver capsule (5 x 9 mm) and acidifying these samples with HCl (1 N) to remove inorganic carbon. The samples were completely oven dried for 24 hours and analysed with the isotope ratio mass spectrometer (Thermo IRMS Delta Plus XP) in conjunction with the elemental analyser (Thermo EA -1112). For the analysis of total nitrogen ( $N_{\text{tot}}$ ) content and  $\delta^{15}\text{N}$  composition,  $30 \pm 1$  mg of each sample was weighed into tin capsules (5 x 9 mm) and analysed using the EA-IRMS. The concentration of inorganic carbon ( $C_{\text{inorg}}$ ) was calculated as the difference between the concentration of  $C_{\text{tot}}$  and  $C_{\text{org}}$ . To estimate the dry bulk density (DBD,  $\text{g cm}^{-3}$ ), the dry weight of sediment was divided by the volume of the wet samples. Isotopic ratios were referenced against standard material obtained from the U.S. National Institute of Standards and Technology and given in the conventional delta notation as ‰ deviation from the standards as follows:

$$\delta^{13}\text{C}_{\text{org}} \text{ or } \delta^{15}\text{N}_{\text{tot}} (\text{‰}) = [(R_{\text{sample}} / R_{\text{standard}}) - 1] \times 10^3$$

where R is the ratio  $^{13}\text{C}/^{12}\text{C}$  or  $^{15}\text{N}/^{14}\text{N}$ .

#### *$^{210}\text{Pb}$ dating*

Sediment accumulation rates during the last decades were determined using the  $^{210}\text{Pb}$ . Sediments were initially analysed through gamma spectrometry method and, as  $^{210}\text{Pb}$  activities resulted lower than the detection limits, further alpha spectrometry analysis was carried on.  $^{210}\text{Pb}$  (half-life = 22.3 years) is a naturally produced radionuclide that has been extensively used in the dating of recent sediments. Dating is based on determination of the vertical distribution of  $^{210}\text{Pb}$  derived from atmospheric fallout (termed unsupported  $^{210}\text{Pb}$ , or  $^{210}\text{Pb}_{\text{excess}}$ ), and the known decay rate of  $^{210}\text{Pb}$  (see Appleby and Oldfield 1992). High resolution gamma spectrometric analysis was performed using HPGe detectors. Samples were counted for at least 8 h on Canberra well-type low background HPGe detectors to determine the activities of  $^{137}\text{Cs}$ ,  $^{210}\text{Pb}$  and other gamma emitting radionuclides. Detectors were calibrated against a mixed radionuclide standard solution. The standard was used to prepare a source of identical geometry to that of the samples. Gamma spectra were analysed, and individual radionuclides quantified using Fitzpeaks spectral deconvolution software (JF Computing Services). Alpha spectrometry method:  $^{210}\text{Pb}$  activity was determined by a proxy method through alpha spectrometric measurement of its granddaughter nuclide  $^{209}\text{Po}$ . The method employed was based on Flynn (1968), using double acid leaching of the sediment with  $^{209}\text{Po}$  as an isotopic tracer. The sample was digested using aqua regia and  $^{209}\text{Po}$  was separated by auto-deposition in the leachate on to silver discs. Detection limits were 1 Bq/kg. All these analysis were performed at the School of Ocean and Earth Science of the University of Southampton (UK).

### *Granulometry*

The first 10 cm of each short sediment core for grain size analysis were pre-treated with hydrogen peroxide and Na-hexa-metaphosphate to remove organic matter and prevent flocculation of the particles. The pretreated sediment was then oven dried at 60°C, dry sieved using a set of sieves up to 63 µm to separate the sediment fractions (gravel > 2 mm, sand 2 mm - 63 µm, pelite < 63 µm) and weighed.

### *Trace metals*

The concentrations of Al, P and trace metals (As, Cd, Co, Cr, Cu, Hg, Ni, Mn, Pb, V and Zn) were measured by ICP-OES after the samples were digested using the microwave-assisted acid digestion method according to USEPA Method 3052 (Hanessian, Stephen; Bennanin, 1996). An amount of 0.6 ± 0.3 g of each sample was acidified in a vessel with a solution of HNO<sub>3</sub>-HF-H<sub>2</sub>O<sub>2</sub> and Milli-Q water, then the vessel was sealed and heated in a microwave system. To check the efficiency of the digestion, a reference sample (NIST Standard Reference Material 2702, Marine Inorganic Sediment) with a known concentration of the investigated elements was also run through the process and analysed. After microwave digestion, the samples were filtered to remove undissolved parts and analysed by ICP-OES.

## **Calculation and data analysis**

### *Elemental stocks*

Elements stocks were estimated as the cumulative product of element concentration, decompressed DBD and decompressed sediment slice thickness in the first 63 cm of sediment depth, to allow comparison between habitats, as this is the length of the shortest core. To allow literature comparison elements stocks were then standardized to 1 meter depth, fitting a linear regression of cumulative stock per slice against sediment depth and expressed as Mg·ha<sup>-1</sup>.

### *<sup>210</sup>Pb dating*

The <sup>210</sup>Pb<sub>excess</sub> activity was estimated by subtraction of the average value of <sup>210</sup>Pb activity in deeper core samples, where total <sup>210</sup>Pb activities had fallen to virtually constant values (Cundy and Croudace 1996). Sediment accretion rates were determined using the CF:CS model of <sup>210</sup>Pb dating (Robbins 1978, Appleby and Oldfield, 1992), where the sedimentation rate is given by the slope of the least squares fit for the natural log of the <sup>210</sup>Pb<sub>excess</sub> activity versus depth.

### *Organic carbon origin*

Coastal sediments receive organic matter from autochthonous sources (i.e. locally produced, such as tissues of *P. oceanica*) and allochthonous sources (i.e. transported from *ex situ* areas, e.g. by rivers, coastal runoff or with the tides). The main sources of organic matter have different  $\delta^{13}\text{C}$  and  $\text{C}_{\text{org}}/\text{N}_{\text{tot}}$  values: the  $\delta^{13}\text{C}$  signature of *P. oceanica* tissues (leaves, roots, rhizomes, blades, detritus) ranges between -19.7 ‰ and -9 ‰ (Calizza et al., 2013; Cardona et al., 2007; Fourqurean et al., 2007; Vizzini & Mazzola, 2003). Terrestrial C3 plants  $\delta^{13}\text{C}$  values are between -32 ‰ and -21 ‰ (Deines et al., 1980), while terrestrial C4 plants  $\delta^{13}\text{C}$  values are between -17 ‰ and -9 ‰ (Deines et al., 1980). Marine POC (particulate organic carbon, such as phytoplankton and zooplankton, in coastal environments generally mixed with terrestrial sources as plants detritus and sewage), typically ranges between -18 ‰ and -21 ‰ (Lamb et al., 2006).  $\text{C}_{\text{org}}/\text{N}_{\text{tot}}$  values of terrestrial and aquatic plants may show considerable overlap. Since the tissues of terrestrial plants are mainly composed of lignin and cellulose, which have a low nitrogen concentration, their  $\text{C}_{\text{org}}/\text{N}_{\text{tot}}$  ratio is generally above 12 (Tyson 1994) and is highly variable due to the fluctuation of nitrogen content (Lamb et al., 2006). Similarly, *P. oceanica*  $\text{C}_{\text{org}}/\text{N}_{\text{tot}}$  ratio ranges between 16 and 135 (Pirc & Wollenweber, 1988; Fourqurean et al., 2007; Vizzini et al., 2002; unpublished data from the Laboratory of Marine Biology and Resources - University of Palermo). Algal and bacterial cells are rich in proteins, therefore the  $\text{C}_{\text{org}}/\text{N}_{\text{tot}}$  values of bacteria and algae are generally lower than terrestrial values, ranging between 4 and 6 for bacteria and below 10 for algae (Meyers, 1994; Tyson, 1995). Similarly,  $\text{C}_{\text{org}}/\text{N}_{\text{tot}}$  values of marine POC, as phytoplankton is nitrogen rich, are typically lower than 8. Sediment organic matter  $\delta^{13}\text{C}$  and the  $\text{C}_{\text{org}}/\text{N}_{\text{tot}}$  ratio of bulk sediment should reflect the relative amounts of sources and have been widely used as indicators of organic matter sources in coastal areas and estuaries (Lamb et al., 2006; Yu et al., 2010; Kemp et al., 2010). A crossplot of the  $\text{C}_{\text{org}}/\text{N}_{\text{tot}}$  ratio against  $\delta^{13}\text{C}$  was used for an initial investigation of the sources of organic matter that have characterized the Gulf of Palermo to date.

### *Trace metals*

To determine the contamination level in the area, in terms of eco-toxicological implications, concentrations of trace metals ( $\text{mg kg}^{-1}$ , not normalized) were compared to the following set of sediment quality guidelines (SQG): TEL (threshold effects level) and PEL (probable effects level); ERL (toxic effects range low) and ERM (toxic effects range medium) (Macdonald et al., 1996; Long et al., 1995). The classification of the SQGs used and the relative effects are described in Tab. 1.



Tab. 1 Classification of SQGs and relative association to toxic effects.

Sediment quality guidelines	Effect	
TEL and PEL	< TEL	Not associated with adverse biological effects
	Between TEL-PEL	May occasionally be associated with adverse biological effects
	> PEL	Frequently associated with adverse biological effects
ERM and ERM	< ERL	Minimal toxic effects range
	Between ERL-ERM	Toxic effects would occasionally occur
	> ERM	Toxic effects would frequently occur

One of the most important factors controlling the natural distribution of trace metals in marine sediments is grain size. To compensate for natural variability due to differences in sediment composition and to compare trace element concentrations between sediment samples, it is therefore necessary to compensate for the effects of grain size. A widely used method for normalising trace element data is the use of inorganic chemical constituents such as Al, Fe, Sc and Cs, which are elementary proxies for mineralogical and granulometric changes in sediments (Loring et al., 1991). In this study, trace element concentrations measured in sediment samples were normalised using Al, measured in the corresponding slices, which is widely used for the normalisation of trace element data from marine sediments (Din, 1992; Cheevaporn et al., 1997; Di Leonardo et al., 2012; Ho et al., 2012), as it has no anthropogenic origin (Qingjie et al. 2008) or is so abundant that the contribution from anthropogenic sources is insignificant, and it has minimal natural variation in sediment.

Enrichment factor (EF), that is an index that allows to distinguish between enrichment of trace metals from anthropogenic or natural sources (Brady et al., 2015) was calculated for each slice. EF is defined as the observed trace element/Al ratio in the sediment sample of interest ( $(TE/Al)_{\text{sediment}}$ ) divided by the background trace element/Al ratio ( $(TE/Al)_{\text{background}}$ ):

$$EF = (TE/Al)_{\text{sediment}} / (TE/Al)_{\text{background}}$$

In this study, background reference concentrations of trace metals and Al are those from the deepest layer of the dead *matte* core, from which TE were measured (27 cm of depth). As dead *matte* is the habitat with the lower sediment accumulation rate, as measured by  $^{210}\text{Pb}$  method, this layer appears the oldest considering the whole habitat analysed, and therefore is a good reference for historical unpolluted sediment in the studied area.

The EF threshold values for sediment quality were described by Qingjie et al. (2008) and enable the classification into six quality classes, which describe the degree of contamination of a sediment, as described in Tab. 2.

Tab. 2 EFs and related sediment quality.

Class	Qualification of sediment	EF value (Qingjie et al., 2008)
0	Unpolluted	EF<1
1	Slightly polluted	1<EF<3
2	Moderately polluted	3<EF<5
3	From moderately polluted to strongly polluted	5<EF<10
4	Strongly polluted	10<EF<25
5	From strongly polluted to extremely polluted	25<EF<50
6	Extremely polluted	EF>50

### *Statistical analysis*

To investigate the differences between the habitat studied, a Kruskal-Wallis test was used to compare sediment DBD ( $\text{g cm}^{-3}$ ), elemental concentration ( $C_{\text{org}}$  %,  $C_{\text{inorg}}$  %,  $N_{\text{tot}}$  %) and isotopic composition ( $\delta^{13}\text{C}$  %,  $\delta^{15}\text{N}$  %) measured in the upper 63 cm of the cores, as well as P% and trace element concentrations normalized to Al, measured in the upper 30 cm the cores. When significant differences between habitats were found, a pairwise Wilcoxon rank sum test, with “Bonferroni” correction, was used to understand which habitat was significantly different from the other.

Kruskal-Wallis test was also used to determine the effects of pollution in the Gulf of Palermo, comparing sediment properties (DBD,  $C_{\text{org}}$ ,  $C_{\text{inorg}}$ ,  $\delta^{13}\text{C}$ ,  $N_{\text{tot}}$ ,  $\delta^{15}\text{N}$ ), and trace element enrichment factors before and after 1950, when the exposure to anthropogenic factors began (Pirrotta et al., 2015). For sediment properties, the comparison has been done considering the last 120 years, dated by  $^{210}\text{Pb}$ , to specifically understand the changes happened in the century during which the main anthropogenic disturbances took place.

Pearson correlation analysis was performed to identify significant trends in the distribution of geochemical variables and trace element concentrations along sediment depth.

Furthermore, threshold regression analysis was performed in order to identify significant change points in the vertical profiles of P % and trace metals, considering the last 120 years, using the *chnppt* package on R software, with the model “segmented” (Fong et al., 2017).

All the analysis were performed using R version 4.3.1. (R Core Team, 2021).

## Results

### Nutrient stocks

Overall, the nutrient stocks in the upper 63 cm of the sediment depth were similar in the three habitats studied (Fig. 2), Natural meadow, Old reforestation, Dead matte. In more detail, the habitat Dead matte had the highest  $C_{\text{org}}$  stock ( $9.5 \text{ kg m}^{-2}$ ) followed by Old reforestation ( $7.4 \text{ kg m}^{-2}$ ) and Natural meadow ( $6.5 \text{ kg m}^{-2}$ ).  $N_{\text{tot}}$  stocks were very similar between habitats ( $0.24 \text{ kg m}^{-2}$ ,  $0.29 \text{ kg m}^{-2}$ ,  $0.29 \text{ kg m}^{-2}$ , respectively for Natural meadow, Old reforestation and Dead matte). Old reforestation showed the highest  $C_{\text{inorg}}$  stock in the upper 63 cm ( $23.9 \text{ kg m}^{-2}$ ), followed by Dead matte ( $19.30 \text{ kg m}^{-2}$ ) and Natural meadow ( $17.8 \text{ kg m}^{-2}$ ).

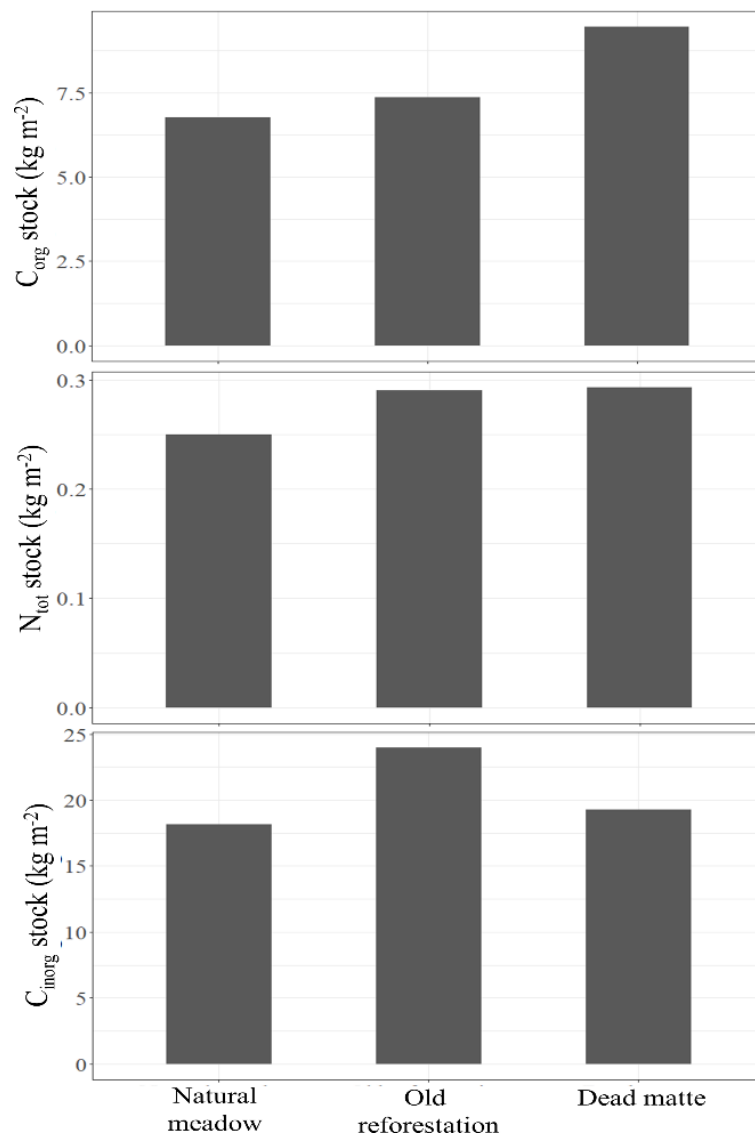


Fig. 2 Barplot of  $C_{\text{org}}$ ,  $N_{\text{tot}}$  and  $C_{\text{inorg}}$  stock ( $\text{kg m}^{-2}$ ) at top 63 cm (maximum common length of cores) at each habitat.

Nutrient stocks extrapolated to the uppermost metre of sediment were 89 Mg C<sub>org</sub> ha<sup>-1</sup>, 306 Mg C<sub>inorg</sub> ha<sup>-1</sup> and 3.5 Mg N<sub>tot</sub> ha<sup>-1</sup> in the Natural meadow; 100 Mg C<sub>org</sub> ha<sup>-1</sup>, 412 Mg C<sub>inorg</sub> ha<sup>-1</sup>, 4.2 Mg N<sub>tot</sub> ha<sup>-1</sup> in the Old reforestation habitat; 134 Mg C<sub>org</sub> ha<sup>-1</sup>, 324 Mg C<sub>inorg</sub> ha<sup>-1</sup>, 4.5 Mg N<sub>tot</sub> ha<sup>-1</sup> in the Dead matte habitat (Tab. 3).

Tab. 3 C<sub>org</sub>, C<sub>inorg</sub> and N<sub>tot</sub> at top 1 meter of sediment at each habitat.

	C <sub>org</sub> stock (Mg ha <sup>-1</sup> ) top 1 m	C <sub>inorg</sub> stock (Mg ha <sup>-1</sup> ) top 1 m	N <sub>tot</sub> stock (Mg ha <sup>-1</sup> ) top 1 m
<b>Natural meadow</b>	88.8	306.2	3.5
<b>Old reforestation</b>	100.1	412.4	4.2
<b>Dead matte</b>	134.0	324.2	4.5

### **<sup>210</sup>Pb dating and accumulation rates**

The <sup>210</sup>Pb<sub>excess</sub> activity (Fig.3) showed a quasi-exponential decline with sediment depth at Old reforestation, while the of <sup>210</sup>Pb profiles at Natural meadow and Dead *matte* showed shifts in the slope. Each profile reaches the supported activity of 7 Bq kg<sup>-1</sup>. <sup>210</sup>Pb<sub>excess</sub> inventories at Natural meadow (1134 Bq m<sup>-2</sup>) and Old reforestation (1144 Bq m<sup>-2</sup>) were similar, while lower <sup>210</sup>Pb<sub>excess</sub> inventories were measured in Dead matte (1085 Bq m<sup>-2</sup>) (Fig. 4). Sediment accumulation rate (SAR) and Mass accumulation rate (MAR) were similar between Old reforestation (0.15 cm y<sup>-1</sup> SAR; 0.15 cm y<sup>-1</sup> MAR) and Natural meadow (0.11 cm y<sup>-1</sup> SAR; 0.12 cm y<sup>-1</sup> MAR), while they were lower for Dead matte (0.05 cm y<sup>-1</sup> SAR; 0.05 cm y<sup>-1</sup> MAR). In the last 120 years the rate of accumulation of C<sub>org</sub>, C<sub>inorg</sub> and N<sub>tot</sub> were lower in Dead matte (10.39 g C<sub>org</sub> m<sup>-2</sup> y<sup>-1</sup>, 10.88 g C<sub>inorg</sub> m<sup>-2</sup> y<sup>-1</sup>, 0.31 g N<sub>tot</sub> m<sup>-2</sup> y<sup>-1</sup>) than in Natural meadow (11.80 g C<sub>org</sub> m<sup>-2</sup> y<sup>-1</sup>, 27.02 g C<sub>inorg</sub> m<sup>-2</sup> y<sup>-1</sup>, 0.47 g N<sub>tot</sub> m<sup>-2</sup> y<sup>-1</sup>) and in Old reforestation (21.16 g C<sub>org</sub> m<sup>-2</sup> y<sup>-1</sup>, 43.74 g C<sub>inorg</sub> m<sup>-2</sup> y<sup>-1</sup>, 0.76 g N<sub>tot</sub> m<sup>-2</sup> y<sup>-1</sup>). This latter habitat had the higher accumulation rate.

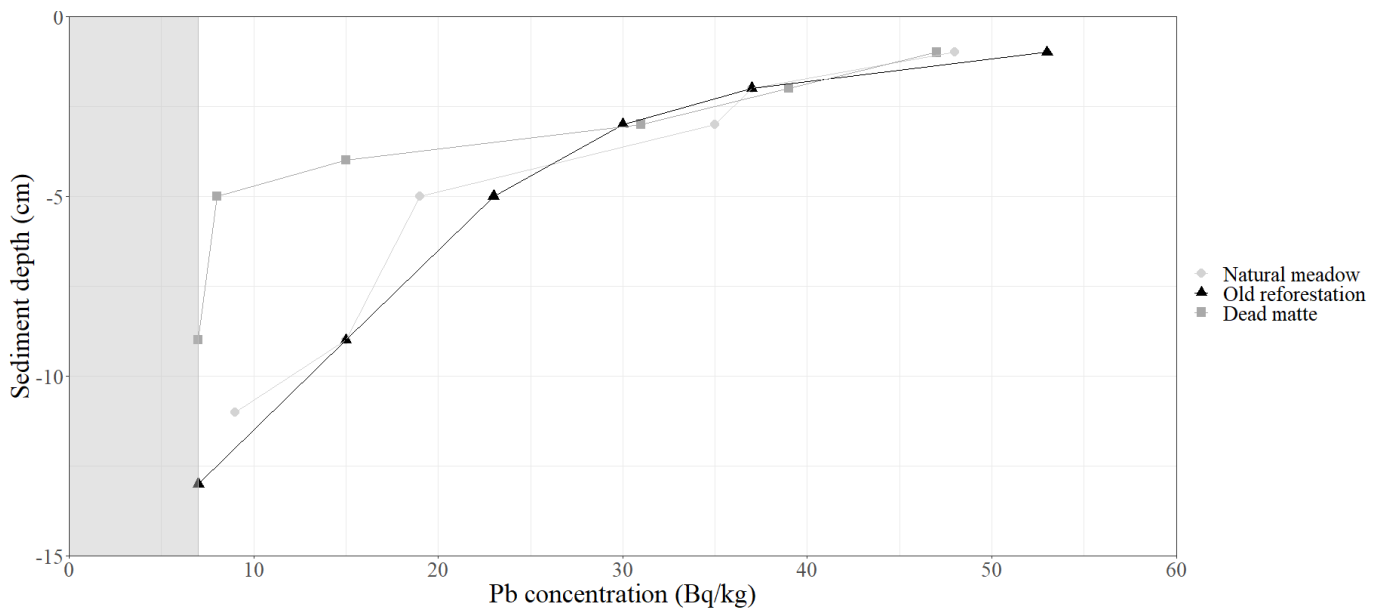


Fig. 3 Total  $^{210}\text{Pb}$  activity ( $\text{Bq kg}^{-1}$ ) with sediment depth. Shaded area represents the supported activity ( $7 \text{ Bq kg}^{-1}$ ).

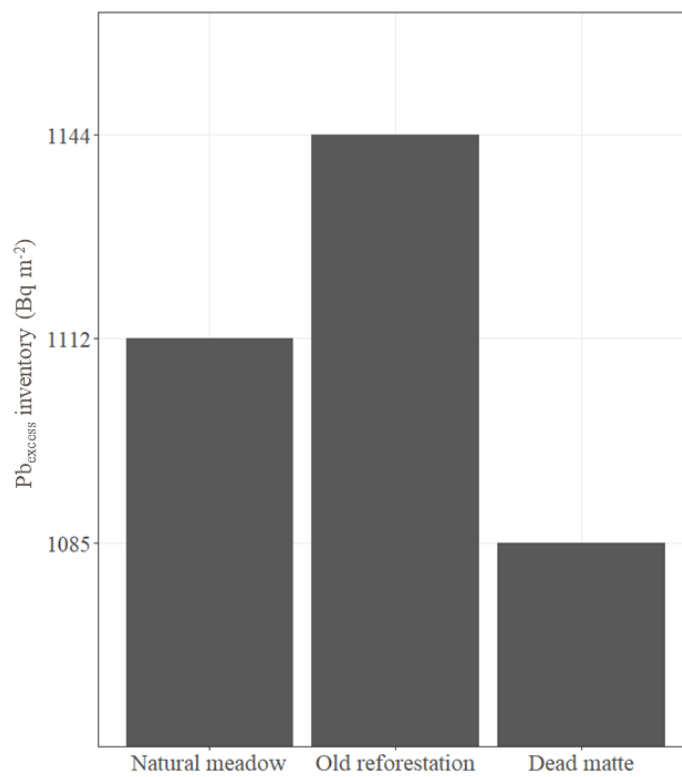


Fig. 4 Inventories of  $^{210}\text{Pb}_{\text{excess}}$  ( $\text{Bq m}^{-2}$ ) at each habitat (in 9 cm of depth).

The sediment beneath each habitat was mainly sandy and the granulometric properties were similar in the habitats studied (Table 4).

The Kruskal-Wallis test revealed significant differences in DBD,  $C_{org}$  content,  $C_{inorg}$  content and  $C_{org}/N_{tot}$  ratio in the uppermost 63 cm between the habitat studied. The pairwise Wilcoxon rank sum test showed that Dead *matte* had significantly lower DBD ( $0.85 \pm 0.18 \text{ g cm}^{-3}$ ) and higher  $C_{org}$  content ( $1.68 \pm 0.83 \text{ } C_{org} \text{ \% DW}$ ) than Old reforestation ( $1.11 \pm 0.20 \text{ g cm}^{-3}$ ;  $1.17 \pm 0.60 \text{ } C_{org} \text{ \% DW}$ ) and Natural meadow ( $1.13 \pm 0.23 \text{ g cm}^{-3}$ ;  $1.2 \pm 0.46 \text{ } C_{org} \text{ \% DW}$ ). Old reforestation showed higher  $C_{inorg}$  content ( $3.58 \pm 0.62 \text{ } C_{inorg} \text{ \% DW}$ ) than Natural meadow ( $3.10 \pm 0.37 \text{ } C_{inorg} \text{ \% DW}$ ) and Dead *matte* ( $3.11 \pm 0.76 \text{ } C_{inorg} \text{ \% DW}$ ). Dead *matte* showed significantly higher  $C_{org}/N_{tot}$  ratio ( $32.80 \pm 11.21$ ) than Natural meadow ( $27.7 \pm 8.10$ ) and Old reforestation ( $25.26 \pm 7.57$ ). No significant difference between Natural meadow, Old reforestation and Dead *matte* was found in  $N_{tot}$  content ( $0.04 \pm 0.01$ ;  $0.05 \pm 0.02$ ;  $0.05 \pm 0.02 \text{ } N_{tot} \text{ \% DW}$ , respectively),  $\delta^{13}\text{C}$  ( $-17.0 \pm 1.4 \text{ ‰}$ ;  $-17.2 \pm 1.6 \text{ ‰}$ ;  $16.8 \pm 2.3 \text{ ‰}$ , respectively) and  $\delta^{15}\text{N}$  ( $3.3 \pm 1.3 \text{ ‰}$ ;  $3.4 \pm 1.1 \text{ ‰}$ ;  $3.8 \pm 1.1 \text{ ‰}$ , respectively) (Table 4 and 5).

Tab. 4 Mean  $\pm$  STDEV of DBD, elements content, stable isotopes and  $C_{org}/N_{tot}$  of each habitat, considering the uppermost 63 cm of sediment depth. Mean  $\pm$ STDEV of the granulometric properties in the uppermost 10 cm of sediment depth.

	Natural meadow	Old reforestation	Dead <i>matte</i>
<b>DBD <math>\text{g cm}^{-3}</math></b>	$1.13 \pm 0.23$	$1.11 \pm 0.20$	$0.85 \pm 0.18$
<b><math>C_{org}</math> (%)</b>	$1.2 \pm 0.46$	$1.17 \pm 0.60$	$1.68 \pm 0.83$
<b><math>C_{inorg}</math> (%)</b>	$3.10 \pm 0.37$	$3.58 \pm 0.62$	$3.11 \pm 0.76$
<b><math>\delta^{13}\text{C}</math> (‰)</b>	$-17.0 \pm 1.4$	$-17.2 \pm 1.6$	$-16.8 \pm 2.3$
<b><math>N_{tot}</math> (%)</b>	$0.04 \pm 0.01$	$0.05 \pm 0.02$	$0.05 \pm 0.02$
<b><math>\delta^{15}\text{N}</math> (‰)</b>	$3.3 \pm 1.3$	$3.4 \pm 1.1$	$3.8 \pm 1.1$
<b><math>C_{org}/N_{tot}</math></b>	$27.7 \pm 8.10$	$25.26 \pm 7.57$	$32.8 \pm 11.21$
<b>Gravel &gt; 2 mm (%)</b>	$3.6 \pm 0.4$	$6.2 \pm 1.0$	$3.0 \pm 0.2$
<b>Sand 2mm-63 <math>\mu\text{m}</math> (%)</b>	$81.9 \pm 2.3$	$79.3 \pm 2.7$	$80.9 \pm 6.1$
<b>Pelite &lt; 63 <math>\mu\text{m}</math> (%)</b>	$14.5 \pm 2.0$	$14.5 \pm 2.3$	$16.0 \pm 6.0$

Tab. 6 Kruskal-Wallis results, comparison between pre- and post-1950 values of DBD, element content, isotopes composition,  $C_{org}/N_{tot}$  and accumulation rates at each habitat, considering the last 120 years.

Habitat	Variable	pre-1950	post-1950	p-value
Natural meadow		(n=4)	(n=5)	
	DBD (g cm <sup>-3</sup> )	0.69 (0.67;0.70)	0.67 (0.65;0.69)	< 0.05
	$C_{org}$ (%)	1.67 (1.45; 1.84)	1.36 (1.30; 1.44)	< 0.05
	$C_{inorg}$ (%)	3.39 (3.24; 3.48)	3.45 (3.10; 3.91)	< 0.05
	$\delta^{13}C$ (‰)	-15.8 (-16.6; -15.0)	-16.4 (-16.7; -16.4)	< 0.05
	$N_{tot}$ (%)	0.05 (0.05; 0.06)	0.07 (0.06; 0.07)	< 0.05
	$\delta^{15}N$ (‰)	4.9 (4.8; 5.2)	5.3 (4.8; 5.5)	n.s.
	$C_{org}/N_{tot}$	28.9 (27.3; 30.6)	20.9 (19.8; 21.8)	< 0.05
	$C_{org}$ acc. rate (g m <sup>-2</sup> y <sup>-1</sup> )	10.2 (9.91; 10.4)	8.86 (7.90; 8.86)	< 0.05
$C_{inorg}$ acc. rate (g m <sup>-2</sup> y <sup>-1</sup> )	23.7 (23.5; 23.8)	20.9 (17.7; 22.0)	< 0.05	
$N_{tot}$ acc. rate (g m <sup>-2</sup> y <sup>-1</sup> )	0.42 (0.42; 0.42)	0.39 (0.34; 0.41)	n.s.	
Old reforestation		(n=7)	(n=8)	
	DBD (g cm <sup>-3</sup> )	0.85 (0.77; 0.98)	0.76 (0.66; 0.83)	< 0.05
	$C_{org}$ (%)	1.54 (1.25;2.06)	1.57 (1.40; 1.95)	n.s.
	$C_{inorg}$ (%)	3.23 (3.14; 3.32)	3.43 (3.37; 3.53)	< 0.05
	$\delta^{13}C$ (‰)	-16.5 (-17.0; -15.2)	-16.0 (-16.5; -15.2)	< 0.05
	$N_{tot}$ (%)	0.05 (0.04; 0.06)	0.06 (0.05; 0.07)	< 0.05
	$\delta^{15}N$ (‰)	4.8 (4.5; 5.0)	4.3 (4.1; 4.4)	n.s.
	$C_{org}/N_{tot}$	25.5 (22.8; 33.2)	25.2 (22.5; 33.4)	n.s.
	$C_{org}$ acc. rate (g m <sup>-2</sup> y <sup>-1</sup> )	18.3 (17.9; 18.5)	16.3 (14.9; 17.0)	< 0.05
$C_{inorg}$ acc. rate (g m <sup>-2</sup> y <sup>-1</sup> )	38.5 (38.4; 38.6)	34.9 (34.2; 37.8)	n.s.	
$N_{tot}$ acc. rate (g m <sup>-2</sup> y <sup>-1</sup> )	0.67 (0.67; 0.68)	0.64 (0.60; 0.65)	< 0.05	
Dead matre		(n=3)	(n=2)	
	DBD (g cm <sup>-3</sup> )	0.61 (0.60; 0.62)	0.7 (0.66; 0.74)	< 0.05
	$C_{org}$ (%)	3.2 (2.95; 3.66)	2.02 (1.60; 2.44)	< 0.05
	$C_{inorg}$ (%)	2.21 (1.87; 2.82)	3.49 (2.90; 3.62)	< 0.05
	$\delta^{13}C$ (‰)	-14.3 (-14.7; -14.0)	-16.0 (-16.3; -15.7)	n.s.
	$N_{tot}$ (%)	0.09 (0.09; 0.09)	0.08 (0.07; 0.08)	< 0.05
	$\delta^{15}N$ (‰)	5.1 (5.4; 5.5)	5.4 (5.0; 5.3)	n.s.
	$C_{org}/N_{tot}$	36.8 (33.9; 42.6)	24.8 (21.1; 28.4)	n.s.
	$C_{org}$ acc. rate (g m <sup>-2</sup> y <sup>-1</sup> )	8.84 (8.14; 8.99)	5.91 (5.37; 6.46)	n.s.
$C_{inorg}$ acc. rate (g m <sup>-2</sup> y <sup>-1</sup> )	10.2 (9.88; 11.1)	13.4 (13.0; 13.8)	n.s.	
$N_{tot}$ acc. rate (g m <sup>-2</sup> y <sup>-1</sup> )	0.28 (0.28; 0.28)	0.28 (0.28; 0.28)	n.s.	

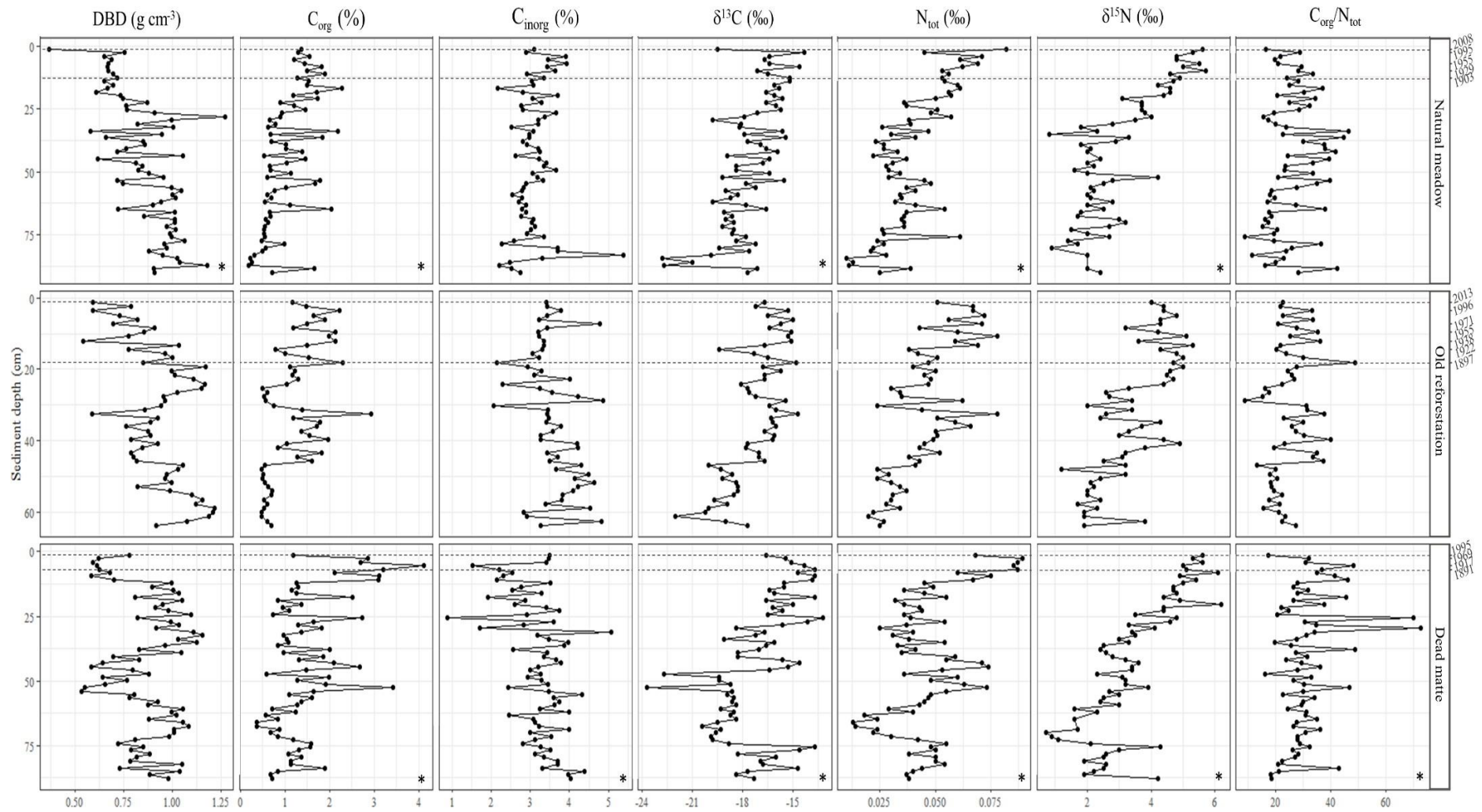


Fig. 3 Vertical profiles of DBD (g cm<sup>-3</sup>), C<sub>org</sub> (DW %), C<sub>inorg</sub> (DW %), δ<sup>13</sup>C (‰), N<sub>tot</sub> (‰), δ<sup>15</sup>N (‰) and C<sub>org</sub>/N<sub>tot</sub> with sediment depth. Temporal trend for the last 120 years is provided on the second y axis and highlighted through dotted lines. Asterisks indicate significant correlation with sediment depth.



## Organic carbon origin

The  $C_{org}/N_{tot}$  vs.  $\delta^{13}C$  crossplot showed that the organic matter in the sediment originated mainly from autochthonous *P. oceanica* sources, and this result is to be expected in *P. oceanica* meadows and mattes. However, due to the relatively low  $C_{org}/N_{tot}$  ratio of the studied cores (24-31 for the pre-1950 sediments, 21-27 for the post-1950 sediment) compared to the broader range of  $C_{org}/N_{tot}$  of *P. oceanica* tissues (20-130), part of the organic matter from the studied sediment could also originate from marine algae, bacteria and POC, as these sources have lower  $C_{org}/N_{tot}$  ratios. The values before and after 1950 partially clustered, as after 1950 there was a slight decrease in the  $C_{org}/N_{tot}$  ratio in Dead *matte* and Natural meadow, and a slight enrichment of  $\delta^{13}C$  in each habitat. This trend was also described in an earlier analysis carried out on two unvegetated sediment cores from the coast of the Gulf of Palermo (Di Leonardo et al., 2012). There, it was suggested that the lower  $C_{org}/N_{tot}$  ratio and the enriched  $\delta^{13}C$  values recorded after 1960 could testify to an increase in the trophic status of the area and in phytoplankton growth and biomass, leading to a greater accumulation of marine organic matter in the sediments. Further studies using stable isotope mixing models are needed to understand the contribution of each potential source to the organic matter of sediment.

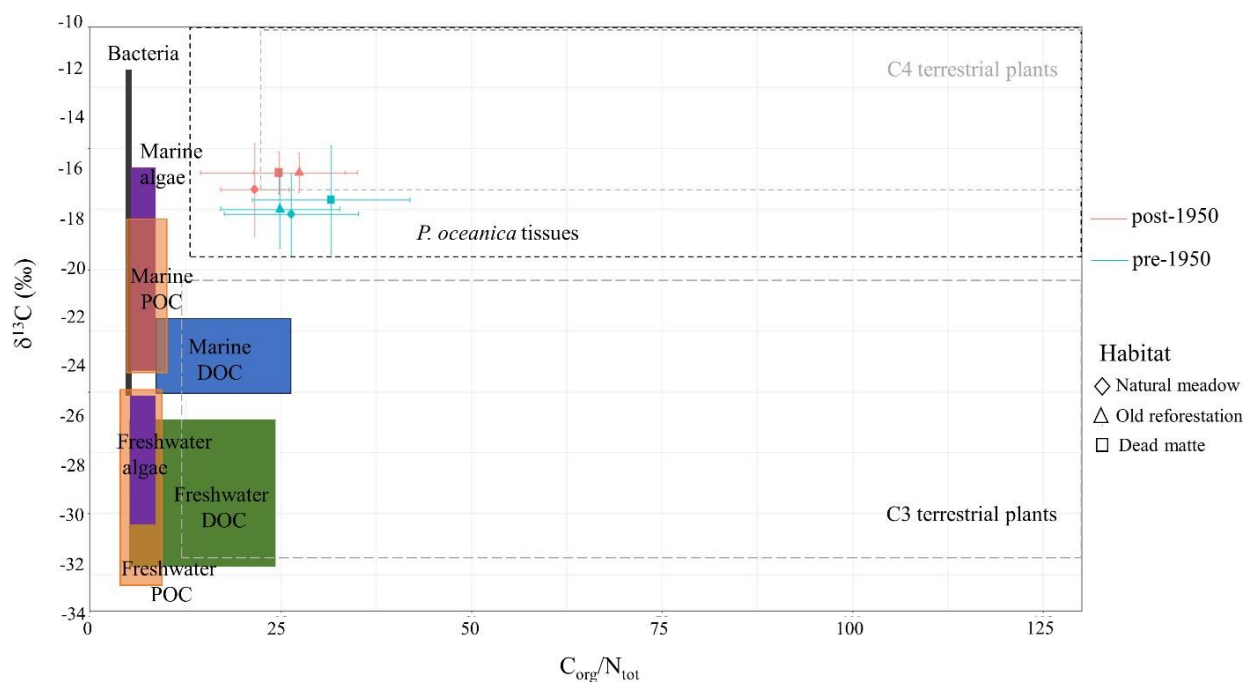


Fig. 4 Mean  $\pm$ STDEV of  $C_{org}/N_{tot}$  vs  $\delta^{13}C$  of Natural meadow, Old reforestation, Dead *matte*, divided into values before and after 1950. Crossplot modified from Lamb et al., 2006.

## Trace metals and phosphorus

Concentrations of trace metals and phosphorus and comparison with offshore and inshore unvegetated sediments collected in previous studies (Di Leonardo et al., 2009, 2012) and with SQGs are provided in Tab. 7. Kruskal-Wallis test revealed significant differences in the concentration of Cu, Zn and Mn, normalized to Al, between the studied habitats (Tab. 8). In particular, pairwise Wilcoxon test showed a significantly higher Cu, Zn and Mn concentration in Natural meadow and Old reforestation than Dead *matte*. In addition, Natural meadow had a significantly higher P % value than the other habitats, Old reforestation had higher P % value than Dead *matte* (Tab. 8).

Normalization to Al changed considerably the depth profiles of trace metals. Vertical profiles of trace metals concentration normalized to Al (Fig. 5) showed a similar trend between habitats. Pearson correlation analysis revealed a significant increase towards the top layers in Natural meadow and Dead *matte* for all trace metals. This increase is particularly evident in Natural meadow after 1968 and in Dead *matte* after 1943.

Threshold-analysis enabled the identification of significant changes in the slope of the profiles, i.e. points after which a significant change in the association between trace metals concentration and depth can be detected. A significant change point in the Cd/Al and Cu/Al profiles in Natural meadow was identified at 7.03 cm depth, corresponding to the year 1955, and a significant change point in As/Al was identified at 12.65 cm depth, corresponding to the year 1903 (Fig. 5). Threshold analysis revealed a significant change point for all trace metals profiles of Old reforestation at 7.2 cm depth, which corresponds to 1971. It can be clearly seen that the vertical profiles of trace metals of Old reforestation show two drastic increases at 1955 and 1971, after which the trace metals concentration returns to pre-1950 values. Significant changes were identified for all trace element profiles of Dead *matte*, at 5.39 cm depth, which corresponds to the year 1917, except for As/Al, which shows a significant change point at 4.04 cm depth (1943). It deserves to be noted that the particular trends of trace metals concentration in Old reforestation have been confirmed by also presenting the vertical profiles of trace metals normalized to C<sub>org</sub> %, to avoid interpretation errors that could result from errors in the measurement of Al concentration (data not shown).

Overall, EF values (Tab. 9, Fig. 6) were higher for each trace metals and habitat in sediment layers stratified after 1950. The Kruskal-Wallis test revealed a significant difference between the EFs of Hg, Cu and Zn before 1950 and after 1950 in Natural meadow. A significant difference between the EFs of Hg, Pb, V and Zn was found in the Dead *matte*. In the Old reforestation, all EF values in the sediment after 1950 were significantly higher than before 1950. Cu is the trace metal with the highest EF value after 1950, in each habitat, followed by Hg and Zn. Overall, the highest EF values were measured in Natural meadow.

Tab. 7 Mean  $\pm$ STDEV of trace metals and phosphorus concentration (mg/kg), for each habitat. Trace metal values refer to the first 20 cm of depth (~ 30 cm decompressed). Comparison with Sediment Quality Guidelines and unvegetated offshore and coastal sediments from the same area (Di Leonardo, 2009; 2012) are also reported.

Trace element (mg kg <sup>-1</sup> )	SQG TEL	SQG SEL	SQG ERL	SQG ERM	Natural meadow (this study)	Old reforestation (this study)	Dead matte (this study)	Coastal unvegetated sediment (Di Leonardo et al., 2012, AC core)	Offshore unvegetated sediment (Di Leonardo et al., 2009)
Cd	0.68	4.21	1.2	9.6	0.25 $\pm$ 0.04	0.26 $\pm$ 0.04	0.28 $\pm$ 0.03	0.05-0.34	-
Hg	-	-	0.01	0.71	0.08 $\pm$ 0.02	0.06 $\pm$ 0.01	0.07 $\pm$ 0.03	0.06-2.34	0.025-0.707
Co	-	-	-	-	6.3 $\pm$ 0.8	6.6 $\pm$ 1.2	7.4 $\pm$ 1.3	1.2-6.5	-
Cr	52.3	160	81	370	17.0 $\pm$ 2.7	15.9 $\pm$ 2.5	16.8 $\pm$ 3.6	6.5-36.6	-
Cu	18.7	108	34	270	13.9 $\pm$ 2.4	12.9 $\pm$ 1.7	11.7 $\pm$ 3.9	2.4-34.9	12.3-38.6
Ni	15.9	30.2	20.9	51.6	13.7 $\pm$ 1.8	13.5 $\pm$ 1.8	14.7 $\pm$ 1.9	2.3-17.8	21.5 – 45.8
Pb	30.2	112	46.7	218	8.81 $\pm$ 1.7	9.13 $\pm$ 2.1	8.86 $\pm$ 2.3	8.4-66.5	11.6-60.2
Zn	124	271	150	410	23.9 $\pm$ 5.2	23.5 $\pm$ 5.7	20.6 $\pm$ 5.3	8.4-83.9	-
V	-	-	-	-	28.2 $\pm$ 3.7	26.6 $\pm$ 3.5	29.8 $\pm$ 5.0	10.4-48.8	-
As	-	-	8.2	70	18.5 $\pm$ 6.1	27.0 $\pm$ 5.7	33.3 $\pm$ 11.3	4.7-32.8	9.6-19.3
Mn	-	-	-	-	207.4 $\pm$ 26	185.2 $\pm$ 30.3	182.4 $\pm$ 34.5	158.4 – 278.6	216-379
P	-	-	-	-	348.8 $\pm$ 80.0	296.2 $\pm$ 34.6	271.1 $\pm$ 63.0	-	-

Tab. 8 Kruskal-Wallis and Pairwise Wilcoxon Rank Sum test, comparison in trace metals concentration, normalized at Al, and P % between Natural meadow, Old reforestation and Dead *matte*.

Kruskal-Wallis test				Pairwise Wilcoxon Rank Sum Test
Variable	DF	Chi-squared	p-value	
Cd/Al	2	4.527	0.10	NAT = OLD = DM
Hg/Al	2	5.643	0.05	NAT = OLD = DM
Co/Al	2	2.806	0.24	NAT = OLD = DM
Cr/Al	2	6.032	0.05	NAT = OLD = DM
Cu/Al	2	8.826	<b>0.01</b>	NAT = OLD > DM
Ni/Al	2	4.647	0.09	NAT = OLD = DM
Pb/Al	2	5.743	0.05	NAT = OLD = DM
V/Al	2	5.335	0.07	NAT = OLD = DM
Zn/Al	2	8.542	<b>0.01</b>	NAT = OLD > DM
As/Al	2	0.7567	0.68	NAT = OLD = DM
Mn/Al	2	7.800	<b>&lt;0.01</b>	NAT = OLD > DM
P %	2	12.09	<b>&lt;0.01</b>	NAT > OLD > DM

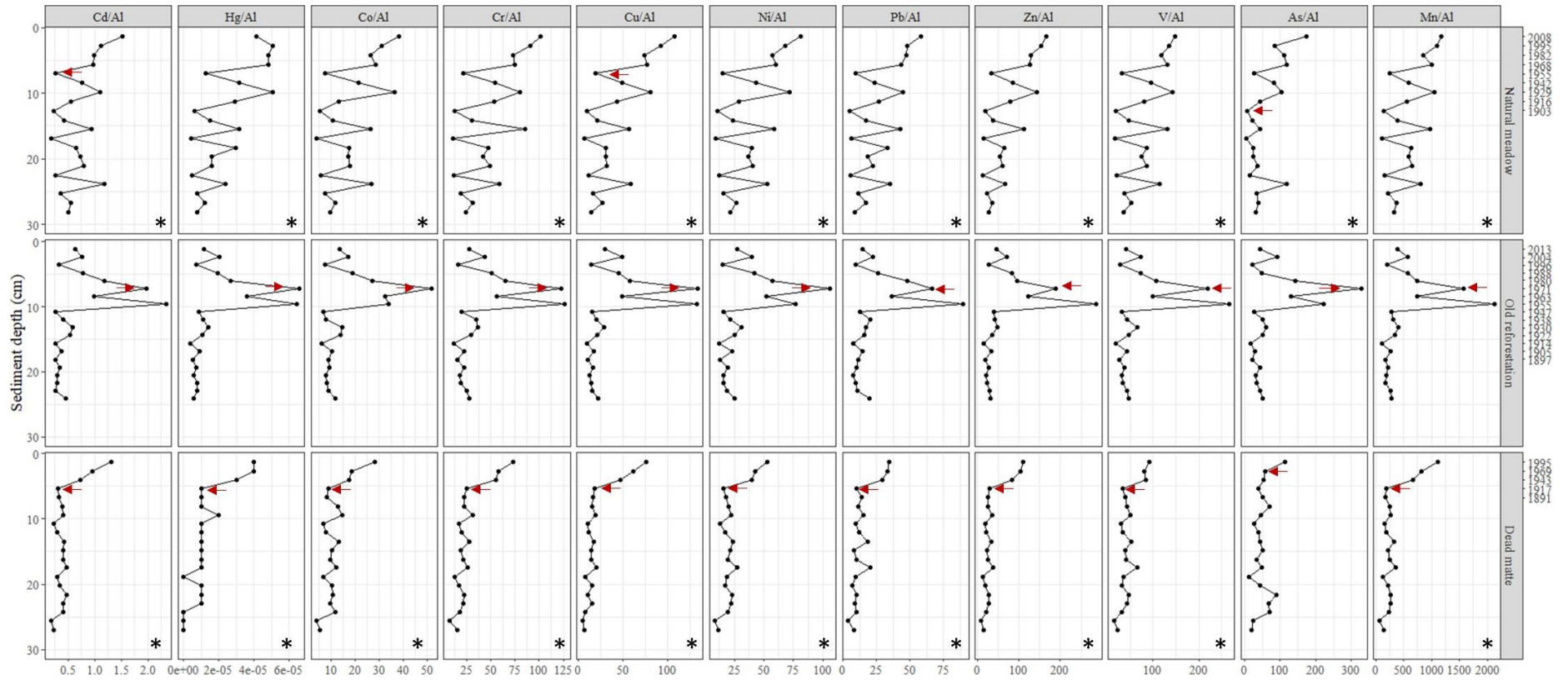


Fig. 5 Vertical profiles of trace metals concentration, normalized at Al, with sediment depth. Temporal trend for the last 120 years is provided on the second y axis. Asterisks indicate significant correlation with sediment depth, red arrows indicate threshold points.

Tab. 9 Kruskal-Wallis results, comparison between pre- and post-1950 EF values.

Habitat	Variable	pre-1950	post-1950	p-value
Natural meadow		(n=15)	(n=5)	
	EF Cd	2.8 ± 1.4	4.4 ± 2.1	n.s.
	EF Hg	4.4 ± 3.1	9.3 ± 3.7	<0.05
	EF Co	3 ± 1.8	5.1 ± 2.2	n.s.
	EF Cr	2.6 ± 1.5	4.7 ± 2.0	n.s.
	EF Cu	4.9 ± 3.2	11.2 ± 5.0	<0.05
	EF Ni	2.9 ± 1.7	5 ± 2.2	n.s.
	EF Pb	2.7 ± 1.7	5.3 ± 2.4	n.s.
	EF V	3 ± 1.8	4.9 ± 2.0	n.s.
	EF Zn	3.7 ± 2.5	8.1 ± 3.5	<0.05
	EF As	2.1 ± 1.7	5.1 ± 2.7	n.s.
	EF Mn	3.4 ± 2.0	5.8 ± 2.5	n.s.
Old reforestation		(n=12)	(n=8)	
	EF Cd	1.6 ± 0.5	5.1 ± 3.1	<0.05
	EF Hg	1.8 ± 0.7	7.3 ± 5.2	<0.05
	EF Co	1.8 ± 0.5	4.9 ± 2.7	<0.05
	EF Cr	1.5 ± 0.5	4.1 ± 2.6	<0.05
	EF Cu	2.6 ± 0.8	9.6 ± 6.7	<0.05
	EF Ni	1.8 ± 0.6	4.6 ± 2.6	<0.05
	EF Pb	1.7 ± 0.6	5 ± 3.5	<0.05
	EF V	1.7 ± 0.5	4.9 ± 3.7	<0.05
	EF Zn	2.1 ± 0.7	7.7 ± 5.7	<0.05
	EF As	1.9 ± 0.7	6.4 ± 5.2	<0.05
	EF Mn	1.7 ± 0.5	5.8 ± 4.4	<0.05
Dead matte		(n=17)	(n=2)	
	EF Cd	1.7 ± 0.6	5.1 ± 1.2	n.s.
	EF Hg	2.3 ± 1.5	8.9 ± 0.1	<0.05
	EF Co	1.9 ± 0.7	4.5 ± 1.3	n.s.
	EF Cr	1.5 ± 0.6	4.2 ± 0.7	n.s.
	EF Cu	2.3 ± 1.4	10.3 ± 1.6	n.s.
	EF Ni	1.8 ± 0.6	4.3 ± 0.6	n.s.
	EF Pb	1.5 ± 0.8	4.3 ± 0.1	<0.05
	EF V	1.8 ± 0.7	3.8 ± 0.4	<0.05
	EF Zn	1.8 ± 1.1	7.2 ± 0.3	<0.05
	EF As	2.3 ± 1.0	4.2 ± 2.0	n.s.
	EF Mn	1.6 ± 0.8	6.5 ± 1.4	n.s.

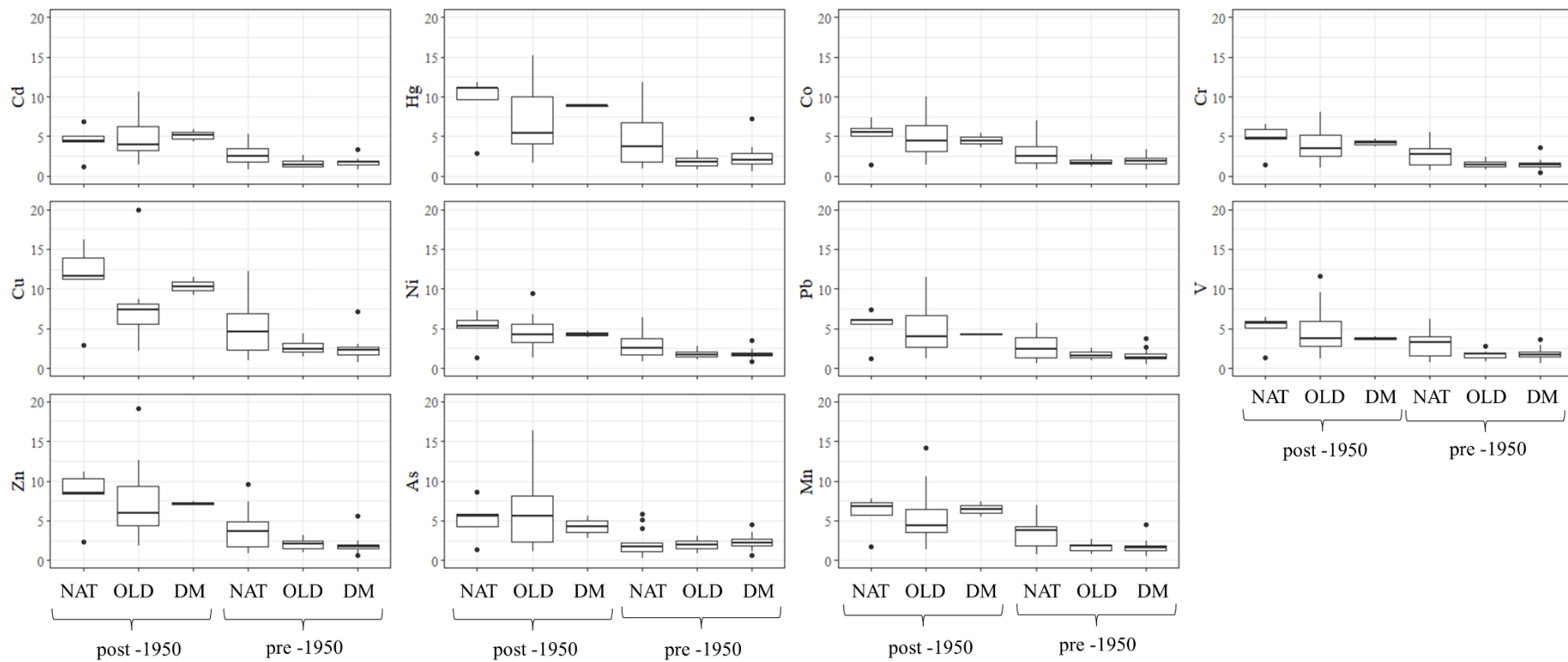


Fig. 6 Boxplot of trace metals enrichment factors EFs ( $TE/AI_{\text{sample}}/TE/AI_{\text{background}}$ ) in the studied habitats (NAT = Natural meadow; OLD = Old reforestation; DM = Dead *matte*) before and after the start of the anthropogenic disturbance (1950).

Likewise trace metals, vertical profiles of P concentration (Fig. 7) showed a significant increase towards the uppermost sediment layers in Natural meadow and Dead *matte*, while no correlation with depth appeared evident in Old reforestation. Threshold analysis allowed to identify a significant change point in the P profile of Dead *matte*, at 5.39 cm depth, which corresponds to the year 1917.

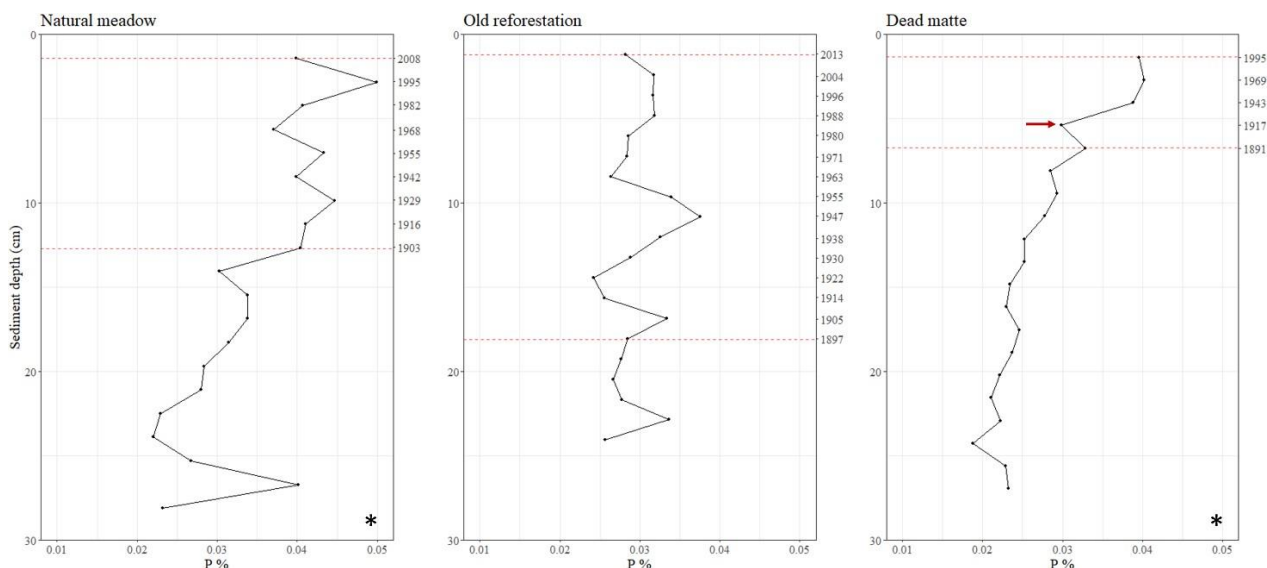


Fig. 7 Vertical profiles of P concentration (%) with sediment depth. Temporal trend for the last 120 years is provided on the second y axis. Asterisks indicate significant correlation with sediment depth, red arrows indicate significant threshold points.



## Discussion

The stocks of organic carbon and inorganic carbon in the sediments of Natural meadow, Old Reforestation and Dead *matte* were within the range described for *Posidonia oceanica* in previous studies (47–755 Mg C<sub>org</sub> ha<sup>-1</sup>; 3–580 Mg C<sub>inorg</sub> ha<sup>-1</sup>; in the upper 1 meter; Romero et al., 1994; Serrano et al., 2014; Mazzarasa et al., 2015; Apostolaki et al., 2019, 2022; Monnier et al., 2022b). Total nitrogen stocks in the sediments were also comparable to those reported elsewhere (3 Mg N ha<sup>-1</sup> in top meter, Apostolaki et al., 2019, 2022). Interesting, Dead *matte* showed higher stocks compared to the naturally vegetated area and to the dead *matte* subjected to reforestation in 2008 (Old reforestation). Higher stocks in dead *matte* sediments compared to vegetated sediments have been previously recorded in the western Sicily (Apostolaki et al., 2022) and it is known that *P. oceanica* necromass and *matte* may persist for several years or even decades (Boudouresque et al., 2015). This may be due to the ability of the seagrasses that previously formed the *matte* to store elements for long period of times, coupled with the lack of mechanical disturbance that can lead to sediment erosion and resuspension of elements after the seagrass loss. However, lower C<sub>org</sub>/N<sub>tot</sub> ratios, concurrent with lower organic carbon concentrations recorded in the most recent layers of Dead *matte* and Natural meadow, compared to the values of the first half of the last century, could reflect a decrease in the capacity of the preservation of the organic matter carried out by the system (Twichell et al. 2002), due to the complete loss of *P. oceanica* in the first habitat, and to a regression in the second, occurred as a result of the anthropogenic impacts in the gulf (Calvo et al., 2021). It is interesting to note that there is no similar decline in the Old reforestation habitat, with organic carbon concentration and C<sub>org</sub>/N<sub>tot</sub> ratio overall stable during the last century, which is a potential proof of the success of the reforestation carried out on the dead *matte* substrate in 2008.

Furthermore, the <sup>210</sup>Pb<sub>excess</sub> profile of Old reforestation suggests a uniform sediment accumulation at this habitat, whereas the <sup>210</sup>Pb<sub>excess</sub> profiles of Dead *matte* and Natural meadow could indicate changes in sediment composition over time, or erosion processes. The very low sediment accumulation rate at Dead *matte*, compared to average values for sediment associated to *P. oceanica* meadows (0.21 cm y<sup>-1</sup>, Serrano et al., 2016) and dead *matte* (0.19 cm y<sup>-1</sup>, Apostolaki et al., 2022), together with the low <sup>210</sup>Pb<sub>excess</sub> concentration and inventory, could confirm that an erosion process is underway at this habitat (Arias-Ortiz et al., 2018).

The increase in total nitrogen and phosphorus content towards the uppermost sediments and the significant difference between the layers stratified after 1950 compared to the first fifty years of the last century, in each of the habitat studied, indicate an increasing eutrophication of the Gulf of Palermo over time and especially from 1950 onwards. Nitrogen occurs in a variety of forms, but ammonia

(NH<sub>3</sub>), ammonium (NH<sub>4</sub>) and nitrate (NO<sup>3-</sup>) are among the most important forms in natural waters. Phosphorus is a very biologically active element whose compounds can be chemically or enzymatically hydrolyzed to orthophosphate in aquatic systems. This is the only form of phosphorus that can be taken up by bacteria, algae and plants (Correll, 1998). Excessive nitrogen and phosphorus concentrations cause algal blooms, anoxic conditions and ocean acidification (Ngadia & Taylor, 2019). Fertilizers, sewage, automobile exhaust and animal wastes are potential anthropogenic sources of phosphorus and nitrogen to aquatic systems (Puckett, 1995; Hole et al., 2002). The observed increases are consistent with findings in the scientific literature, as high concentrations of P-PO<sub>4</sub> (3-45 mmol L<sup>-1</sup>) and chlorophyll-*a* (2-35 mmol L<sup>-1</sup>) were recorded in 1980 (Genchi et al., 1981). Furthermore, a similar increase in nitrogen and phosphorus was found in sediment cores from the same area in previous studies (Di Leonardo et al., 2009; Di Leonardo et al., 2012).

The enrichment in both  $\delta^{13}\text{C}$  and  $\delta^{15}\text{N}$  sediments and the decrease in  $C_{\text{org}}/N_{\text{tot}}$  ratio observed in the Natural meadow and Dead matte cores may represent a further confirmation of the change in trophic state in the area, although not evident in the Old Reforestation habitat. Indeed, increased nutrient input leads to increased primary production, which affects  $\delta^{13}\text{C}$  levels, as intensive primary production causes lower  $^{12}\text{C}/^{13}\text{C}$  fractionation through photosynthesis (Neumann et al., 2002; Oczkowski et al., 2014). Animal nitrogen sources, including domestic sewage, have more enriched  $\delta^{15}\text{N}$  values than marine continental shelf sources (Heaton 1986). The  $\delta^{15}\text{N}$  values from human sources are often higher than 10 ‰, while the  $\delta^{15}\text{N}$  values from the sea off the continental shelf are below 6 ‰ (Fry, 2002; Oczkowski et al., 2014). The enrichment in  $\delta^{15}\text{N}$  in the sediments examined contrasts with earlier results relating to the same coastal area. In fact, Di Leonardo et al. (2012) described a decline in the values of  $\delta^{15}\text{N}$  measured in two unvegetated sediment cores, towards the present, and attributed this trend to the increased input of fertilizers. Synthetic fertilizers are indeed generally depleted in  $\delta^{15}\text{N}$  with values comprised between -2 and 2 ‰ (Bateman et al., 2007). However, the depletion of  $\delta^{15}\text{N}$  is doubtful in a polluted urban area where enrichment in  $\delta^{15}\text{N}$  is expected due to eutrophication (Voß & Struck, 1997; Voss et al., 2000). The difference in the  $\delta^{15}\text{N}$  trends between the present and the cited study could be due to the natural variability of sediment properties and to the scarce capacity of the unvegetated sediment to entrap nutrients. Similar to the present results, Di Leonardo's studies (2009, 2012) reports a decrease in the  $C_{\text{org}}/N_{\text{tot}}$  ratio in the second half of the last century, which could be due to a greater accumulation of marine organic matter in the sediments caused by greater phytoplankton and algal growth, which is further evidence of the increase in trophic status. This decrease however, as highlighted above, could also reflect a decreased preservation of the organic matter buried, due to the loss of vegetation.

Regarding the inorganic contamination in the area, trace metal concentration do not exceed the sediment quality guideline values (Macdonald et al., 1996; Long et al., 1995), except for Hg and As, whose concentration were between the ERL and ERM values, posing potential threat to marine life, as toxic effects may occasionally occur. However, both Hg and As remained slightly lower than the ERM values.

Trace metals pose a major environmental problem due to their toxic properties, their non-degradability and their accumulation behaviour. Important sources predominantly include industrial and agricultural activities, scrap metal recycling, commercial ports, discharge of sewage sludge, leachates from reclamation areas and landfilling, animal wastes, fertilizers and pesticides, fossil fuel combustion and atmospheric deposition, mining (Birch & Taylor, 1999; Bradl 2005; Qi et al., 2010; Christophoridis et al., 2019). Furthermore, it is know that the cements used in the building industry are often characterized by a significant presence of heavy metals of particular environmental concern (Van Der Sloot, 2000). Cements could contain mineral additions such as slags and coal fly ashes. Building materials, aggregates of concrete, pavement materials, coarse could contain post-industrial solid waste as admixture (Huang et al., 2021; Olejarczyk et al., 2022; (J. N. Wang et al., 2023). The leaching of heavy metals from building materials and its impact on aquatic systems has already been identified as a matter of concern (Malik 2021; A.J.H. van Breemen 2007).

The vertical profiles of trace metals of each habitat analysed in this study reflect the increase in the input of contaminants, started in the middle of the last century, mainly derived from domestic and urban sewage, harbour and shipyards activities and to the illegal dumping of building materials along the coast at the Gulf of Palermo (Genchi et al., 1982; Calvo et al., 2021; Di Leonardo et al., 2009). This is particularly evident in the Old reforestation habitat, where two significant increases in trace metals concentration has been recorded between the 1950s and 1970s, gradually decreasing back to pre-1950 values after the 1980s.

Considering the background levels, the EFs before 1950 allowed these layers to be classified as slightly polluted overall. Instead, all post-1950 sediments had higher EFs and can be considered moderately to strongly polluted, especially for Cu, Hg, Zn, Mn and As.

The EF values for Cu, Ni, Pb, Mn and As of post-1950 sediments are higher than those previously estimated for distal unvegetated sediments from the Gulf of Palermo (Di Leonardo et al., 2009), confirming that nearshore sites are more affected by anthropogenic pollution, as observed by Di Leonardo et al. (2012) in an earlier comparison between nearshore and offshore sediments collected in the gulf. EF values for Cu and Zn are higher also if compared to those previously measured from adjacent unvegetated sediments (Di Leonardo et al., 2012, core AC). However, EF values for Hg in

the present study are 4-5 times lower than the values measured in both distal (BC12) and coastal (AC) unvegetated sediment cores. This difference could be attributed to the natural variability of sediments or it could be possible that *P. oceanica* is absorbing Hg in its tissues, through phytoextraction (uptake of metals from the surrounding environment by belowground tissues and translocation in above-ground tissues) and phytostabilization (accumulation of metals in the below-ground tissues and decreasing mobility of metals in substrate), carrying on a phytoremediation process (Lee et al., 2019; Pergent et al., 2011; Ahmad et al., 2014; Bonanno & Raccuia, 2018). Further analyses could focus on measuring the concentration of trace metals in different compartments of *P. oceanica* (leaves, roots, rhizomes, epiphytes).

## Conclusion

The sediment cores collected in the Gulf of Palermo, off the coast of the Bandita locality, represent an archive of past anthropogenic contamination and a biogeochemical sink. The vertical/temporal profiles of the geochemical variables and trace metals testify an increase in the trophic status and the accumulation of inorganic contaminants, resulting from the impacts that this area has been subjected to during the last century. However, the concentrations of trace metals measured in this study do not exceed the sediment quality guidelines, showing that toxic effects on fauna could only occur occasionally. A reduced sediment trapping capacity and possible slight erosion observed in the dead *matte*, as evidenced by the low  $^{210}\text{Pb}$  stocks and very low accumulation rates in this habitat, was not observed in the dead *matte* that was reforested in 2008. The decrease in  $C_{\text{org}}$  concentration and  $C_{\text{org}}/N_{\text{tot}}$  ratio observed in the dead *matte* and natural meadow, occurred in the last 120 years, was not observed in the restored habitat. These is further evidence of the success of the past reforestation intervention, carried out in this habitat, using dead *matte* as substrate and further support to pursue this restoration strategy in degraded coastal areas.

## General conclusion

There is an urgent need in marine science to fill the current gaps in understanding the role of coastal vegetated ecosystems in mitigating climate change, combating eutrophication, and controlling pollution to ensure clear information for coastal management and secure the future of the world's seagrass ecosystems.

Seagrass meadows are coastal marine ecosystems known as Blue Carbon ecosystems, as they store organic carbon, formed by refractory belowground biomass, seagrass detritus and allochthonous organic matter, in their underlying sediments, and preserve it up to millennia time scale (Duarte et al., 2005). Therefore, seagrass ecosystems represent nature-based solution for the mitigation of climate change (Macreadie et al., 2014). They are also known as filtering habitats for nutrients, as they enhance nitrogen removal from the water column through its burial in the sediment, playing an important role in counteracting coastal eutrophication (Aoki et al., 2020). Seagrass meadows have recently been identified as possible hotspots for microplastics (Sanchez-Vidal et al., 2021) and seagrass sediment have been used as tool to reconstruct centennial-scale trends of chemical contamination in coastal environments (Serrano et al., 2016). Unfortunately, several studies have assessed the general decline of seagrass meadows worldwide, due to a broad spectrum of anthropogenic causes such as habitat destruction, pollution, introduction of non-native species and climate change (Duarte, 2002; Barbieri et al., 2017). The loss of seagrass vegetation could lead to the resuspension of previously protected sediment and, therefore, of carbon, nutrients, and pollutants, possibly invalidating the important role of seagrass meadows as Blue Carbon habitats and nutrients and pollutants filtering ecosystems (Macreadie et al, 2015; Moksnes et al, 2021; Unsworth et al., 2022). The loss of seagrass vegetation worldwide must have already led to important new inputs of carbon, nitrogen, and pollutants, previously removed from the surrounding environment and from the biogeochemical cycles. For this reason, nowadays conservation efforts have been carried on, and the ecological restoration of seagrass habitats through transplantation measures seems to be a promising tool to improve the resilience of these ecosystems (Calvo et al., 2021).

However, despite the importance of the afore-mentioned ecosystem services provided by seagrass meadows and the threats these ecosystems are counteracting, there are still gaps in knowledge about the factors driving the variability of seagrass storage capacity, as well as the need to investigate the role they play as traps for pollutants of emerging interest (microplastics) and for the fate of carbon, nutrient and pollutant stocks following the loss or restoration of seagrasses.

The present work contributes to expand our knowledge on the interaction between abiotic factors and seagrass traits in driving the storage of carbon, nutrients, and pollutants. Furthermore, investigation on the geochemical changes and the current state of a transplanted area allowed to assess the effects of a

restoration project. Through this dissertation, the multifaceted roles of seagrasses in carbon sequestration, nutrient regulation, and pollutant removal were investigated.

In summary, this research has yielded several key findings. First, the results highlighted the importance of seagrass traits but also of granulometry and hydrodynamics in driving the carbon and nitrogen storage capacity. The type of seagrass species, which have a different structure and functionality, influences the ability of a system to store carbon in different ways. *Posidonia oceanica* (L.) Delile showed the highest carbon stocks and accumulation rates accordingly to the literature (Forqurean 2012; Pergent-Martini 2021) mainly due to its higher biomass and structural complexity. However, this species is in decline throughout the Mediterranean Sea and is mostly replaced by pioneer species such as *Cymodocea nodosa* Ucria Ascherson. In this thesis, the comparison between *C. nodosa*, *P. oceanica* and unvegetated sediments also highlighted the importance of the former as a carbon sink. The interaction between environmental factors (*i.e.*, temperature, salinity, depth, substrate type, water currents) and the characteristics of seagrass species must be considered when evaluating the ability of these habitats to provide ecosystem services such as carbon sequestration. Based on the results of this work, higher stocks may be found in areas where higher seagrass biomass, a higher proportion of mud in the sediment and lower hydrodynamics interact to promote the deposition and preservation of carbon and nutrients, while higher hydrodynamics seems to lead to higher stocks of inorganic carbon in the sediments. The literature data in this field focus on the relationship between environmental factors, seagrass traits and carbon storage, while less attention has been paid to the factors determining nitrogen and inorganic carbon storage. Furthermore, much of our knowledge on seagrass stocks is based on studies of *P. oceanica*, while less information is available on the storage capacity of other seagrass species. Gaining insights into these gaps could be an address for future research on Blue Carbon science and seagrass ecosystems in general.

This study also confirms the role of seagrass beds in the retention of pollutants, such as microplastics, into the underlying sediment, which, indeed, accumulate microplastics to a larger extent than the water column. The results showed that hydrodynamics and geomorphology can also influence the abundance of microplastics in the environment. When assessing the role of trophic ecology of marine organisms in influencing the likelihood of microplastic ingestion, a holistic perspective that also considers environmental variables can help to define causes and consequences. Very few studies have used trophic niche characteristics (trophic position, isotopic niche width and Layman metrics) to relate the trophic ecology of organisms to the likelihood of microplastic ingestion. Results reported in the literature, from studies that describe the trophic ecology of marine organisms in other ways (e.g. fish stomach contents, known feeding strategies of species) are controversial, as many of them come to opposite conclusions. Intuitively, increasing the number of individuals sampled may help to obtain concrete results that

improve the understanding of the relationship between trophic ecology and ingestion of these pollutants. The number of the individuals analysed could also be a limitation of the present study. However, the sampling effort and especially the time required to visualise and identify all particles found in different compartments such as water, sediment and biota, made a selection necessary. In these cases, one recommendation could be to reduce the number of species analysed but increase the number of individuals per species. Based on recent evidence of the presence of microplastics on the surface of seagrass leaves and blades (Cozzolino et al., 2020; Li et al., 2023), further research in this field may consider this other compartment when linking the distribution of microplastics in the seagrass ecosystem to the likelihood of microplastics ingestion by the associated fauna. Seagrass beds and coastal environments should be priority habitats when assessing the impact of microplastics on the marine environment, as these habitats are characterized by high microplastics concentrations that may affect the associated fauna.

Finally, the comparison between three *P. oceanica* habitats (a pristine meadow, a meadow transplanted onto dead matte, unvegetated dead matte) allowed to determine differences in their function as carbon sinks and filtering habitats over time and to infer on the effects of the transplantation project. Both dead matte and vegetated seagrass sediments appear to be important biogeochemical sinks and archives of past ecosystem changes in historically contaminated areas, which could represent another ecosystem service provided by these environments. Results showed reduced sediment trapping capacity and possibly erosion in the dead matte, while the area characterized by the transplanted meadow appeared stable, suggesting a positive effect of the past reforestation effort. Restoration by transplanting onto *P. oceanica* dead matte seems a promising method to promote the resilience and recovery of damaged meadows, counteract sediment erosion and thus maintain the ability of seagrass meadows to act as carbon and nutrient sinks and prevent the resuspension of pollutants.

Accurate knowledge of what factors positively influence or negatively affect the ability of coastal vegetation to store carbon, nutrients and pollutants can help in the management of restoration and conservation projects to mitigate the impacts of anthropogenic pollution on marine ecosystems. Indeed, the implications of this research extend beyond scientific inquiry to encompass broader societal and environmental concerns. By recognizing the ecological value of seagrass ecosystems, policymakers, stakeholders, and the public can work collaboratively to implement effective conservation and restoration measures and promote sustainable management practices. Through the promotion and protection of the ecological services provided by seagrass ecosystems, we can foster resilient coastal environments and secure a sustainable future for generations to come.

## References

- Abbasi, S. (2021). Prevalence and physicochemical characteristics of microplastics in the sediment and water of Hashilan Wetland, a national heritage in NW Iran. *Environmental Technology and Innovation*, 23, 101782. <https://doi.org/10.1016/j.eti.2021.101782>
- Acharya, S., Rumi, S. S., Hu, Y., & Abidi, N. (2021). Microfibers from synthetic textiles as a major source of microplastics in the environment: A review. *Textile Research Journal*, 91(17–18), 2136–2156. <https://doi.org/10.1177/0040517521991244>
- Agnesi V., Macaluso T., Orrù P. & Ulzega A., 1993 — Paleografia dell'arcipelago delle Egadi (Sicilia) nel Pleistocene sup.- Olocene. — *Naturalista sicil.*, 17: 3-22.
- Ahmad, F., Azman, S., Said, M. I. M., Lavania-Baloo, L., Sabri, S., & Salmiati, S. (2014). Metals in tropical seagrass-accumulation of mercury and lead. *World Applied Sciences Journal*, 32(8), 1468–1473. <https://doi.org/10.5829/idosi.wasj.2014.32.08.1028>
- Andolina, C., Franzoi, P., Cavraro, F., Jackson, A. L., Mazzola, A., & Vizzini, S. (2022). Trophic adaptability shapes isotopic niche of the resident fish *Aphanius fasciatus* across lagoon habitats. *Estuarine, Coastal and Shelf Science*, 264(October 2021), 107685. <https://doi.org/10.1016/j.ecss.2021.107685>
- Andrady, A. L. (2011). Microplastics in the marine environment. *Marine Pollution Bulletin*, 62(8), 1596–1605. <https://doi.org/10.1016/j.marpolbul.2011.05.030>
- Angus, S. (2017). Scottish saline lagoons: Impacts and challenges of climate change. *Estuarine, Coastal and Shelf Science*, 198, 626–635. <https://doi.org/10.1016/j.ecss.2016.07.014>
- Aoki, L. R., McGlathery, K. J., & Oreska, M. P. J. (2020). Seagrass restoration reestablishes the coastal nitrogen filter through enhanced burial. *Limnology and Oceanography*, 65(1), 1–12. <https://doi.org/10.1002/lno.11241>
- Apostolaki, E. T., Caviglia, L., Santinelli, V., Cundy, A. B., Tramati, C. D., Mazzola, A., & Vizzini, S. (2022). The Importance of Dead Seagrass (*Posidonia oceanica*) Matte as a Biogeochemical Sink. *Frontiers in Marine Science*, 9(March), 1–15. <https://doi.org/10.3389/fmars.2022.861998>
- Apostolaki, E. T., Vizzini, S., Santinelli, V., Kaberi, H., Andolina, C., & Papathanassiou, E. (2019). Exotic *Halophila stipulacea* is an introduced carbon sink for the Eastern Mediterranean Sea. *Scientific Reports*, 9(1), 1–13. <https://doi.org/10.1038/s41598-019-45046-w>



- Arias-Ortiz, A., Masqué, P., Garcia-Orellana, J., Serrano, O., Mazarrasa, I., Marbá, N., Lovelock, C. E., Lavery, P. S., & Duarte, C. M. (2018). Reviews and syntheses: 210Pb-derived sediment and carbon accumulation rates in vegetated coastal ecosystems - Setting the record straight. *Biogeosciences*, 15(22), 6791–6818. <https://doi.org/10.5194/bg-15-6791-2018>
- Barbier, E. B., Hacker, S. D., Kennedy, C., Koch, E. W., Stier, A. C., & Silliman, B. R. (2011). The value of estuarine and coastal ecosystem services. *Ecological Monographs*, 81(2), 169–193. <https://doi.org/10.1890/10-1510.1>
- Bateman A.S. & Kelly S. D. (2007) Fertilizer nitrogen isotope signatures. *Isotopes in Environmental and Health Studies*, 43(3), 237-247, <https://doi.org/10.1080/10256010701550732>
- Bergamaschi, B. A., Tsamakis, E., Keil, R. G., Eglinton, T. I., Montluçon, D. B., & Hedges, J. I. (1997). The effect of grain size and surface area on organic matter, lignin and carbohydrate concentration, and molecular compositions in Peru Margin sediments. *Geochimica et Cosmochimica Acta*, 61(6), 1247–1260. [https://doi.org/10.1016/S0016-7037\(96\)00394-8](https://doi.org/10.1016/S0016-7037(96)00394-8)
- Birch, G., & Taylor, S. (1999). Source of heavy metals in sediments of the Port Jackson estuary, Australia. *Science of the Total Environment*, 227(2–3), 123–138. [https://doi.org/10.1016/S0048-9697\(99\)00007-8](https://doi.org/10.1016/S0048-9697(99)00007-8)
- Bonanno, G., & Raccuia, S. A. (2018). Seagrass *Halophila stipulacea*: Capacity of accumulation and biomonitoring of trace elements. *Science of the Total Environment*, 633, 257–263. <https://doi.org/10.1016/j.scitotenv.2018.03.196>
- Boudouresque, C. F., Bernard, G., Bonhomme, P., Charbonnel, E., Diviacco, G., Meinesz, A., Pergent, G., Pergent-Martini, C., Ruitton, S.T.L., 2012. Protection and conservation of *Posidonia oceanica* meadows. RAMOGE and RAC/SPA publisher. Tunis, pp. 1–202. [http://racspa.org/sites/default/files/doc\\_vegetation/ramoge\\_en.pdf](http://racspa.org/sites/default/files/doc_vegetation/ramoge_en.pdf).
- Boudouresque, C. F., Blanfuné, A., Pergent, G., & Thibaut, T. (2021). Restoration of seagrass meadows in the Mediterranean Sea: A critical review of effectiveness and ethical issues. *Water (Switzerland)*, 13(8), 1–34. <https://doi.org/10.3390/w13081034>
- Brady, J. P., Ayoko, G. A., Martens, W. N., & Goonetilleke, A. (2015). Development of a hybrid pollution index for heavy metals in marine and estuarine sediments. *Environmental Monitoring and Assessment*, 187(5). <https://doi.org/10.1007/s10661-015-4563-x>

- Brito, A. C., Newton, A., Tett, P., & Fernandes, T. F. (2012). How will shallow coastal lagoons respond to climate change? A modelling investigation. *Estuarine, Coastal and Shelf Science*, 112, 98–104. <https://doi.org/10.1016/j.ecss.2011.09.002>
- Buapet, P., Gullström, M., & Björk, M. (2013). Photosynthetic activity of seagrasses and macroalgae in temperate shallow waters can alter seawater pH and total inorganic carbon content at the scale of a coastal embayment. *Marine and Freshwater Research*, 64(11), 1040–1048. <https://doi.org/10.1071/MF12124>
- Björk, M., & Gullström, M. (2016). Sediment properties as important predictors of carbon storage in *Zostera marina* meadows: A comparison of four European areas. *PLoS ONE*, 11(12), 1–21. <https://doi.org/10.1371/journal.pone.0167493>
- Cai, Y., Yang, T., Mitrano, D. M., Heuberger, M., Hufenus, R., & Nowack, B. (2020). Systematic Study of Microplastic Fiber Release from 12 Different Polyester Textiles during Washing. *Environmental Science and Technology*, 54(8), 4847–4855. <https://doi.org/10.1021/acs.est.9b07395>
- Calizza, E., Costantini, M. L., Carlino, P., Bentivoglio, F., Orlandi, L., & Rossi, L. (2013). *Posidonia oceanica* habitat loss and changes in litter-associated biodiversity organization: A stable isotope-based preliminary study. *Estuarine, Coastal and Shelf Science*, 135, 137–145. <https://doi.org/10.1016/j.ecss.2013.07.019>
- Cancemi, G., Buia, M. C., & Mazzella, L. (2002). Structure and growth dynamics of *Cymodocea nodosa* meadows. *Scientia Marina*, 66(4), 365–373. <https://doi.org/10.3989/scimar.2002.66n4365>
- Cardona, L., Revelles, M., Sales, M., Aguilar, A., & Borrell, A. (2007). Meadows of the seagrass *Posidonia oceanica* are a significant source of organic matter for adjoining ecosystems. *Marine Ecology Progress Series*, 335, 123–131. <https://doi.org/10.3354/meps335123>
- Carrascal, L. M., Galván, I., & Gordo, O. (2009). Partial least squares regression as an alternative to current regression methods used in ecology. *Oikos*, 118(5), 681–690. <https://doi.org/10.1111/j.1600-0706.2008.16881.x>
- Cera, A., Sighicelli, M., Sodo, A., Lecce, F., Menegoni, P., & Scalici, M. (2022). Microplastics distribution and possible ingestion by fish in lacustrine waters (Lake Bracciano, Italy). *Environmental Science and Pollution Research*, 29(45), 68179–68190. <https://doi.org/10.1007/s11356-022-20403-x>
- Chaudhry, A. K., & Sachdeva, P. (2021). Microplastics' origin, distribution, and rising hazard to aquatic organisms and human health: Socio-economic insinuations and management solutions. *Regional Studies in Marine Science*, 48, 102018. <https://doi.org/10.1016/j.rsma.2021.102018>

- Chefaoui, R.M., Assis, J., Duarte, C. M., & Serrão, E. A. (2016). Large-Scale Prediction of Seagrass Distribution Integrating Landscape Metrics and Environmental Factors: The Case of *Cymodocea nodosa* (Mediterranean–Atlantic). *Estuaries and Coasts*, 39(1), 123–137.  
<https://doi.org/10.1007/s12237-015-9966-y>
- Chefaoui, Rosa M, Duarte, C. M., & Serrão, E. A. (2018). Dramatic loss of seagrass habitat under projected climate change in the Mediterranean Sea. <https://doi.org/10.1111/gcb.14401>
- Coppock, R. L., Cole, M., Lindeque, P. K., Queirós, A. M., & Galloway, T. S. (2017). A small-scale, portable method for extracting microplastics from marine sediments. *Environmental Pollution*, 230, 829–837. <https://doi.org/10.1016/j.envpol.2017.07.017>
- Costa, V., Mazzola, A., Rossi, F., & Vizzini, S. (2019). Decomposition rate and invertebrate colonization of seagrass detritus along a hydrodynamic gradient in a Mediterranean coastal basin: The Stagnone di Marsala (Italy) case study. *Marine Ecology*, 40(6), 1439-1448.  
<https://doi.org/10.1111/maec.12570>
- Cozzolino, L., Nicastro, K. R., Zardi, G. I., de los Santos, C. B., (2020). Species-specific plastic accumulation in the sediment and canopy of coastal vegetated habitats. *Science of The Total Environment*, 723, 138018. <https://doi.org/10.1016/j.scitotenv.2020.138018>.
- Dahl, M., Deyanova, D., Gütschow, S., Asplund, M. E., Lyimo, L. D., Karamfilov, V., Santos, R., Björk, M., & Gullström, M. (2016). Sediment properties as important predictors of carbon storage in *Zostera marina* meadows: A comparison of four European areas. *PLoS ONE*, 11(12), 1–21.  
<https://doi.org/10.1371/journal.pone.0167493>
- de los Santos, C. B., Egea, L. G., Martins, M., Santos, R., Masqué, P., Peralta, G., Brun, F. G., & Jiménez-Ramos, R. (2022). Sedimentary Organic Carbon and Nitrogen Sequestration Across a Vertical Gradient on a Temperate Wetland Seascape Including Salt Marshes, Seagrass Meadows and Rhizophytic Macroalgae Beds. *Ecosystems*. <https://doi.org/10.1007/s10021-022-00801-5>
- de Marchis, M., Ciruolo, G., Nasello, C., & Napoli, E. (2012). Wind- and tide-induced currents in the Stagnone lagoon (Sicily). *Environmental Fluid Mechanics*, 12(1), 81–100.  
<https://doi.org/10.1007/s10652-011-9225-0>
- Di Leonardo, R., Cundy, A. B., Bellanca, A., Mazzola, A., & Vizzini, S. (2012). Biogeochemical evaluation of historical sediment contamination in the Gulf of Palermo (NW Sicily): Analysis of pseudo-trace elements and stable isotope signals. *Journal of Marine Systems*, 94, 185–196.  
<https://doi.org/10.1016/j.jmarsys.2011.11.022>

- Din, Z. B. (1992). Use of aluminium to normalize heavy-metal data from estuarine and coastal sediments of Straits of Melaka. *Marine Pollution Bulletin*, 24(10), 484–491.  
[https://doi.org/10.1016/0025-326X\(92\)90472-I](https://doi.org/10.1016/0025-326X(92)90472-I)
- Duarte, C. M., Fourqurean, J. W., Krause-jensen, D., & Olesen, B. (2006). Seagrasses: Biology, Ecology and Conservation. *Seagrasses: Biology, Ecology and Conservation*, May 2014.  
<https://doi.org/10.1007/1-4020-2983-7>
- Duarte, C. M., Kennedy, H., Marbà, N., & Hendriks, I. (2013). **Assessing** the capacity of seagrass meadows for carbon burial: Current limitations and future strategies. *Ocean and Coastal Management*, 83, 32–38. <https://doi.org/10.1016/j.ocecoaman.2011.09.001>
- Duarte, C. M. (2002). The future of seagrass meadows. *Environmental Conservation*, 29(2), 192-206.  
<https://doi:10.1017/S0376892902000127>
- Enríquez, S., & Schubert, N. (2014). Direct contribution of the seagrass *Thalassia testudinum* to lime mud production. *Nature Communications*, 5(May). <https://doi.org/10.1038/ncomms4835>
- Fernández-González, V., Andrade-Garda, J. M., López-Mahía, P., & Muniategui-Lorenzo, S. (2022). Misidentification of PVC microplastics in marine environmental samples. *TrAC - Trends in Analytical Chemistry*, 153. <https://doi.org/10.1016/j.trac.2022.116649>
- Fernández-Torquemada, Y., & Sánchez-Lizaso, J. L. (2011). Responses of two Mediterranean seagrasses to experimental changes in salinity. *Hydrobiologia*, 669(1), 21–33.  
<https://doi.org/10.1007/s10750-011-0644-1>
- Fong, Y., Huang, Y., Gilbert, P. B., & Permar, S. R. (2017). chngpt: Threshold regression model estimation and inference. *BMC Bioinformatics*, 18(1), 1–7. <https://doi.org/10.1186/s12859-017-1863-x>
- Fourqurean, J. W., Marbà, N., Duarte, C. M., Diaz-Almela, E., & Ruiz-Halpern, S. (2007). Spatial and temporal variation in the elemental and stable isotopic content of the seagrasses *Posidonia oceanica* and *Cymodocea nodosa* from the Illes Balears, Spain. *Marine Biology*, 151(1), 219–232.  
<https://doi.org/10.1007/s00227-006-0473-3>
- Fourqurean, James W., Duarte, C. M., Kennedy, H., Marbà, N., Holmer, M., Mateo, M. A., Apostolaki, E. T., Kendrick, G. A., Krause-Jensen, D., McGlathery, K. J., & Serrano, O. (2012). Seagrass ecosystems as a globally significant carbon stock. *Nature Geoscience*, 5(7), 505–509.  
<https://doi.org/10.1038/ngeo1477>

- Frias, J. P. G. L., & Nash, R. (2019). Microplastics: Finding a consensus on the definition. *Marine Pollution Bulletin*, 138(November 2018), 145–147. <https://doi.org/10.1016/j.marpolbul.2018.11.022>
- Frias, J., Pagter, E., Nash, R., O'Connor, I., Carretero, O., Filgueiras, A., Viñas, L., Gago, J., Antunes, J., Bessa, F., Sobral, P., Goruppi, A., Tirelli, V., Pedrotti, M. L., Suaria, G., Aliani, S., Lopes, C., Raimundo, J., Caetano, M., Gerds, G. (2018). Standardised protocol for monitoring microplastics in sediments. *JPI-Oceans BASEMAN Project*, 33. <https://doi.org/10.13140/RG.2.2.36256.89601/1>
- Gacia, E., Duarte, C. M., & Middelburg, J. J. (2002). Carbon and nutrient deposition in a Mediterranean seagrass (*Posidonia oceanica*) meadow. *Limnology and Oceanography*, 47(1), 23–32. <https://doi.org/10.4319/lo.2002.47.1.0023>
- Garcia, T. D., Cardozo, A. L. P., Quirino, B. A., Yofukuji, K. Y., Ganassin, M. J. M., dos Santos, N. C. L., & Fugi, R. (2020). Ingestion of Microplastic by Fish of Different Feeding Habits in Urbanized and Non-urbanized Streams in Southern Brazil. *Water, Air, and Soil Pollution*, 231(8). <https://doi.org/10.1007/s11270-020-04802-9>
- Gazal, A. A., & Gheewala, S. H. (2020). Plastics, microplastics and other polymer materials—A threat to the environment. *Journal of Sustainable Energy & Environment*, 11, 113-122.
- Govers, L. L., Lamers, L. P. M., Bouma, T. J., Eygensteyn, J., de Brouwer, J. H. F., Hendriks, A. J., Huijbers, C. M., & van Katwijk, M. M. (2014). Seagrasses as indicators for coastal trace metal pollution: A global meta-analysis serving as a benchmark, and a Caribbean case study. *Environmental Pollution*, 195, 210–217. <https://doi.org/10.1016/j.envpol.2014.08.028>
- Guerrero-Meseguer, L., Marín, A., & Sanz-Lázaro, C. (2017). Future heat waves due to climate change threaten the survival of *P. oceanica* seedlings. *Environmental Pollution*, 230, 40–45. <https://doi.org/10.1016/j.envpol.2017.06.039>
- Guidetti, P., Lorenti, M., Buia, M. C., & Mazzella, L. (2002). Temporal dynamics and biomass partitioning in three Adriatic seagrass species: *Posidonia oceanica*, *Cymodocea nodosa*, *Zostera marina*. *Marine Ecology*, 23(1), 51–67. <https://doi.org/10.1046/j.1439-0485.2002.02722.x>
- Gullström, M., Lyimo, L. D., Dahl, M., Samuelsson, G. S., Eggertsen, M., Anderberg, E., Rasmusson, L. M., Linderholm, H. W., Knudby, A., Bandeira, S., Nordlund, L. M., & Björk, M. (2018). Blue Carbon Storage in Tropical Seagrass Meadows Relates to Carbonate Stock Dynamics, Plant–Sediment Processes, and Landscape Context: Insights from the Western Indian Ocean. *Ecosystems*, 21(3), 551–566. <https://doi.org/10.1007/s10021-017-0170-8>

- Hamilton, B. M., Rochman, C. M., Hoellein, T. J., Robison, B. H., Van Houtan, K. S., & Choy, C. A. (2021). Prevalence of microplastics and anthropogenic debris within a deep-sea food web. *Marine Ecology Progress Series*, 675, 23–33. <https://doi.org/10.3354/meps13846>
- Heaton, T. H. E. (1986). Isotopic studies of nitrogen pollution in the hydrosphere and atmosphere: A review. *Chemical Geology: Isotope Geoscience Section*, 59, 87-102. <https://api.semanticscholar.org/CorpusID:97546078>
- Hendriks, I. E., Duarte, C. M., Olsen, Y. S., Steckbauer, A., Ramajo, L., Moore, T. S., Trotter, J. A., & McCulloch, M. (2015). Biological mechanisms supporting adaptation to ocean acidification in coastal ecosystems. *Estuarine, Coastal and Shelf Science*, 152, A1–A8. <https://doi.org/10.1016/j.ecss.2014.07.019>
- Hendriks, I. E., Escolano-Moltó, A., Flecha, S., Vaquer-Sunyer, R., Wesselmann, M., & Marbà, N. (2022). Mediterranean seagrasses as carbon sinks: methodological and regional differences. *Biogeosciences*, 19(18), 4619–4637. <https://doi.org/10.5194/bg-19-4619-2022>
- Hendriks, I. E., Sintès, T., Bouma, T. J., & Duarte, C. M. (2008). Experimental assessment and modeling evaluation of the effects of the seagrass *Posidonia oceanica* on flow and particle trapping. *Marine Ecology Progress Series*, 356, 163–173. <https://doi.org/10.3354/meps07316>
- Hidalgo-ruz, V., Gutow, L., Thompson, R. C., & Thiel, M. (2012). Microplastics in the Marine Environment: A Review of the Methods Used for Identification and Quantification. *Environ. Sci. Technol.* 46(6), 3060-3075. <https://doi.org/10.1021/es2031505>
- Hisham A. Maddah. (2016). Polypropylene as a Promising Plastic: A Review. *American Journal of Polymer Science*, 6(1), 1–11. <https://doi.org/10.5923/j.ajps.20160601.01>
- Ho, H. H., Swennen, R., Cappuyns, V., Vassilieva, E., & Van Tran, T. (2012). Necessity of normalization to aluminum to assess the contamination by heavy metals and arsenic in sediments near Haiphong Harbor, Vietnam. *Journal of Asian Earth Sciences*, 56, 229–239. <https://doi.org/10.1016/j.jseaes.2012.05.015>
- Hoffman, D. K., McCarthy, M. J., Newell, S. E., Gardner, W. S., Niewinski, D. N., Gao, J., & Mutchler, T. R. (2019). Relative Contributions of DNRA and Denitrification to Nitrate Reduction in *Thalassia testudinum* Seagrass Beds in Coastal Florida (USA). *Estuaries and Coasts*, 42(4), 1001–1014. <https://doi.org/10.1007/s12237-019-00540-2>

Howard, G. T. (2002). Biodegradation of polyurethane: A review. *International Biodeterioration and Biodegradation*, 49(4), 245–252. [https://doi.org/10.1016/S0964-8305\(02\)00051-3](https://doi.org/10.1016/S0964-8305(02)00051-3)

Huang, Y., Xiao, X., Effiong, K., Xu, C., Su, Z., Hu, J., Jiao, S., & Holmer, M. (2021). New Insights into the Microplastic Enrichment in the Blue Carbon Ecosystem: Evidence from Seagrass Meadows and Mangrove Forests in Coastal South China Sea. *Environmental Science & Technology*. <https://doi.org/10.1021/acs.est.0c07289>

Jackson, A. L., Inger, R., Parnell, A. C., & Bearhop, S. (2011). Comparing isotopic niche widths among and within communities: SIBER - Stable Isotope Bayesian Ellipses in R. *Journal of Animal Ecology*, 80(3), 595–602. <https://doi.org/10.1111/j.1365-2656.2011.01806.x>

Jackson, M. C., Donohue, I., Jackson, A. L., Britton, J. R., Harper, D. M., & Grey, J. (2012). Population-level metrics of trophic structure based on stable isotopes and their application to invasion ecology. *PLoS ONE*, 7(2), 1–12. <https://doi.org/10.1371/journal.pone.0031757>

Juma, G. A., Magana, A. M., Michael, G. N., & Kairo, J. G. (2020). Variation in Seagrass Carbon Stocks Between Tropical Estuarine and Marine Mangrove-Fringed Creeks. *Frontiers in Marine Science*, 7(August), 1–11. <https://doi.org/10.3389/fmars.2020.00696>

Kennedy, H., Pagès, J. F., Lagomasino, D., Arias-Ortiz, A., Colarusso, P., Fourqurean, J. W., Githaiga, M. N., Howard, J. L., Krause-Jensen, D., Kuwae, T., Lavery, P. S., Macreadie, P. I., Marbà, N., Masqué, P., Mazarrasa, I., Miyajima, T., Serrano, O., & Duarte, C. M. (2022). Species Traits and Geomorphic Setting as Drivers of Global Soil Carbon Stocks in Seagrass Meadows. *Global Biogeochemical Cycles*, 36(10), 1–18. <https://doi.org/10.1029/2022GB007481>

Kennedy, Hilary, Beggins, J., Duarte, C. M., Fourqurean, J. W., Holmer, M., Marbà, N., & Middelburg, J. J. (2010). Seagrass sediments as a global carbon sink: Isotopic constraints. *Global Biogeochemical Cycles*, 24(4), 1–8. <https://doi.org/10.1029/2010GB003848>

Kindeberg, T., Ørberg, S. B., Röhr, M. E., Holmer, M., & Krause-Jensen, D. (2018). Sediment stocks of carbon, nitrogen, and phosphorus in Danish eelgrass meadows. *Frontiers in Marine Science*, 5(DEC), 1–14. <https://doi.org/10.3389/fmars.2018.00474>

Kreitsberg, R., Raudna-Kristoffersen, M., Heinlaan, M., Ward, R., Visnapuu, M., Kisand, V., Meitern, R., Kotta, J., & Tuvikene, A. (2021). Seagrass beds reveal high abundance of microplastic in sediments: A case study in the Baltic Sea. *Marine Pollution Bulletin*, 168, 112417. <https://doi.org/10.1016/j.marpolbul.2021.112417>

- Kucheryavskiy, S. (2020). mdatools – R package for chemometrics. *Chemometrics and Intelligent Laboratory Systems*, 198, 103937. <https://doi.org/10.1016/j.chemolab.2020.103937>
- La Loggia, G., Calvo, S., Ciraolo, G., Mazzola, A., Pirrotta, M., Sarà, G., Tomasello, A., & Vizzini, S. (2004). Influence of hydrodynamic conditions on the production and fate of *Posidonia oceanica* in a semi-enclosed shallow basin (Stagnone di Marsala, western Sicily). *Chemistry and Ecology*, 20(3), 183–201. <https://doi.org/10.1080/02757540410001689786>
- Lamb, A. L., Wilson, G. P., & Leng, M. J. (2006). A review of coastal palaeoclimate and relative sea-level reconstructions using  $\delta^{13}\text{C}$  and C/N ratios in organic material. *Earth-Science Reviews*, 75(1–4), 29–57. <https://doi.org/10.1016/j.earscirev.2005.10.003>
- Lavery, P. S., Mateo, M. Á., Serrano, O., & Rozaimi, M. (2013). Variability in the Carbon Storage of Seagrass Habitats and Its Implications for Global Estimates of Blue Carbon Ecosystem Service. *PLoS ONE*, 8(9). <https://doi.org/10.1371/journal.pone.0073748>
- Layman, C. A., & Post, D. M. (2008). Can stable isotope ratios provide for community-wide measures of trophic structure? reply. *Ecology*, 89(8), 2358–2359. <https://doi.org/10.1890/08-0167.1>
- Lee, G., Suonan, Z., Kim, S. H., Hwang, D. W., & Lee, K. S. (2019). Heavy metal accumulation and phytoremediation potential by transplants of the seagrass *Zostera marina* in the polluted bay systems. *Marine Pollution Bulletin*, 149, 110509. <https://doi.org/10.1016/j.marpolbul.2019.110509>
- Leiva-Dueñas, C., Graversen, A. E. L., Banta, G. T., Holmer, M., Masque, P., Stæhr, P. A. U., & Krause-Jensen, D. (2023). Capturing of organic carbon and nitrogen in eelgrass sediments of southern Scandinavia. *Limnology and Oceanography*, 68(3), 631–648. <https://doi.org/10.1002/lno.12299>
- Li, C., Zhu, L., Li, W. T., & Li, D. (2023). Microplastics in seagrass ecosystems: A critical review. *Science of the Total Environment*, 902, 166152. <https://doi.org/10.1016/j.scitotenv.2023.166152>
- Li, Y., Chen, F., Zhou, R., Zheng, X., Pan, K., Qiu, G., Wu, Z., Chen, S., & Wang, D. (2023). A review of metal contamination in seagrasses with an emphasis on metal kinetics and detoxification. *Journal of Hazardous Materials*, 454, 131500. <https://doi.org/10.1016/j.jhazmat.2023.131500>
- Lloret, J., Marín, A., & Marín-Guirao, L. (2008). Is coastal lagoon eutrophication likely to be aggravated by global climate change? *Estuarine, Coastal and Shelf Science*, 78(2), 403–412. <https://doi.org/10.1016/j.ecss.2008.01.003>



- Macdonald, D. D., Carr, R. S., Calder, F. D., Long, E. R., & Ingersoll, C. G. (1996). Development and evaluation of sediment quality guidelines for Florida coastal waters. *Ecotoxicology*, 5(4), 253–278. <https://doi.org/10.1007/BF00118995>
- Macreadie, P. I., Baird, M. E., Trevathan-Tackett, S. M., Larkum, A. W. D., & Ralph, P. J. (2014). Quantifying and modelling the carbon sequestration capacity of seagrass meadows - A critical assessment. *Marine Pollution Bulletin*, 83(2), 430–439. <https://doi.org/10.1016/j.marpolbul.2013.07.038>
- Macreadie, Peter I., Costa, M. D. P., Atwood, T. B., Friess, D. A., Kelleway, J. J., Kennedy, H., Lovelock, C. E., Serrano, O., & Duarte, C. M. (2021). Blue carbon as a natural climate solution. *Nature Reviews Earth and Environment*, 2(12), 826–839. <https://doi.org/10.1038/s43017-021-00224-1>
- Mahbub, M. S., & Shams, M. (2022). Acrylic fabrics as a source of microplastics from portable washer and dryer: Impact of washing and drying parameters. *Science of the Total Environment*, 834(February), 155429. <https://doi.org/10.1016/j.scitotenv.2022.155429>
- Marmara, D., Katsanevakis, S., Brundo, M. V., Tiralongo, F., Ignoto, S., & Krasakopoulou, E. (2023). Microplastics ingestion by marine fauna with a particular focus on commercial species: a systematic review. *Frontiers in Marine Science*, 10(September), 1–16. <https://doi.org/10.3389/fmars.2023.1240969>
- Marbà, N., Díaz-almela, E., & Duarte, C. M. (2014). Mediterranean seagrass (*Posidonia oceanica*) loss between 1842 and 2009. *Biological Conservation*, 176, 183–190. <https://doi.org/10.1016/j.biocon.2014.05.024>
- Marbà, N., & Duarte, C. M. (1998). Rhizome elongation and seagrass clonal growth. *Marine Ecology Progress Series*, 174, 269–280. <https://doi.org/10.3354/meps174269>
- Marbà, N., & Duarte, C. M. (2010). Mediterranean warming triggers seagrass (*Posidonia oceanica*) shoot mortality. *Global Change Biology*, 16(8), 2366–2375. <https://doi.org/10.1111/j.1365-2486.2009.02130.x>
- Mazarrasa, I., Lavery, P., Duarte, C. M., Lafratta, A., Lovelock, C. E., Macreadie, P. I., Samper-Villarreal, J., Salinas, C., Sanders, C. J., Trevathan-Tackett, S., Young, M., Steven, A., & Serrano, O. (2021). Factors Determining Seagrass Blue Carbon Across Bioregions and Geomorphologies. *Global Biogeochemical Cycles*, 35(6), 1–17. <https://doi.org/10.1029/2021GB006935>

- Mazarrasa, I., Marbà, N., Garcia-Orellana, J., Masqué, P., Arias-Ortiz, A., & Duarte, C. M. (2017). Effect of environmental factors (wave exposure and depth) and anthropogenic pressure in the C sink capacity of *Posidonia oceanica* meadows. *Limnology and Oceanography*, 62(4), 1436–1450. <https://doi.org/10.1002/lno.10510>
- Mazarrasa, I., Samper-villarreal, J., Serrano, O., Lavery, P. S., Lovelock, C. E., Marbà, N., Duarte, C. M., & Cortés, J. (2018). Habitat characteristics provide insights of carbon storage in seagrass meadows. *Marine Pollution Bulletin*, 134(January), 106–117. <https://doi.org/10.1016/j.marpolbul.2018.01.059>
- Miyajima, T., Hori, M., Hamaguchi, M., Shimabukuro, H., & Yoshida, G. (2017). Geophysical constraints for organic carbon sequestration capacity of *Zostera marina* seagrass meadows and surrounding habitats. *Limnology and Oceanography*, 62(3), 954–972. <https://doi.org/10.1002/lno.10478>
- Olejarczyk, M., Rykowska, I., & Urbaniak, W. (2022). Management of Solid Waste Containing Fluoride—A Review. *Materials*, 15(10), 1–23. <https://doi.org/10.3390/ma15103461>
- Oliveira, V. H., Fonte, B. A., Costa, F., Sousa, A. I., Henriques, B., Pereira, E., Dolbeth, M., Díez, S., & Coelho, J. P. (2023). The effect of *Zostera noltei* recolonization on the sediment mercury vertical profiles of a recovering coastal lagoon. *Chemosphere*, 345(March), 140438. <https://doi.org/10.1016/j.chemosphere.2023.140438>
- Olsen, Y. S., Sánchez-Camacho, M., Marbà, N., & Duarte, C. M. (2012). Mediterranean Seagrass Growth and Demography Responses to Experimental Warming. *Estuaries and Coasts*, 35(5), 1205–1213. <https://doi.org/10.1007/s12237-012-9521-z>
- Omollo, D. J., Wang'ondou, V. W., Githaiga, M. N., Gorman, D., & Kairo, J. G. (2022). The Contribution of Subtidal Seagrass Meadows to the Total Carbon Stocks of Gazi Bay, Kenya. *Diversity*, 14(8). <https://doi.org/10.3390/d14080646>
- Palacios-Mateo, C., van der Meer, Y., & Seide, G. (2021). Analysis of the polyester clothing value chain to identify key intervention points for sustainability. *Environmental Sciences Europe*, 33(1). <https://doi.org/10.1186/s12302-020-00447-x>
- Pedersen, M. F., Duarte, C. M., & Cebrián, J. (1997). Rates of changes in organic matter and nutrient stocks during seagrass *Cymodocea nodosa* colonization and stand development. *Marine Ecology Progress Series*, 159, 29–36. <https://doi.org/10.3354/meps159029>

- Pergent-Martini, C., Pergent, G., Monnier, B., Boudouresque, C. F., Mori, C., & Valette-Sansevin, A. (2021). Contribution of *Posidonia oceanica* meadows in the context of climate change mitigation in the Mediterranean Sea. *Marine Environmental Research*, 165(August 2020).  
<https://doi.org/10.1016/j.marenvres.2020.105236>
- Piehlner, M. F., & Smyth, A. R. (2011). Habitat-specific distinctions in estuarine denitrification affect both ecosystem function and services. *Ecosphere*, 2(1), 1–17. <https://doi.org/10.1890/ES10-00082.1>
- Piñeiro-Juncal, N., Kaal, J., Moreira, J. C. F., Martínez Cortizas, A., Lambais, M. R., Otero, X. L., & Mateo, M. A. (2021). Cover loss in a seagrass *Posidonia oceanica* meadow accelerates soil organic matter turnover and alters soil prokaryotic communities. *Organic Geochemistry*, 151.  
<https://doi.org/10.1016/j.orggeochem.2020.104140>
- Piro, A., Marín-Guirao, L., Serra, I. A., Spadafora, A., Sandoval-Gil, J. M., Bernardeau-Esteller, J., Fernandez, J. M. R., & Mazzuca, S. (2015). The modulation of leaf metabolism plays a role in salt tolerance of *Cymodocea nodosa* exposed to hypersaline stress in mesocosms. *Frontiers in Plant Science*, 6(JUNE), 1–12. <https://doi.org/10.3389/fpls.2015.00464>
- Post, D. M. (2002). Using stable isotopes to estimate trophic position: models, methods, and assumptions. *Ecology*, 3(83), 703–718. <https://doi.org/10.2307/3071875>
- Qi, S., Leipe, T., Rueckert, P., Di, Z., & Harff, J. (2010). Geochemical sources, deposition and enrichment of heavy metals in short sediment cores from the Pearl River Estuary, Southern China. *Journal of Marine Systems*, 82(SUPPL.), S28–S42. <https://doi.org/10.1016/j.jmarsys.2010.02.003>
- Röhr, M. E., Boström, C., Canal-Vergés, P., & Holmer, M. (2016). Blue carbon stocks in Baltic Sea eelgrass (*Zostera marina*) meadows. *Biogeosciences*, 13(22), 6139–6153. <https://doi.org/10.5194/bg-13-6139-2016>
- Romeo, T., Pietro, B., Pedà, C., Consoli, P., Andaloro, F., & Fossi, M. C. (2015). First evidence of the presence of plastic debris in the stomach of large pelagic fish in the Mediterranean Sea. *Marine Pollution Bulletin*, 95(1), 358–361. <https://doi.org/10.1016/j.marpolbul.2015.04.048>
- Salinas, C., Duarte, C. M., Arias-ortiz, A., Leon, J. X., Lavery, P. S., Masque, P., Callaghan, D., & Kendrick, G. G. A. (2020). Seagrass losses since mid-20th century fueled CO<sub>2</sub> emissions from soil carbon stocks. *Global Change Biology*, 26(2), 743–752. <https://doi.org/10.1111/gcb.15204>
- Salk, K. R., Erler, D. V., Eyre, B. D., Carlson-Perret, N., & Ostrom, N. E. (2017). An unexpectedly high degree of anammox and DNRA in seagrass sediments: Description and application of a revised

isotope pairing technique. *Geochimica et Cosmochimica Acta*, 211, 64–78.

<https://doi.org/10.1016/j.gca.2017.05.012>

Samper-Villarreal, J., Lovelock, C. E., Saunders, M. I., Roelfsema, C., & Mumby, P. J. (2016).

Organic carbon in seagrass sediments is influenced by seagrass canopy complexity, turbidity, wave height, and water depth. *Limnology and Oceanography*, 61(3), 938–952.

<https://doi.org/10.1002/lno.10262>

Sanchez-Vidal, A., Canals, M., de Haan, W. P., Romero, J., & Veny, M. (2021). Seagrasses provide a novel ecosystem service by trapping marine plastics. *Scientific Reports*, 11(1), 1–7.

<https://doi.org/10.1038/s41598-020-79370-3>

Santos, C. B. D. L., Krång, A., & Infantes, E. (2021). Microplastic retention by marine vegetated canopies: Simulations with seagrass meadows in a hydraulic flume. *Environmental Pollution*, 269,

116050. <https://doi.org/10.1016/j.envpol.2020.116050>

Senturk, Y., Emanet, M., Ceylan Y., & Aytan, U. (2023). The First Evidence of Microplastics Occurrence in Greater Pipefish (*Syngnathus acus Linnaetabus*, 1758) in the Black Sea. *Turkish Journal of Fisheries and Aquatic Sciences*, 23(9). <https://doi.org/10.4194/trjfas23764>

Serrano, O., Lavery, P. S., Rozaimi, M., & Mateo, M. Á. (2014). Global Biogeochemical Cycles. 950–961. <https://doi.org/10.1002/2014GB004872>.

Serrano, O., Lavery, P. S., Duarte, C. M., Kendrick, G. G. A., Calafat, A., York, P. H., Steven, A., & Macreadie, P. I. (2016). Can mud (silt and clay) concentration be used to predict soil organic carbon content within seagrass ecosystems? *Biogeosciences*, 13, 4915–4926. <https://doi.org/10.5194/bg-13-4915-2016>

Serrano, O., Ricart, A. M., Lavery, P. S., Mateo, M. A., Arias-Ortiz, A., Masque, P., Rozaimi, M., Steven, A., & Duarte, C. M. (2016). Key biogeochemical factors affecting soil carbon storage in *Posidonia* meadows. *Biogeosciences*, 13(15), 4581–4594. <https://doi.org/10.5194/bg-13-4581-2016>

Tan, Y. M., Dalby, O., Kendrick, G. A., Statton, J., Sinclair, E. A., Fraser, M. W., Macreadie, P. I., Gillies, C. L., Coleman, R. A., Waycott, M., van Dijk, K. J., Vergés, A., Ross, J. D., Campbell, M. L., Matheson, F. E., Jackson, E. L., Irving, A. D., Govers, L. L., Connolly, R. M., Sherman, C. D. H. (2020). Seagrass Restoration Is Possible: Insights and Lessons From Australia and New Zealand. *Frontiers in Marine Science*, 7(617). <https://doi.org/10.3389/fmars.2020.00617>

- Terrados, J., & Duarte, C. M. (2000). Experimental evidence of reduced particle resuspension within a seagrass (*Posidonia oceanica* L.) meadow. *Journal of Experimental Marine Biology and Ecology*, 243(1), 45–53. [https://doi.org/10.1016/S0022-0981\(99\)00110-0](https://doi.org/10.1016/S0022-0981(99)00110-0)
- Thabit, F. N., El-Shater, A. H., & Soliman, W. (2023). Role of silt and clay fractions in organic carbon and nitrogen stabilization in soils of some old fruit orchards in the Nile floodplain, Sohag Governorate, Egypt. *Journal of Soil Science and Plant Nutrition*, 23(2), 2525–2544. <https://doi.org/10.1007/s42729-023-01209-3>
- Trevathan-Tackett, S. M., Macreadie, P. I., Sanderman, J., Baldock, J., Howes, J. M., & Ralph, P. J. (2017). A global assessment of the chemical recalcitrance of seagrass tissues: Implications for long-term carbon sequestration. *Frontiers in Plant Science*, 8 (925), 1–18. <https://doi.org/10.3389/fpls.2017.00925>
- Tsangaris, C., Panti, C., Compa, M., Pedà, C., Digka, N., Bains, M., D'Alessandro, M., Alomar, C., Patsiou, D., Giani, D., Romeo, T., Deudero, S., & Fossi, M. C. (2021). Interlaboratory comparison of microplastic extraction methods from marine biota tissues: A harmonization exercise of the Plastic Busters MPAs project. *Marine Pollution Bulletin*, 164, 111992. <https://doi.org/10.1016/j.marpolbul.2021.111992>
- Twichell, S. C., Meyers, P. A., Diester-Haass, L. (2002). Significance of high C/N ratios in organic carbon-rich Neogene sediments under the Benguela Current upwelling system. *Organic Geochemistry*, 33(7), 715–722. [https://doi.org/10.1016/S0146-6380\(02\)00042-6](https://doi.org/10.1016/S0146-6380(02)00042-6)
- Unsworth, R. K. F., Cullen-Unsworth, L. C., Jones, B. L. H., & Lilley, R. J. (2022). The planetary role of seagrass conservation. *Science*, 377(6606), 609–613. <https://doi.org/10.1126/science.abq6923>
- Unsworth, R. K. F., McKenzie, L. J., Collier, C. J., Cullen-Unsworth, L. C., Duarte, C. M., Eklöf, J. S., Jarvis, J. C., Jones, B. L., & Nordlund, L. M. (2019). Global challenges for seagrass conservation. *Ambio*, 48(8), 801–815. <https://doi.org/10.1007/s13280-018-1115-y>
- Unsworth, R. K. F., van Keulen, M., & Coles, R. G. (2014). Seagrass meadows in a globally changing environment. *Marine Pollution Bulletin*, 83(2), 383–386. <https://doi.org/10.1016/j.marpolbul.2014.02.026>
- Van Der Sloot, H. A. (2000). Comparison of the characteristic leaching behaviour of cements using standard (EN 196-1) cement mortar and an assessment of their long-term environmental behaviour in construction products during service life and recycling. *Cement and Concrete Research*, 30(7), 1079–1096. [https://doi.org/10.1016/S0008-8846\(00\)00287-8](https://doi.org/10.1016/S0008-8846(00)00287-8)

- Vizzini, Salvatrice, Costa, V., Tramati, C., Gianguzza, P., & Mazzola, A. (2013). Trophic transfer of trace elements in an isotopically constructed food chain from a semi-enclosed marine coastal area (Stagnone di Marsala, Sicily, Mediterranean). *Archives of Environmental Contamination and Toxicology*, 65(4), 642–653. <https://doi.org/10.1007/s00244-013-9933-1>
- Vizzini, Salvatrice, & Mazzola, A. (2006). Sources and transfer of organic matter in food webs of a Mediterranean coastal environment: Evidence for spatial variability. *Estuarine, Coastal and Shelf Science*, 66(3–4), 459–467. <https://doi.org/10.1016/j.ecss.2005.10.004>
- Vizzini, Salvatrice, & Mazzola, A. (2009). Stable isotopes and trophic positions of littoral fishes from a Mediterranean marine protected area. *Environmental Biology of Fishes*, 84(1), 13–25. <https://doi.org/10.1007/s10641-008-9381-3>
- Vizzini, S., & Mazzola, A. (2003). Seasonal variations in the stable carbon and nitrogen isotope ratios ( $^{13}\text{C}/^{12}\text{C}$  and  $^{15}\text{N}/^{14}\text{N}$ ) of primary producers and consumers in a western Mediterranean coastal lagoon. *Marine Biology*, 142(5), 1009–1018. <https://doi.org/10.1007/s00227-003-1027-6>
- Wang, J. N., Chen, F. X., Yu, R., Fan, D. Q., & Zhang, T. S. (2023). Effect of heavy metal (Mn, Pb and Cr) on the properties and hydration in low water/binder cement-based composites (LW/B-CC). *Construction and Building Materials*, 386 (April). <https://doi.org/10.1016/j.conbuildmat.2023.131567>
- Wang, Y., Zou, X., Peng, C., Qiao, S., Wang, T., Yu, W., Khokiattiwong, S., & Kornkanitnan, N. (2020). Occurrence and distribution of microplastics in surface sediments from the Gulf of Thailand. *Marine Pollution Bulletin*, 152(February), 110916. <https://doi.org/10.1016/j.marpolbul.2020.110916>
- Welsh, D., Castadelli, G., Bartoli, M., Poli, D., Careri, M., De Wit, R., & Viaroli, P. (2001). Denitrification in an intertidal seagrass meadow, a comparison of  $^{15}\text{N}$ -isotope and acetylene-block techniques: Dissimilatory nitrate reduction to ammonia as a source of  $\text{N}_2\text{O}$ ? *Marine Biology*, 139(6), 1029–1036. <https://doi.org/10.1007/s002270100672>
- Wesselmann, M., Gherardi, N. R., Duarte, C. M., Garcia-Orellana, J., Díaz-Rúa, R., Arias-Ortiz, A., Hendriks, I. E., Apostolaki, E. T., & Marbà, N. (2021). Seagrass (*Halophila stipulacea*) invasion enhances carbon sequestration in the Mediterranean Sea. *Global Change Biology*, 27(11), 2592–2607. <https://doi.org/10.1111/gcb.15589>

## Acknowledgements

I would like to thank sincerely all of the people that contributed to realisation of my PhD project, who guided, supported and encouraged me in many different ways during this three-year pathway.

I am grateful to my supervisor Prof. Titti Vizzini for the opportunity to work with her, for the teachings, the scientific rigor and for the understanding during the less easy moments.

A special thank goes to the colleagues of the research group of the University of Palermo. I thank Dr. Laura Ciriminna and Dr. Roberta Bardelli, who gave me invaluable help from the field samplings to daily work. I thank Dr. Cristina Andolina and Dr. Geraldina Signa for giving me a special help in understanding the work to be done and in carrying out certain analyses. I really thank Drs. Giovanna Ciluffo for the support I received in understanding and carrying out the statistical analysis. I thank Dr. Andrea Savona and Dr. Cecilia Tramati for the very important technical support and the laboratory assistance.

I am very grateful to Prof. Maria Cristina Fossi and Dr. Cristina Panti, for giving me the opportunity to work in their research team at the University of Siena, to carrying out the research on microplastics. A special thank goes to Dr. Margherita Concato and Dr. Matteo Baini, who gave me invaluable support in the laboratory activities.

I would like to thank Drs. Eugenia Apostolaki, who hosted me during a period abroad at the Hellenic Centre for Marine Research in Crete, for all her advice and guidance in organising the work and writing a research paper.

Furthermore, I am grateful to Prof. Andrew Cundy for hosting me during a wonderful period abroad at the University of Southampton, for the important teachings in the field of  $^{210}\text{Pb}$  dating.